Congestion management of electric distribution networks through market based methods

Huang, Shaojun

Publication date:
2017

Document Version
Publisher's PDF, also known as Version of record

CONGESTION MANAGEMENT OF ELECTRIC DISTRIBUTION NETWORKS THROUGH MARKET BASED METHODS

Shaojun Huang

Kongens Lyngby 2016
CEE-PhD-2016

Congestion Management of Electric Distribution Networks through Market Based Methods

Author:
Shaojun Huang

Supervisors:
Associate Professor: Qiuwei Wu, CEE, DTU
Associate Professor: Arne Hejde Nielsen, CEE, DTU

Examiners:
Associate Professor: Chresten Træholt, CEE, DTU
Professor: Sami Petteri Repo, Tampere University of Technology
Professor: Benjamin F. Hobbs, The Johns Hopkins University

Center for Electric Power and Energy
Eletrovej, Building 325, 1st Floor
2800 Kgs. Lygnby
Denmark

Release date: August 2016

Class: 1 (public)

Edition: 1st Edition

Comment: This dissertation is submitted to the faculty of Department of Electrical Engineering at Technical University of Denmark in partial fulfillment of the requirements for the degree of PhD.

ABSTRACT

Rapidly increasing share of intermittent renewable energy production poses a great challenge of the management and operation of the modern power systems. Deployment of a large number of flexible demands, such as electrical vehicles (EVs) and heat pumps (HPs), is believed to be a promising solution for handling the challenge. Equipped with batteries and hot water storage systems, EVs and HPs are able to shift the consumption according to the production level of renewable energy. However, most of today's distribution networks are not able to accommodate such large number of flexible demands if coordination is not exercised. Congestion can occur on distribution networks if the EVs and HPs consume power simultaneously. This thesis is dedicated to handle the congestion problems on distribution networks when there is high penetration of distributed energy resources (DERs), including EVs and HPs.

Market-based congestion management methods are the focus of the thesis. They handle the potential congestion at the energy planning stage; therefore, the aggregators can optimally plan the energy consumption and have the least impact on the customers. After reviewing and identifying the shortcomings of the existing methods, the thesis fully studies and improves the dynamic tariff (DT) method, and proposes two new market-based congestion management methods, namely the dynamic subsidy (DS) method and the flexible demand swap method.

The thesis improves the DT method from four aspects. Firstly, the formulation of the DT method has been improved. Based on the locational marginal pricing (LMP) concept, the DT method has been proposed in several previous works for congestion management in a decentralized manner. However, linear programming models are not suitable for determining DT due to the multiple-response issue (one price set can have multiple flexible demand responses from aggregators). The thesis proposes a quadratic programming model for the DT method which can avoid the multiple-response issue and make the DT method an efficient decentralized congestion

management method. Secondly, the combination of the DT method and direct control methods is studied and the feeder reconfiguration based DT method is proposed for more efficient congestion management and loss reduction on distribution networks. Thirdly, the stochastic nature of flexible demands is studied and a method for uncertainty management of the DT method is proposed. The probability of congestion events is controlled to be under a certain level through the modified DT method, where the behavior and parameters of the flexible demands have a given probability distribution. At last, a convex relaxation based AC optimal power flow (OPF) model is proposed for determining DT where voltage constraints are included. Moreover, a sufficient condition for exact convex relaxation is proposed and validated. The condition is that there is no reverse power flow, or only active or reactive reverse power flow on the distribution network.

After the study of the DT method, the thesis proposes the DS method for day-ahead congestion management, which is conceptually opposite to the DT method; however, it doesn't discriminate the customers. Finally, the thesis proposes the flexible demand swap method for real-time congestion management, which handles the residual congestion after the day-ahead market and the congestion caused by forecast errors and contingent events. As such, a series of market-based methods, including DT, DS and flexible demand swap, are formed systematically in this thesis for handling congestion more comprehensively and efficiently.

ABSTRACT (DANISH)

Den øgede integration af vedvarende energikilder i el-nettet udgør en udfordring for stabilliteten af fremtidens el-system. En lovende løsning på problemet ved den periodiske produktion af vedvarende energi syntes at ligge i at kontrollere det fleksible forbrug fra elbiler og varmepumper. Ved brug af hhv. batterier og varmtvandsbeholdere kan elbiler og varmepumper ændre deres forbrug til at ligge i perioder med høj produktion af vedvarende energi. Denne strategi medfører dog en ny udfordring, da den nuværende infrastruktur ikke er i stand til at servicere en stor mængde fleksibelt forbrug uden koordinering af de enkelte forbrugere. Hvis der opstår en situation hvor et stort antal elbiler og varmepumper forbruger elektricitet samtidigt, kan det medføre overbelastninger i distributionsnettet. Denne afhandling omhandler overbelastningsproblemer i distributionsnettet hvortil en stor mængde distribuerede energi ressourcer, inkl. elbiler og varmepumper, er tilsluttet.

Denne afhandling fokuserer på metoder der håndterer overbelastningsproblemer med en markedsbaseret tilgang. Disse metoder kan tage højde for eventuelle overbelastninger af el-nettet i planlægningsfasen, hvilket muliggør at aggregatorer kan udregne de optimale forbrugsmønstre og have mindst mulig negativ effekt på kunderne. Efter en gennemgang af eksisterende metoder og identifikation af deres mangler, beskriver denne afhandling en forbedret dynamisk tarif metode og præsenterer to nye markedsbaserede metoder til håndtering af overbelastning. De to nye metoder er kaldt den dynamiske tilskuds metode og fleksibelt forbrugs swap metoden.

Den dynamiske tarif metode er forbedret på fire punkter i denne afhandling. Først og fremmest er den matematiske formulering af metoden forbedret. Den dynamiske tarif metode er baseret på lokalitets marginal prissætning konceptet og er blevet præsenteret i adskillige tidligere udgivelser som en metode til decentraliseret overbelastningshåndtering. På trods af dette, er den lineære programmerings model ikke egnet til udregningen af den dynamiske tarif pga. degenerering. Denne afhandling foreslår en ny formulering af den dynamiske tarif metode baseret på kvadratisk

programmering, hvilket afhjælper degenereringsproblemet og dermed forbedrer den dynamiske tarif metode til håndtering af overbelastningsproblemer. For det andet beskrives en kombination af den dynamiske tarif metode og direkte overbelastnings kontrol, og distributionsnetværk re-konfigurations dynamisk tarif metoden er foreslået som en mere effektiv metode til håndtering af overbelastning og tabsbegrænsning i distributionsnet. For det tredje undersøges den stokastiske natur af det fleksible forbrug og en metode til usikkerhedshåndtering i den dynamiske tarif metode foreslås. Sandsynligheden for overbelastning i el-nettet er kontrolleret til at være under et givet niveau i den dynamiske tarif metode, hvor både adfærd og parametre af det fleksible forbrug har en given sandsynlighedsfordeling. Til sidst præsenteres den konveks afslapnings-baserede vekselstrøms optimalt effekt flow metode som en metode til at udregne den dynamiske tarif når der er taget højde for spændingsbegrænsninger i distributionsnettet. Derudover er en tilstrækkelig betingelses konveks afslapning foreslået og bekræftet. For denne betingelse er det nødvendigt at der ikke er omvendt power flow eller at der kun er aktive eller reaktive omvendte power flows i distributionsnettet.

Efter den dybdegående undersøgelse af dynamisk tarif metoden forslås denne afhandling dynamisk tilskuds metoden, som er begrebsmæssig det modsatte af dynamisk tarif metoden. Forskellen er at dynamisk tilskuds metoden ikke diskriminerer kunderne. Til sidst forslår denne afhandling fleksibelt forbrugs swap metoden til realtids håndtering af overbelastninger, som håndterer den resterende overbelastning efter spotmarkedet og den overbelastning der måtte skyldes prognose fejl og uforudsete hændelser. Derved indeholder denne afhandling en systematisk oversigt over markedsbaserede metoder, inklusiv dynamisk tarif, dynamisk tilskud og fleksibelt forbrugs swap, til mere omfattende og effektiv håndtering af overbelastning i el-nettet.

ACKNOWLEDGEMENTS

First of all, I would like to express my deepest gratitude to my supervisors Associate Prof. Qiuwei Wu and Associate Prof. Arne Hejde Nielsen for their continuous support, patient supervision and wise mentoring during the last three years of my Ph.D. program. I would like to thank them for offering me freedom and encouragement to develop my own ideas in both the project and research while contributing their expertise to the technical analysis in the program.

I would like to thank Prof. Shmuel S. Oren for hosting my external stay at University of California at Berkeley and being an amazing mentor throughout my stay there. His insightful guidance and contagious enthusiasm give me an example of how a world class researcher should be. I am grateful to Assistant Prof. Javad Lavaei and their graduate students in the research group for their great questions and suggestions regarding my research topic during the external stay.

I would like to thank Prof. Mohammad Shahidehpour from Illinois Institute of Technology, for the great discussions and suggestions on my research topic during his visiting at CEE in summer, 2016. He offered me a different view of my research from the perspective of a much wider background, which was a great help during the final stage of my PhD study.

Special gratitude goes to Theis Bo Rasmussen, a fellow PhD student at CEE, for his help of translating the abstract of this thesis to Danish. Special gratitude also goes to Zhaoxi Liu, Jakob Møller, and Haoran Zhao, for their careful proofreading of the final version of this thesis.

My gratitude also goes to Guangya Yang, Louise Busch-Jensen, Hjörtur Jóhannsson, Pauli Petersen, Angel Perez, Junjie Hu, Shi You, Xue Han, Xiaowei Song, Tue Vissing Jensen, Martin Lindholm Wittrock, Chunyu Zhang, Qi Wang, Trine Lyberth Barksmann, Anne Due and all the wonderful colleagues in CEE for the warm welcoming and intellectually rich environment they have brought to me.

Finally, I am deeply grateful to my family for their love and unwavering support. Most importantly, I would like to thank my wife Dongdong and our loving son Yichen, for their support, encouragement, understanding and tremendous love.

TABLE OF CONTENTS

LIST OF TABLES

LIST OF FIGURES

LIST OF ABBREVIATIONS

AD	active demand
BRP	balance responsible party
COP	coefficient of performance
CRP	conditional re-profiling
CRP-2	bi-directional conditional re-profiling
CB	circuit breakers
DR	demand response
DLMP	distribution locational marginal price
DSO	distribution system operator
DT	dynamic tariff
DS	dynamic subsidy
DER	distributed energy resource
DG	distributed generator
EV	electric vehicle
FLECH	flexibility service clearing house
FR	feeder reconfiguration
GAMS	general algebraic modeling system
HP	heat pump
HTC	heat transfer coefficient
ISO	independent system operator
ICT	information and communication technology
LMP	locational marginal price
LV	low voltage
LSE	load serving entities
LP	linear programming / load point
LM	Lagrange multiplier
MV	medium voltage
MIP	mixed integer programming
NLP	nonlinear programming
NP-hard	non-deterministic polynomial-time hard
OPF	optimal power flow
PTDF	power transfer distribution factor
PV	photovoltaics
QP	quadratic programming

RES	renewable energy source
RP	regulation price
RBTS	Roy Billinton test system
SOCP	second-order cone programming
SDP	semidefinite programming
SOC	state of charge
SP	solar power
SRP	scheduled re-profiling
TSO	transmission system operator
WP	wind power

LIST OF SYMBOLS

Some specific sets:

$\mathcal{B}$	set of aggregators
$\mathcal{E}$	set of edges/lines of the whole network
$\mathcal{E}_i$	set of edges of the subtree from node i
$\mathcal{E}^s$	subset of lines with sectionalizing switch
$\mathcal{N}$	set of nodes of the whole network
$\mathcal{N}^+$	subset of nodes, excluding node 0, named as plus nodes
$\mathcal{N}_i$	set of nodes of the subtree from node i
$\mathcal{N}_i^+$	subset of nodes of the subtree, excluding node i
$\mathcal{N}_d$	set of demand bus/load points
$\mathcal{R}^n$	real n-vector/matrix ($n \times 1$)
$\mathcal{P}$	feasible (active) injection region of the OPF
$\mathcal{P}^+$	feasible (active) sub-injection region of the OPF
$\mathcal{S}$	feasible injection region of the OPF
$\mathcal{S}^+$	feasible sub-injection region of the OPF
$\tilde{\mathcal{S}}$	feasible injection region of the SOCP
$\tilde{\mathcal{S}}^+$	feasible sub-injection region of the SOCP
$\mathcal{T}$	set of planning periods
$\mathcal{I}$	set of swaps
$\mathcal{V}$	set of EVs
$\mathcal{V}_i$	set of EVs connected to node i
$\mathcal{Z}$	set of positive integer numbers
$\mathcal{Z}^-$	set of negative integer numbers

Some specific parameters:

$A_{i,t,t\_}$	coefficient matrix, describe the relations between the power consumption and temperature change of the household
$B_{i,t}$	matrix of the price sensitivity coefficient
B	reduced incidence matrix regarding electric nodes

C	reduced incidence matrix regarding graphic nodes
C_a	heat capacity of the inside air
C_s	heat capacity of the house structure (walls, etc.)
D	power transfer distribution factor (PTDF)
E_i	customer to load bus mapping matrix
F_t	line loading limit
K	temperature of the house outside
K^a	house inside temperature
K^s	temperature of the house structure
$K_{i,t}^{a,\min}$	lower temperature limit
$K_{i,t}^{a,\max}$	upper temperature limit
M	a sufficient large number
Q^e	thermal energy produced by HP
S_t^1	solar irradiation to the inside air
S_t^2	solar irradiation to the structure
$\bar{S}$	line capacity (absolute value) upper limit
V_n	nominal voltage
$a_{t,t\_}$	coefficients between power and temperature
a_{kt}	EV availability
b	coefficients
b_{it}	conventional consumption, complex number
c_{jk}^s	average cost of switching on/off
c_t	baseline price
c_s	price of a swap
$d_{i,t}$	discharging power of EVs due to driving
$e_i^{\min}$	lower limit of the state of charge (SOC) level
$e_i^{\max}$	upper limit of the SOC level
$e_{i,0}$	initial SOC level
$\overline{e_k}$	EV charging power upper limit, active power
f_t	line loading limit available for flexible demands
$\bar{\mathbf{i}}$	(square of the magnitude) line current upper limit
k_1	heat transfer coefficient (HTC) between the inside and the outside of the household (ventilation)
k_2	HTC between the inside and the house structure
k_3	HTC between the house structure and the outside

m_i	the number of customers of aggregator i
p_t^c	non-flexible (conventional) demand/resource of load bus
p_s	power of one swap
$p_{i,t}^c$	conventional power consumption of households of one aggregator
$p_{i,t}^{\min}$	lower charging power limit of EVs
$p_{i,t}^{\max}$	upper charging power limit of EVs
$\hat{p}_i^{\min}$	lower power limit of HPs
$\hat{p}_i^{\max}$	upper power limit of HPs
$\bar{p}$	real part of $\bar{s}$
$\bar{q}$	imaginary part of $\bar{s}$
r	resistance
r_{jk}	resistance of line jk
$\bar{s}$	upper limit of the sub-injection
$\underline{s}$	lower limit of the sub-injection
$u_{i,t}$	constant relating to initial temperature and solar radiation
$\mathbf{v}_0$	(square) voltage of node 0, real number
$\underline{\mathbf{v}}_i$	(square) voltage of plus nodes, lower limit
$\overline{\mathbf{v}}_i$	(square) voltage of plus nodes, upper limit
x	reactance
$x_{jk,0} \in \{0,1\}$	initial status of sectionalizing switch
z	impedance, $z = r + \mathrm{j}x$
y_t	predicted price including the baseline part and the sensitive part
α_i	(alpha) sensitivity coefficients
β_t	(beta) price sensitivity coefficient
η	(eta) the confidence level
σ^2	(sigma square) variance
ε	(epsilon) predefined overloading percentage
ϕ	(phi) energy consumption per km for EV

Some specific variables:

K_t	fictitious transferring power
P_t	active power flow
P	reverse line flow, active part
$\hat{P}$	linear approximation of the reverse line flow, active part
Q	reverse line flow, reactive part
$\hat{Q}$	linear approximation of the reverse line flow, reactive part

S	reverse line flow, complex number
$\hat{S}$	linear approximation of the reverse line flow, complex number
c_t^{DT}	dynamic tariff
e	EV charging power, active power
$\mathbf{i}$	(square of the magnitude) line current
p, p_i	real part of s
p_0	real part of s_0
p_t	charging power of an EV
$p_{i,t}$	charging power of EVs of one aggregator
$\hat{p}_t$	power consumption of an HP
$\hat{p}_{i,t}$	power consumption of HPs of one aggregator
q, q_i	imaginary part of s
r_t	distributional regulation price, can be dynamic tariff or subsidy
s, s_i	injection of plus nodes ($i>0$), i.e. sub-injection
s_0	injection of node 0, complex number
$\mathbf{v}, \mathbf{v}_i$	(square) voltage of plus nodes, real number, $i>0$
$\hat{\mathbf{v}}_i$	linear approximation of (square) voltage
$x_{jk,t} \in \{0,1\}$	status of sectionalizing switch
$x \in \{0,1\}$	the indicator of whether the load point is selected
$y \in \{0,1\}$	the indicator of whether the load point is selected
$y_{jk,t}$	counting switching operations
λ_t	(lambda) Lagrange multiplier (LM) of line loading limit constraint
$\lambda_t^+ \in R^{n_L}$	(lambda) LM of line loading limit constraint (right side)
$\lambda_t^- \in R^{n_L}$	(lambda) LM of line loading limit constraint (left side)
ρ, ρ_a, ρ_d	(rho) probability
ρ_t	(rho) LM of load flow equations (DC load flow)
$\mu_{i,t}^+$	(mu) LM of SOC upper limit constraint
$\mu_{i,t}^-$	(mu) LM of SOC lower limit constraint
$\hat{\mu}_{i,t}^+$	(mu) LM of upper temperature limit constraint
$\hat{\mu}_{i,t}^-$	(mu) LM of lower temperature limit constraint
$\varsigma_{i,t}^+$	(sigma) LM of EV charging power upper limit constraint
$\varsigma_{i,t}^-$	(sigma) LM of EV charging power lower limit constraint
$\hat{\varsigma}_{i,t}^+$	(sigma) LM of HP power upper limit constraint
$\hat{\varsigma}_{i,t}^-$	(sigma) LM of HP power lower limit constraint

$\psi^{+}_{jk,t}$	(psi) LM of topo constraint (determined by the switching status of the sectionalizing switches)
$\psi^{-}_{jk,t}$	(psi) LM of topo constraint

Other Symbols

$\mathbf{1}$	a vector with all ones
$\|*\|_1$	L-1 norm of vector $*$
$\{*\}_j$	j-th element of vector $*$
$*^T$	transpose of matrix/vector $*$
n_*	the number of elements of set $*$

CHAPTER 1.

INTRODUCTION

1.1 Background

Denmark, as one of the countries that strive for CO_2 emission reduction and energy supply security, has adopted energy strategies that aim at achieving independence from fossil fuels by 2050 [1]. After the world leaders met 2015 in Paris to address the climate change, China promised to reduce 60% of the major pollutant emissions from the power sector by 2020. In order to realize such ambitious goals, renewable energy, such as hydro power, wind power (WP) and solar power (SP), and distributed energy resources (DERs), such as distributed generators (DGs), electric vehicles (EVs) and heat pumps (HPs), will be extensively used and play an important role in future power systems.

The installation of WP around the world increased rapidly since the beginning of this century. Table 1-1 shows the statistics of the global installed wind power till 2015 [2]. The wind power in Denmark covered 42% of the total electricity consumption in 2015 [3].

TABLE 1-1. GLOBAL INSTALLED WIND POWER CAPACITY (MW)

	Africa, Middle East	Asia	Europe	Latin America, Caribbean	North America	Pacific Region	World Total
End 2014	2,536	141,973	134,251	8,568	77,935	4,442	369,705
New 2015	953	33,859	13,805	3,652	10,817	381	63,467
End 2015	3,489	175,831	147,771	12,220	88,749	4,823	432,883

SP experiences the same rapid speed of development and installation as WP. There are 22 countries that have enough SP capacity to cover at least 1% of their total electricity demand [4]. Italy, Greece and Germany have SP production to cover respectively 8%, 7.4% and 7.1% of their total annual electricity consumption. The top 5 countries by the end of 2015 for cumulative installed PV capacity are listed in Table 1-2.

TABLE 1-2. TOP 5 COUNTRIES TILL END 2015 FOR CUMULATIVE INSTALLED CAPACITY (GW)

	China	Germany	Japan	USA	Italy
End 2015	43.5	39.7	34.4	25.6	18.9

Impacts of the renewable energy on the power systems have been widely studied [5], [6]. The intermittent nature of WP and SP needs a revolution at the demand side, because the conventional non-shiftable loads can't maximize the utilization of the intermittent renewable energy. The flexible demands, such as EV and HP equipped with energy storage devices, are able to harvest the benefits of the intermittent renewable energy and support the stability of the power system. Thanks to the advancement of the technologies and the support from the government policies, the sales of plug-in light vehicles had a fast growth in the past five years in the major markets [7], as shown in Fig. 1-1.

1.2 Problem Statement

It is a great challenge to manage and operate the power system with high penetration of the abovementioned new power sources, namely WP, SP, EVs and HPs. The challenge includes the issue of imbalance between production and consumption, and the issue of the congestion due to simultaneous discharge / charge (production / consumption) of DERs.

The key to coping with this challenge is smart grid technology based on information and communication technologies (ICT). The smart grid technology enables advanced coordination between the components of the power system. It also enables a more sophisticated management and control of the new members to handle the imbalance and congestion issues. Both issues are critical to the power system operation; however, the PhD study focuses only on the congestion issue, specifically, the potential congestion on distribution networks due to high penetration of DERs. Congestion problems in distribution networks are envisaged as voltage problems (bus voltage is close to or exceeding the limit, typically +/–10%) and

overloading problems (loading is close to or exceeding the thermal limit of the power components).

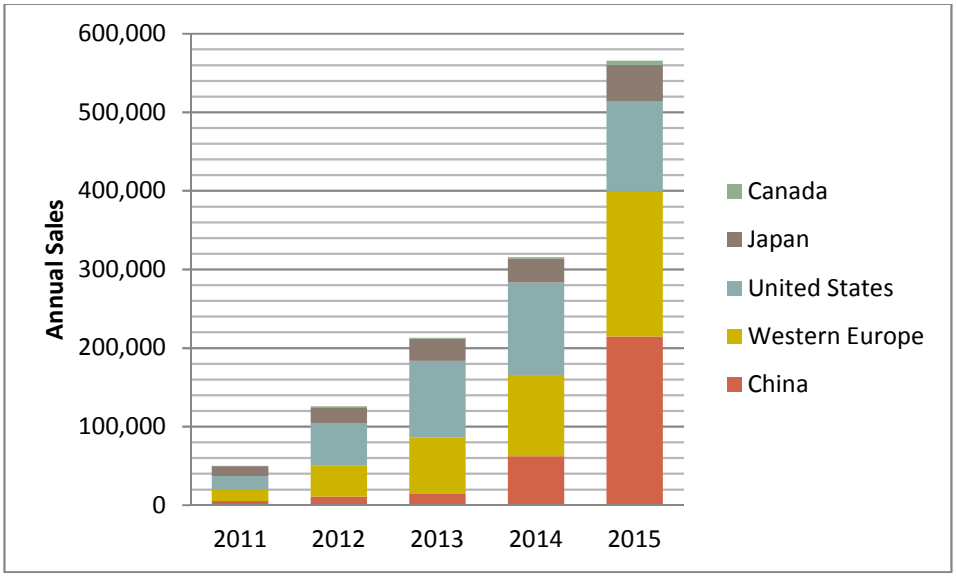

Fig. 1-1. Global plug-in light vehicle sales, 2011-2015

The goal of a distribution network is to efficiently deliver active power p_d (shown in Fig. 1-2) as required to the customers with high reliability. The customers can absorb some reactive power (e.g. induction motor) in the allowed range (according to the grid code). Delivering active and reactive power through a feeder will lead to voltage drop problems. Similarly, in the case of receiving renewable energy production, p_d can be negative and it can lead to over-voltage problems. In both cases, if the power flow exceeds the thermal limits of the power components, it will lead to overloading problems.

1.3 Existing Research Work on Congestion Management

To solve (or alleviate) the under-voltage or over-voltage issues and overloading issues discussed in the above section, distribution system operators (DSOs) can reinforce the distribution network (i.e. use cables/lines with higher current carrying capability and smaller impedance). The DSO can also change the total active and

reactive power at Bus 2 (Fig. 1-2) by installing local new DGs and FACTS devices, such as static VAR compensators (SVCs), or by motivating the customers to change p_d and q_d via market-based methods or directly controlling p_d and q_d under pre-agreements with the customers.

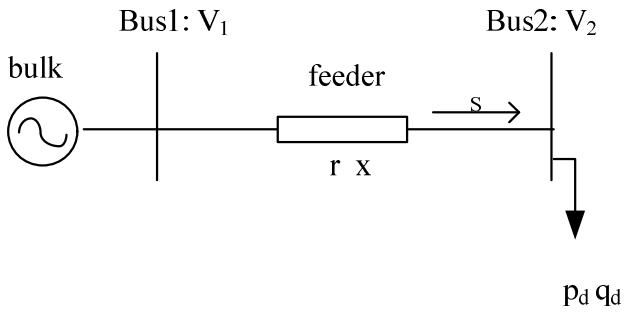

Fig. 1-2. Illustration of a simple distribution grid

Market-based methods or indirect control methods, as the main topic of this thesis, are defined as the methods that employ prices or incentives to influence the behavior of DERs such that congestion on distribution networks is alleviated. Direct control methods refer to those methods in which the DSO can directly control power system components, such as sectioning switches (network reconfiguration), on-load tap changers (OLTC), SVC, grid-owned DGs and in some cases, customer-owned DGs. There are scenarios that the coordination between the market-based methods and the direct control methods is beneficial. One example is the reconfiguration-based dynamic tariff (DT) method, which will be discussed in Chapter 3.

Several market-based methods have been developed in previous literature, which are reviewed in the following subsection. Market-based methods rely on the underlying market structure. It's very often that a market-based method will interact with the markets; therefore, a good understanding of the fundamental market structure is very important. In Appendix B, the market structure of the Nordic electricity market is reviewed, which is the fundamental assumption for discussing the market-based methods in this thesis unless specified otherwise.

1.3.1 Price-based Congestion Management Methods

By extending the locational marginal price (LMP) concept [8] from transmission networks to distribution networks, [9]–[13] have developed the distribution LMP (DLMP) concept and applied it to handle the congestion issues in distribution networks with distributed generators (DGs). Through the DLMP concept, the local DGs will make profits if they produce more power and reduce the energy requirement of the local bus from remote areas during the congestion hours. DLMP is determined through an OPF method, which is very similar to LMP calculation. In the DLMP method, the LMP at the bulk grid connection point is the reference price for DLMP, i.e. the energy exported to or imported from the bulk grid has a price as LMP. However, whether this LMP is a forecast price or an actual price in the DLMP method has not been pointed out in the abovementioned references. In addition, as a market clearing method on the distribution level, its relation with the major market clearing on the transmission level is not clear.

References [14], [15] employ the dynamic tariff (DT) concept (a detailed introduction can be seen in Chapter 2) to solve congestion due to flexible demands in distribution networks. The flexible demands may create congestion if the price is not properly set; on the other hand, they can help the congestion management if they are controlled through proper price signals. In [14], [15], the congestion management is conducted in a decentralized manner where the aggregators independently determine the energy plans for the flexible demands managed by them without considering network constraints. The network constraint information is contained in DT. However, due to the linear formulation of the DT method proposed in [14], [15], multiple-response issue may occur, which can cause a failure of the DT method for congestion management as a decentralized indirect control method.

The DT method shares many similar features of the DLMP method, e.g., both methods employ OPF methods and the marginal cost concept (Lagrange multipliers), and the DT per node is equal to the congestion cost element of the corresponding DLMP. But there are differences between them. First of all, the DT method is not a market clearing method while DLMP is. The DT method relies on the existing day-ahead market, e.g. the spot market in Nordic area, and it can be seamlessly integrated into the existing market. Second of all, the DT method is a decentralized control method, which is implemented through two steps of optimizations, while DLMP is a centralized clearing method through one step of optimization.

Also based on OPF methods and the marginal cost concept, a distribution network capacity reallocation method was proposed in [16]–[19]. However, unlike the DT

method, it determines the marginal cost and the network capacity for each aggregator through an iterative process between the DSO and the aggregators. One of the benefits of this method is that it can protect the privacy of the aggregators, but the efficiency of this method is questionable due to the high communication burden from the multiple iterative steps.

In theory, the abovementioned three methods will converge to same prices if setups are the same. However, the implementation of these methods is quite different. Only the DT method has no requirement of binding between DSO and aggregators, so the aggregators can be fairly easy to enter the day-ahead market, which makes it suitable for being integrated with the day-ahead market.

1.3.2 Incentive-based Congestion Management Methods

The authors of [20] proposed a new method to solve the congestion: FLECH- flexibility service clearing house. The aggregators do not need to buy distribution grid capacity, i.e. they can make their own demand plan without considering the distribution grid limitations. Instead, the DSO needs to buy flexibility services to solve the congestion problem, e.g. buy a service which is to reduce the demands at a certain time and a certain location. In [20], the possible flexibility services are classified as: Flexibility Service of Overload Planned (FSOP), Flexibility Service of Overload Urgent (FSOU), Flexibility Service of Overload Reserve (FSOR), Flexibility Service of Overload Cap (FSOC) and Flexibility Service of Overload Maximum (FSOM). A similar idea, i.e. the active demand (AD) product, has been proposed in [21]. AD products are classified as: Scheduled Re-Profiling (SRP), Conditional Re-Profiling (CRP) and Bi-directional Conditional Re-Profiling (CRP-2). However, both the FLECH method and the AD method are still in a fairly conceptual phase without detailed investigation of implementation method.

Reference [22] has proposed a coupon incentive-based demand response program that can benefit both the load serving entities (LSEs) and the customers. In US and Europe, LSE refers to retailers or aggregators. LSEs buy electricity from markets and sell it to their customers. Outside of US and Europe, LSE may refer to different entities due to different structures of the electricity markets. One of the shortcomings of the coupon based incentive program is that it only considers the economic profit of LSEs, without considering the limits of distribution networks and the intertemporal effect of flexible demands.

A monetary incentive based method was proposed in [23] for coordinating and rescheduling flexible demands, where the capacity limit of distribution networks was

taken into account. With this method, the flexible demands will be rewarded if they are willing to reduce consumption during the congestion hours. However, the method to determine a proper incentive is not optimal for the following reason. The authors of [23] choose the best one from a finite set of predefined incentives, however, it is not necessarily global optimal due to limited size of the finite set. The rebound effect, i.e., the reduced flexible demand will cause an increase in a future period, is not considered because the method only handles one period at each execution. Another issue is that it does not consider the location of the incentives. Demand responses for solving congestion are usually needed at specific areas or nodes. Locational incentives can improve the efficiency of solving congestion because the responses of flexible demands from uncritical areas or nodes (e.g. the upstream nodes to the congested point) have a limited effect.

1.4 Contributions of the Thesis

Motivated by the issues associated with the abovementioned existing methods for congestion management on distribution networks, several new market-based congestion management methods/concepts were proposed in this thesis, including: A new formulation to strengthen the DT concept; The uncertainty management method and the convex relaxation based AC OPF model for supporting the DT concept; The combination of the DT and reconfiguration method; The DS method; The flexible demand swap method for real-time congestion management. These methods can be organized chronologically as shown in Fig. 1-3, to form a series of market-based methods for congestion management. The time frame for these methods spans from the time day-ahead to the time near the operation; therefore, they can handle the potential congestion appearing from the day-ahead energy planning stage to the near operation stage. These methods are proposed to outperform the existing methods, not from the economic point of view (the proposed methods have as good economic efficiency as the existing methods, such as the DLMP method), but rather from the practical point of view. All these methods have taken into account the rules of the day-ahead market; therefore, they are hopefully more acceptable to the stakeholders from the industry.

The first contribution is to strengthen the DT concept for congestion management, which is the most important and fundamental concept in this thesis. The quadratic programming based optimization model for determining DT was proposed to handle the multiple-response issue associated with the linear programming based optimization model.

The second contribution is to propose a method for the DT concept to manage the uncertainties due to the stochastic nature of flexible demands and the inevitable forecast errors. The third contribution is to propose a sufficient condition for exact convex relaxation of the AC OPF model, which can be employed to determine DT with voltage constraints included.

The fourth contribution is to investigate the combination of the DT method and the direction control method, such as reconfiguration. The fifth contribution is to propose a new concept, i.e. DS, to replace the DT method and avoid regulation issues nowadays.

The last contribution is the proposal of the flexible demand swap method for real-time congestion management, which can handle the unsolved congestion from the day-ahead market and the potential congestion occurring near the operation time. This method is the last-minute method for congestion management through market-based methods.

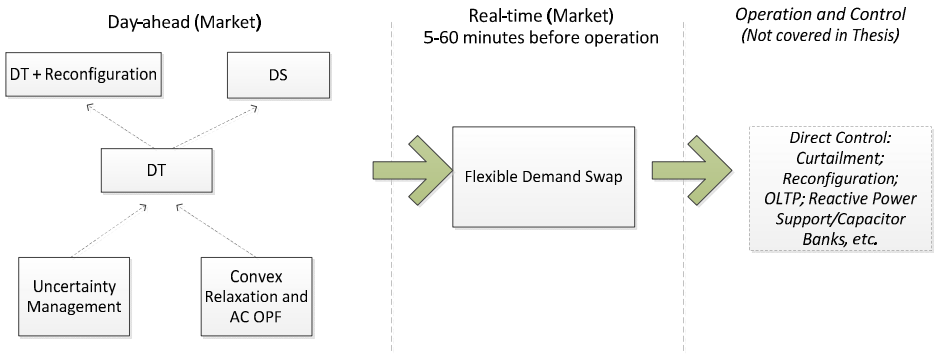

Fig. 1-3. Structure of the proposed congestion management methods/concepts, organized chronologically; dashed arrows show the support function between the two methods, solid arrows show the chronological relation among the methods.

The publications completed during the PhD study include:

1. **S. Huang**, Q. Wu, S. S. Oren, R. Li, and Z. Liu, "Distribution locational marginal pricing through quadratic programming for congestion management in distribution networks," IEEE Trans. Power Syst., vol.30, no.4, pp. 2170–2178, Jul. 2015.
2. **S. Huang**, Q. Wu, L. Cheng, and Z. Liu, "Optimal Reconfiguration-Based Dynamic Tariff for Congestion Management and Line Loss Reduction in Distribution Networks," IEEE Trans. Smart Grid, vol.7, no.3, pp. 1295–1303, May 2016.
3. **S. Huang**, Q. Wu, L. Cheng, Z. Liu, H. Zhao, "Uncertainty management of dynamic tariff method for congestion management in distribution networks", IEEE Trans. Power Syst., in press
4. **S. Huang**, Q. Wu, J. Wang, H. Zhao, "A sufficient condition on convex relaxation of AC optimal power flow in distribution networks", IEEE Trans. Power Syst., in press

5. **S. Huang**, Q. Wu, "Dynamic subsidy method for congestion management in distribution networks", IEEE Trans. Smart Grid, in press
6. **S. Huang**, Q. Wu, "Real-time congestion management in distribution networks by flexible demand swap", IEEE Trans. Smart Grid, in press
7. **S. Huang**, Q. Wu, H. Zhao, and Z. Liu, "Geometry of power flows and convex-relaxed power flows in distribution networks with high penetration of renewables," Energy Procedia, accepted
8. **S. Huang**, Q. Wu, A. H. Nielsen, Z. Liu, and H. Zhao, "Long Term Incentives for Residential Customers Using Dynamic Tariff," in Proc. 2015 IEEE PES Asia-Pacific Power and Energy Engineering Conference.
9. **S. Huang**, Q. Wu, Z. Liu, and H. Zhao, "Sensitivity analysis of dynamic tariff method for congestion management in distribution networks," in Proc. 2015 IEEE Power & Energy Society General Meeting, pp. 1–6.
10. **S. Huang**, Q. Wu, Z. Liu, and A. H. Nielsen, "Review of congestion management methods for distribution networks with high penetration of distributed energy resources," in Proc. 2014 IEEE PES Innovative Smart Grid Technologies, Europe, pp. 1–6.

The publications 1-6 are incorporated in this thesis, while the rest are cited as references wherever relevant.

1.5 Structure of the Thesis

The thesis is organized as follows.

Chapter 2: This chapter is to provide a rigorous theoretical foundation for the DT concept through mathematical formulations and proofs. Quadratic programming optimization model is employed to handle the multiple-response issue of the DT method.

Chapter 3: This chapter is to investigate the possibilities of combining the DT method with direct control methods, such as feeder reconfiguration, for a more efficient congestion management on distribution networks.

Chapter 4: This chapter is to provide a method to handle the uncertainties related to the DT method for congestion management.

Chapter 5: This chapter will present a method to solve AC OPF through exact convex relaxation and its application for EV energy planning and DT determination where voltage constraints are included.

Chapter 6: In this chapter, the dynamic subsidy method will be presented, which is opposite to the DT method and has less regulation concerns.

Chapter 7: This chapter will present a congestion management method, i.e. flexible demand swap, which can be employed near the operation time.

Chapter 8: Conclusion is made and the possible future work is discussed in this chapter.

CHAPTER 2.

DYNAMIC TARIFF THROUGH QUADRATIC PROGRAMMING[1]

This chapter is to provide a sound theoretical foundation for the DT concept through mathematical reformulations and proofs.

2.1 Introduction

A DSO, who has the main responsibility for resolving congestion in distribution networks, can choose to reinforce the network through their long term planning or employ market-based methods [14], [18], [19] to influence DERs to respect the system capacity limits. Compared to direct control methods for congestion management [24], [25], market-based methods can maximize the social welfare, cause the least discomfort to customers and encourage more participation in the energy planning.

Reference [14] employs the dynamic tariff (DT) concept to solve the congestion due to flexible demands in distribution networks. However, the method proposed in [14] did not consider the inter-temporal characteristics of flexible demands. In [15], taking into account the inter-temporal characteristics, a linear formulation for determining DT was proposed. The method proposed in [15] works in many cases. However, the aggregator optimization may have multiple solutions because of the linear programming formulation, leading to multiple possible responses from the aggregator side. The multiple-response issue of the aggregator optimization in the DT concept was discussed in [26]. The multiple-response issue may cause the centralized DSO optimization and the decentralized aggregator optimization not to

[1] This chapter is based on paper: S. Huang, Q. Wu, S. Oren, R. Li and Z. Liu, "Distribution Locational Marginal Pricing Through Quadratic Programming for Congestion Management in Distribution Networks", IEEE Tr. Power System, vol: 30, issue: 4, pages: 2170 - 2178, July 2015.

converge, and the decentralized congestion management to fail. Motivated by the multiple-response issue of the decentralized aggregator optimization, this chapter is dedicated to solve the non-convergence problem of the centralized DSO optimization and the decentralized aggregator optimization by proposing a new formulation with quadratic programming (QP).

The chapter begins with an introduction of the spot price prediction method and the optimal energy planning model of EVs and HPs, which are the basic elements of the DT method. DT is determined through an optimal energy planning of flexible demands in the distribution network by the DSO based on the predicted day-ahead electricity price, energy requirements of the demands and the production from distributed renewables. Next, the non-convergence issue of the linear programming formulation and how to solve it through QP formulation, including the proof of the convergence through QP, are presented. Finally, the case studies are presented and discussed.

2.2 Optimal Energy Planning for EVs and HPs

EVs and HPs meet their energy needs for driving and heating by procuring energy in the day-ahead electricity market. Such purchases can be done through an aggregator representing the EV and HP users by submitting bids on their behalf in the day-ahead electricity market. As such, the individual users shift the burden of market participation to aggregators, and the aggregators get enough capacity to participate in different markets. This section is to derive EV and HP planning models respectively, which later on will be used in Section 2.3.3 for the integrated energy planning at DSO side and the distributed energy planning at aggregator side.

2.2.1 Spot Price Prediction

Before submitting their bids, the aggregators need to determine an optimal energy plan based on the predicted spot prices. The electricity prices are plan-dependent, which poses some difficulty in determining an optimal energy plan because the price is a discontinuous function of the energy plan. A price sensitivity based spot price prediction method was proposed in [16], [27] to deal with such difficulty. Specifically, the predicted price consists of a baseline price plus a linear component proportional to the demand. Therefore, the predicted spot price at time t (hour) is given by,

$$y_t = c_t + \beta_t p_t, \tag{2.1}$$

where c_t is the baseline price, β_t is the sensitivity coefficient and p_t is the total power of flexible demands.

The price sensitivity coefficient β is determined by evaluating the merit order of the power plants in the electricity market [27]. The production of renewable energy resources, such as WP and SP, is deducted from the conventional demands first. Then the net demands and the flexible demands are met by conventional power plants according to the order of their marginal cost. The function of marginal cost versus demand is fit by an exponential function and β is the first order coefficient of the Taylor expansion of the fit function. The concept of the price sensitivity is illustrated in Fig. 2-1. The coefficient β estimated in the above method is scaled up by the total number of available flexible demands (EVs and HPs) in order to be used for individual flexible demand, which is still denoted as β without causing ambiguity.

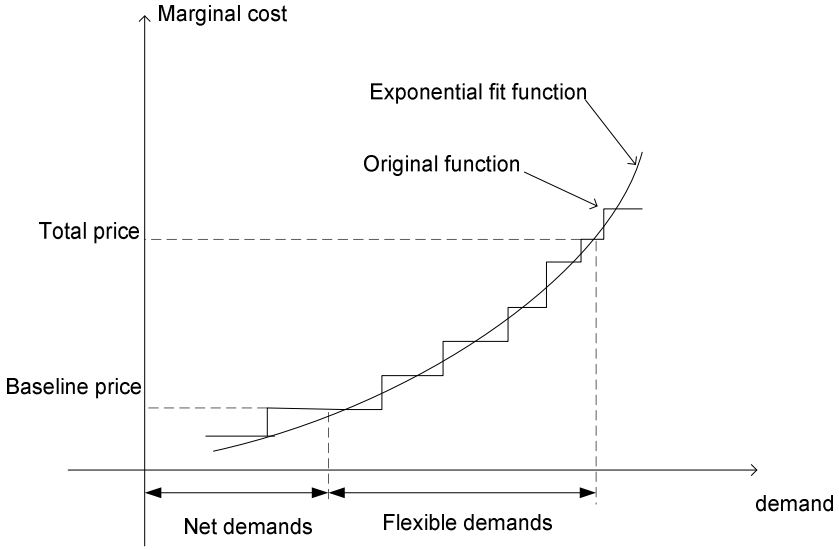

Fig. 2-1. Concept of the price sensitivity

2.2.2 Optimal EV Charging

The optimal EV charging aims to meeting the energy needs of EVs with minimum energy cost. Taking into account the price sensitivity, the cost function of the EV charging becomes a quadratic function. The total charging cost of an EV is,

$$\sum_{t\in N_T} y_t p_t = \sum_{t\in N_T} (c_t + \beta_t p_t) p_t = \sum_{t\in N_T} \beta_t p_t^2 + c_t p_t \,, \tag{2.2}$$

where p_t is the charging power of one EV and β_t is the average sensitivity coefficient for one flexible demand.

With the aggregator concept, the charging plan of the EVs managed by aggregator i at period t can be expressed as a vector $p_{i,t} \in \mathcal{R}^{m_i}$, where m_i is the number of EVs of the aggregator i.

As such, the optimal EV charging plan can be found by solving the optimization problem below.

$$\min_{p_{i,t}} \sum_{i\in\mathcal{B},t\in\mathcal{T}} (\frac{1}{2} p_{i,t}{}^T B_{i,t} p_{i,t} + (c_t \mathbf{1})^T p_{i,t}) \tag{2.3}$$

subject to,

$$e_i^{\min} \le \sum_{t\_\le t} (p_{i,t\_} - d_{i,t\_}) + e_{i,0} \le e_i^{\max}, \forall t \in \mathcal{T}, i \in \mathcal{B}, (\mu_{i,t}^-, \mu_{i,t}^+) \tag{2.4}$$

$$p_{i,t}^{\min} \le p_{i,t} \le p_{i,t}^{\max}, \forall t \in \mathcal{T}, i \in \mathcal{B}, (\varsigma_{i,t}^-, \varsigma_{i,t}^+) \tag{2.5}$$

In the above equations, vector $e_i^{\min}$ and $e_i^{\max}$ are the minimum SOC and maximum SOC of the batteries (absolute value with unit kWh), vector d is the discharging power, vector $e_{i,0}$ is the initial SOC, $\mathcal{B}$ is the set of the aggregators and $\mathcal{T}$ is the set of planning periods. Elements of the diagonal matrix B is the sensitivity coefficient β_t. Vector μ and ς are Lagrange multipliers. Constraint (2.4) ensures that the SOC levels of the batteries are within the specified range. It is assumed that one planning period is one hour; therefore, the charging power in kW is equivalent to the energy change in kWh, i.e. $(p_{i,t\_} - d_{i,t\_}) = (p_{i,t\_} - d_{i,t\_})\Delta t$ in (2.4). Equations (2.3)-(2.5) form a QP problem.

2.2.3 Optimal HP Planning

The optimal HP planning is to schedule the energy consumption of HPs so as to maintain the house temperature within a specified range at the minimum energy cost. The heat transfer process of the air source HP can be represented by an electric circuit [28] which is illustrated in Fig. 2-2. Thus, the following thermal balance equations can be derived [28].

$$Q_t^e + S_t^1 - k_1(K_t^a - K_t) - k_2(K_t^a - K_t^s) = C_a(K_t^a - K_{t-1}^a),\ \forall t \in \mathcal{T} \tag{2.6}$$

$$S_t^2 + k_2(K_t^a - K_t^s) - k_3(K_t^s - K_t) = C_s(K_t^s - K_{t-1}^s),\ \forall t \in \mathcal{T} \tag{2.7}$$

In the above equations, $k$is the heat transfer coefficient of one time unit, K is the temperature, $S$is the solar radiation of one time unit, C is the heat capacity and Q is the thermal energy produced by the HP of one time unit. Here, the time unit is chosen to be one planning period, e.g. 1 hour. The right side of (2.6) and (2.7) are the heat energy needed to change the temperature from K_{t-1}^a and K_{t-1}^s to K_t^a and K_t^s, which are the temperatures of the inside air and the house structure at the beginning and the end of one planning period respectively.

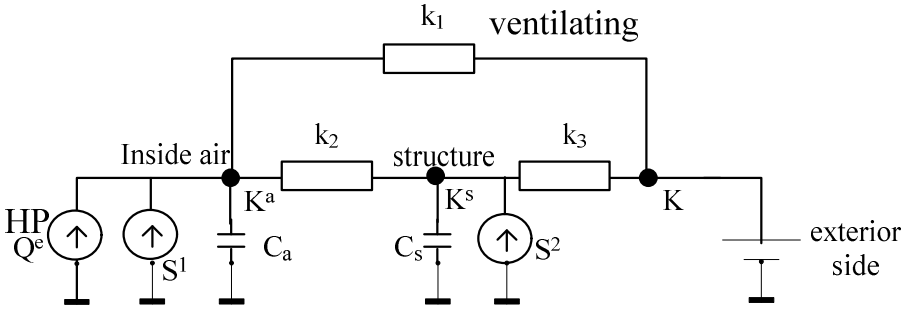

Fig. 2-2. Heat transferring process of the house

Equations (2.6) and (2.7) can be solved iteratively. As a result, the house inside air temperature K_t^a will be a linear combination of all the previous and the current thermal energy (Q_t^e) plus an initial state. Because Q_t^e has a linear relation (by the

coefficient of performance (COP)) to the active power $\hat{p}_t$ consumed by the HP, the house inside air temperature can be expressed as,

$$K_t^a = \sum_{t\_\le t} a_{t,t\_}\hat{p}_{t\_} + u_t \quad \forall \mathrm{t} \in \mathcal{T}, \tag{2.8}$$

where a is the coefficient and u is the constant relating to the initial temperature and the given solar radiation profile.

Finally, the optimization problem of the HP energy plan can be formed as,

$$\min_{\hat{p}_{i,t}} \quad \sum_{i\in\mathcal{B},t\in\mathcal{T}} \frac{1}{2}\hat{p}_{i,t}{}^T B_{i,t}\hat{p}_{i,t} + (c_t\mathbf{1})^T\hat{p}_{i,t} \tag{2.9}$$

subject to,

$$K_{i,t}^{a,\min} \le \sum_{t\_\le t} A_{i,t,t\_}\hat{p}_{i,t\_} + u_{i,t} \le K_{i,t}^{a,\max}, \forall i \in \mathcal{B}, \mathrm{t} \in \mathcal{T}, (\hat{\mu}_{i,t}^-, \hat{\mu}_{i,t}^+), \tag{2.10}$$

$$\hat{p}_{i,t}^{\min} \le \hat{p}_{i,t} \le \hat{p}_{i,t}^{\max}, \forall i \in \mathcal{B}, \mathrm{t} \in \mathcal{T}, (\hat{\varsigma}_{i,t}^-, \hat{\varsigma}_{i,t}^+), \tag{2.11}$$

where $A_{i,t,t\_} \in \mathcal{R}^{m_i \times m_i}$ is a diagonal matrix, and $u_{i,t} \in \mathcal{R}^{m_i}$ represents the constant values.

2.3 DT through QP

2.3.1 Decentralized Congestion Management through the DT Concept

According to [14], [15], the procedure of using the DT concept to solve the congestion problem in a decentralized manner can be summarized as follows. Firstly, the DSO obtains the flexible demand data, such as energy requirements and the availability, from the aggregators or by its own prediction. The DSO also needs the network information and the predicted spot price. Secondly, DTs are calculated through the optimal schedule respecting the network constraints, and the DTs are published to all the aggregators. Thirdly, after receiving the DTs, the aggregators make their own optimal plans independently with both the predicted spot prices and the DTs. At last, the aggregators submit their energy plans/bids to the spot market (the energy cost will be paid to the day-ahead market).

2.3.2 Multiple-response Issue of the Aggregator Optimization with Linear Programming Formulation

The multiple-response issue of the aggregator optimization through linear programming was pointed out by the discussers of [26] based on the observation of the case study results of [15]. According to the observation, there are an infinite number of optimal solutions of the aggregator optimization due to the equal DTs at some load points[2]. The multiple-response issue of the aggregator optimization through linear programming is further discussed by the following analysis.

Assume that there is one EV (or HP) in the distribution network and it is available for energy planning in two periods. It is also assumed that the energy requirement cannot be fulfilled by consuming power in only one period due to the network constraints. For such a case, the DSO optimization is,

$$\min_p \; c_1 p_1 + c_2 p_2 , \tag{2.12}$$

subject to,

$$D p_1 \le f_1, \; (\lambda_1) , \tag{2.13}$$

$$D p_2 \le f_2, \; (\lambda_2) , \tag{2.14}$$

$$a_1 p_1 + a_2 p_2 \ge b, \;\; (\mu) , \tag{2.15}$$

$$p_1, p_2 \ge 0, \;\; (\varsigma_1, \varsigma_2) , \tag{2.16}$$

where the scalar (or matrix with one element) D is power transfer distribution factor (PTDF), f is the remaining capacity for the flexible demands, λ is Lagrange multiplier. The decision variables p_1 and p_2 represent the energy consumption at the two periods respectively. Constraints (2.13) and (2.14) are network constraints for the two periods, constraint (2.15) is the energy requirement (derived from (2.4) and (2.10), parameter b is the summation of all constants of (2.4) and (2.10); the upper limit is ignored for simplicity), and constraint (2.16) is to set the lower limit

[2] Note that there is a relationship to Danzig-Wolfe decomposition, in which the master problem states prices, and the subproblem returns quantities. To avoid the problem occurring here, the master problem considers schedules that have been proposed and chooses a convex combination. However, a DW approach to this market wouldn't work because there's not a market-based way for aggregators and the DSO to iterate to generate multiple candidate schedules.

of the consuming power (p_1, p_2) (the upper limit is ignored for simplicity). Coefficients a_1 and a_2 are positive ($a_1 = a_2 = 1$ when it is EV).

According to the KKT conditions, the DTs are calculated by (note that $\varsigma_1, \varsigma_2 = 0$ and $p_1, p_2 > 0$, because the energy requirement cannot be fulfilled by any one of them),

$$\begin{aligned} c_1 + D^T \lambda_1 &= \mu a_1 \\ c_2 + D^T \lambda_2 &= \mu a_2 \end{aligned}, \tag{2.17}$$

where the terms $D^T \lambda_1$ and $D^T \lambda_2$ are the DTs and should be sent to the aggregator.

The aggregator optimization (no network constraints) is,

$$\min_p \ (c_1 + \lambda_1^T D) p_1 + (c_2 + \lambda_2^T D) p_2, \tag{2.18}$$

subject to,

(2.15) and (2.16).

It can be seen that such a linear programming has an infinite number of optimal solutions due to the proportional coefficients. The aggregator optimization and the DSO optimization do not converge. For instance, the optimal energy plan of the aggregator optimization, where $p_1 = 0$, is infeasible for the DSO optimization because the energy requirement cannot be fulfilled by any one of p_1, p_2 , as stated in the assumption.

When there are many flexible demands in a distribution network, the above analysis is still valid, as there is at least one flexible demand behaving like the one in the above example. As such, the decentralized congestion management formulated through linear programming fails.

2.3.3 QP Formulation and the Proof of Convergence

2.3.3.1 DSO Optimization through QP

In this chapter, it is assumed that the aggregators are willing to share the flexible demand information (energy requirement, availability, etc.) with the DSO; therefore, the DSO can have detailed information for modelling the optimal EV and HP planning. However, this assumption is relaxed in chapter 4 (see section 4.2.1). The DSO optimization in the second step of the procedures in Section 2.3.1 is,

$$\min_{p_{i,t},\hat{p}_{i,t}} \sum_{\forall i\in\mathcal{B},t\in\mathcal{T}} \frac{1}{2} {p_{i,t}}^T B_{i,t} p_{i,t} + (c_t 1)^T p_{i,t} + \frac{1}{2} {\hat{p}_{i,t}}^T B_{i,t} \hat{p}_{i,t} + (c_t 1)^T \hat{p}_{i,t}, \tag{2.19}$$

subject to,

$$\sum_{i\in\mathcal{B}} DE_i(p_{i,t} + \hat{p}_{i,t}) \le f_t, \forall t \in \mathcal{T}, \ (\lambda_t), \tag{2.20}$$

and (2.4), (2.5), (2.10) and (2.11).

Matrix E is a mapping from the customers to the load busses. The conventional household demands are assumed to be inflexible. Therefore, they are not included in the objective function (2.19), but reflected in the line loading limits f_t, which are the total line capacities F_t excluding the loadings induced by the conventional demands.

The DTs, equal to $D^T\lambda_t$, will be published by the DSO before the day-ahead market clears. Parameters c_t and β_t (B) used by the DSO are shared with the aggregators since the aggregators need them in their optimization problems.

2.3.3.2 Aggregator Optimization through QP

Aggregator i first forms the prices for each of his customers, i.e. $c_t\mathbf{1} + {E_i}^T D^T \lambda$. Then, the optimal energy plan of aggregator *i* can be formulated as,

$$\min_{p_{i,t},\hat{p}_{i,t}} \sum_{t\in\mathcal{T}} \frac{1}{2} {p_{i,t}}^T B_{i,t} p_{i,t} + (c_t \mathbf{1} + {E_i}^T D^T \lambda_t)^T p_{i,t} + \frac{1}{2} {\hat{p}_{i,t}}^T B_{i,t} \hat{p}_{i,t} + (c_t \mathbf{1} + {E_i}^T D^T \lambda_t)^T \hat{p}_{i,t}, \tag{2.21}$$

subject to,

$$e_i^{\min} \le \sum_{t\_\le t} (p_{i,t\_} - d_{i,t\_}) + e_{i0} \le e_i^{\max}, \forall t \in \mathcal{T}, (\mu_{i,t}^-, \mu_{i,t}^+), \tag{2.22}$$

$$p_{i,t}^{\min} \le p_{i,t} \le p_{i,t}^{\max} \quad \forall t \in \mathcal{T}, (\varsigma_{i,t}^-, \varsigma_{i,t}^+), \tag{2.23}$$

$$K_{i,t}^{a,\min} \le \sum_{t\_\le t} A_{i,t,t\_} \hat{p}_{i,t\_} + u_{i,t} \le K_{i,t}^{a,\max}, \forall t \in \mathcal{T}, (\hat{\mu}_{i,t}^-, \hat{\mu}_{i,t}^+), \tag{2.24}$$

$$\hat{p}_{i,t}^{\min} \le \hat{p}_{i,t} \le \hat{p}_{i,t}^{\max} \quad , \forall t \in \mathcal{T}, (\hat{\varsigma}_{i,t}^-, \hat{\varsigma}_{i,t}^+). \tag{2.25}$$

As discussed in section 4.2.2, price sensitive coefficients ($B_{i,t}$) can be the one from the DSO, who publishes this information together with DTs. The rationale behind the aggregators using this coefficient matrix is that the individual planning of flexible demands will affect the final energy price of the day-ahead market. Although it should be an aggregated effect, the individual owner or the aggregator can only rely on its own consumption data (quantity of each hour) and a predicted coefficient that describes the relation of the individual consumption and the final price. This is a sort of multiplayer game. Everyone wishes to consume energy at low price hour and hope others not to do the same, otherwise the final price can be much higher than expected. Under this circumstance, the sensitive coefficient matrix can give the aggregators an indication of how their own consumption will affect the final price, though not very accurate. An accurate coefficient matrix is almost impossible to obtain; therefore, the DSO should use some judgement in addition to prediction and estimation. Whether this strategy (using sensitive coefficient matrix) can lead to an equilibrium of the multiplayer game is not investigated.

2.3.3.3 Proof of the Convergence of the DSO Optimization and the Aggregator Optimization through QP

The KKT conditions of the DSO optimization are,

$$B_{i,t}p_{i,t}+c_t\mathbf{1}+E_i^{\,T}D^T\lambda_t+\sum_{t\_\le t}(\mu_{i,t\_}^{+}-\mu_{i,t\_}^{-})+(\varsigma_{i,t}^{+}-\varsigma_{i,t}^{-}) \\ =0,\forall i\in\mathcal{B},t\in\mathcal{T} \quad , \tag{2.26}$$

$$B_{i,t}\hat{p}_{i,t}+c_t\mathbf{1}+E_i^{\,T}D^T\lambda_t+\sum_{t\_\le t}(\hat{\mu}_{i,t\_}^{+}-\hat{\mu}_{i,t\_}^{-})+(\hat{\varsigma}_{i,t}^{+}-\hat{\varsigma}_{i,t}^{-}) \\ =0,\forall i\in\mathcal{B},t\in\mathcal{T} \quad , \tag{2.27}$$

$$(\sum_{i\in\mathcal{B},}DE_i p_{i,t}-f_t)\cdot\lambda_t=0,\ \ t\in\mathcal{T}\ , \tag{2.28}$$

$$(\sum_{t\_\le t}(p_{i,t\_}-d_{i,t\_})+e_{i,0}-e_i^{\max})\cdot\mu_{i,t}^{+}=0,\forall t\in\mathcal{T},i\in\mathcal{B}, \tag{2.29}$$

$$(\sum_{t\_\le t}(p_{i,t\_}-d_{i,t\_})+e_{i,0}-e_i^{\min})\cdot\mu_{i,t}^{-}=0,\forall t\in\mathcal{T},i\in\mathcal{B}, \tag{2.30}$$

$$(p_{i,t}-p_{i,t}^{\max})\cdot\varsigma_{i,t}^{+}=0,\forall t\in\mathcal{T},i\in\mathcal{B}, \tag{2.31}$$

$$(p_{i,t}-p_{i,t}^{\min})\cdot\varsigma_{i,t}^{-}=0\ ,\ \forall t\in\mathcal{T},i\in\mathcal{B}, \tag{2.32}$$

$$(\sum_{t\_\le t}A_{i,t,t\_}\hat{p}_{i,t\_}+u_{i,t}-K_{i,t}^{a,\max})\cdot\hat{\mu}_{i,t}^{+}=0,\forall t\in\mathcal{T},i\in\mathcal{B}, \tag{2.33}$$

$$(\sum_{t\_\le t}A_{i,t,t\_}\hat{p}_{i,t\_}+u_{i,t}-K_{i,t}^{a,\min})\cdot\hat{\mu}_{i,t}^{-}=0,\forall t\in\mathcal{T},i\in\mathcal{B}, \tag{2.34}$$

$$(\hat{p}_{i,t}-\hat{p}_{i,t}^{\max})\cdot\hat{\varsigma}_{i,t}^{+}=0,\forall t\in\mathcal{T},i\in\mathcal{B}, \tag{2.35}$$

$$(\hat{p}_{i,t}-\hat{p}_{i,t}^{\min})\cdot\hat{\varsigma}_{i,t}^{-}=0,\forall t\in\mathcal{T},i\in\mathcal{B}, \tag{2.36}$$

$$\lambda_t\ge 0,\forall\, t\in\mathcal{T}\ , \tag{2.37}$$

$$\mu_{i,t}^{+},\mu_{i,t}^{-},\varsigma_{i,t}^{+},\varsigma_{i,t}^{-},\hat{\mu}_{i,t}^{+},\hat{\mu}_{i,t}^{-},\hat{\varsigma}_{i,t}^{+},\hat{\varsigma}_{i,t}^{-}\ge 0,\forall \mathrm{t}\in\mathcal{T},i\in\mathcal{B}, \tag{2.38}$$

together with the constraints (2.4), (2.5), (2.10), (2.11) and (2.20).

Similarly, the KKT conditions of the aggregator i optimization are,

$$\begin{aligned} B_i p_{i,t} + c_t \mathbf{1} + E_i^T D^T \lambda_t + \sum_{t\_\le t} (\mu_{i,t\_}^+ - \mu_{i,t\_}^-) + (\varsigma_{i,t}^+ - \varsigma_{i,t}^-) \\ = 0, \forall t \in \mathcal{T} \end{aligned}, \tag{2.39}$$

$$\begin{aligned} B_i \hat{p}_{i,t} + c_t \mathbf{1} + E_i^T D^T \lambda_t + \sum_{t\_\le t} (\hat{\mu}_{i,t\_}^+ - \hat{\mu}_{i,t\_}^-) + (\hat{\varsigma}_{i,t}^+ - \hat{\varsigma}_{i,t}^-) \\ = 0, \forall t \in \mathcal{T} \end{aligned}, \tag{2.40}$$

$$(\sum_{t\_\le t} (p_{i,t\_} - d_{i,t\_}) + e_{i,0} - e_i^{\max}) \cdot \mu_{i,t}^+ = 0, \forall t \in \mathcal{T}, \tag{2.41}$$

$$(\sum_{t\_\le t} (p_{i,t\_} - d_{i,t\_}) + e_{i,0} - e_i^{\min}) \cdot \mu_{i,t}^- = 0, \forall t \in \mathcal{T}, \tag{2.42}$$

$$(p_{i,t} - p_{i,t}^{\max}) \cdot \varsigma_{i,t}^+ = 0, \forall t \in \mathcal{T}, \tag{2.43}$$

$$(p_{i,t} - p_{i,t}^{\min}) \cdot \varsigma_{i,t}^- = 0, \forall t \in \mathcal{T}, \tag{2.44}$$

$$(\sum_{t\_\le t} A_{i,t,t\_} \hat{p}_{i,t\_} + u_{i,t} - K_{i,t}^{a,\max}) \cdot \hat{\mu}_{i,t}^+ = 0, \forall t \in \mathcal{T}, \tag{2.45}$$

$$(\sum_{t\_\le t} A_{i,t,t\_} \hat{p}_{i,t\_} + u_{i,t} - K_{i,t}^{a,\min}) \cdot \hat{\mu}_{i,t}^- = 0, \forall t \in \mathcal{T}, \tag{2.46}$$

$$(\hat{p}_{i,t} - \hat{p}_{i,t}^{\max}) \cdot \hat{\varsigma}_{i,t}^+ = 0, \forall t \in \mathcal{T}, \tag{2.47}$$

$$(\hat{p}_{i,t} - \hat{p}_{i,t}^{\min}) \cdot \hat{\varsigma}_{i,t}^- = 0, \forall t \in \mathcal{T}, \tag{2.48}$$

together with (2.22)-(2.25) and (2.38).

It can be seen that the objective function (2.19) of the DSO problem is a quadratic function with all quadratic terms being positive and no cross terms. Therefore, the Hessian matrix can be found by observation. Particularly, it is a diagonal matrix with the elements being the coefficients of the quadratic terms in (2.19), which are

all positive. A diagonal matrix with all elements being positive is a positive definite matrix; therefore, the Hessian matrix of (2.19) is positive definite.

Since the objective function (2.19) is a quadratic function with positive definite Hessian matrix and all the constraints, i.e. (2.4), (2.5), (2.10), (2.11) and (2.20) are affine functions, the DSO optimization problem is a strict convex QP problem, which has a unique minimizer [29] assuming the problem is feasible. Moreover, the KKT conditions of the DSO optimization problem are necessary and sufficient [29].

Similarly, it can be inferred from (2.21)-(2.25) that each aggregator optimization problem is also a strict convex QP problem. Therefore, each of them has a unique minimizer and the KKT conditions are necessary and sufficient.

Now, suppose

$$(p_{i,t}^{*},\hat{p}_{i,t}^{*},\lambda_t^{*},\mu_{i,t}^{+*},\mu_{i,t}^{-*},\varsigma_{i,t}^{+*},\varsigma_{i,t}^{-*},\hat{\mu}_{i,t}^{+*},\hat{\mu}_{i,t}^{-*},\hat{\varsigma}_{i,t}^{+*},\hat{\varsigma}_{i,t}^{-*})$$

is a solution of the KKT conditions of the DSO problem ((2.4), (2.5), (2.10), (2.11), (2.20) and (2.26)-(2.38)), implying that $(p_{i,t}^{*},\hat{p}_{i,t}^{*})$ is an optimal solution of the DSO problem. By comparing the KKT conditions, it can be seen that, with respect to aggregator i,

$$(p_{i,t}^{*},\hat{p}_{i,t}^{*},\mu_{i,t}^{+*},\mu_{i,t}^{-*},\varsigma_{i,t}^{+*},\varsigma_{i,t}^{-*},\hat{\mu}_{i,t}^{+*},\hat{\mu}_{i,t}^{-*},\hat{\varsigma}_{i,t}^{+*},\hat{\varsigma}_{i,t}^{-*})$$

is also satisfying (2.22)-(2.25) and (2.38)-(2.48), i.e. the KKT conditions of the aggregator problem. This means $(p_{i,t}^{*},\hat{p}_{i,t}^{*})$ is also an optimal solution of the aggregator problem. Because any solution of the DSO problem must satisfy the KKT conditions of it, it can be concluded that any solution of the DSO problem is also a solution to the aggregator problem.

On the other hand, a solution that satisfies the KKT conditions of the aggregator problems does not necessarily satisfy the KKT conditions of the DSO problem, because the switching condition (2.28) of the DSO problem is not respected by the aggregator problems. However, due to the uniqueness of the solution to the DSO problem and the aggregator problems, any solution of the aggregator problems must also be a solution of the DSO problem. This can be proven by contradiction.

Suppose $(p_{i,t}^{**}, \hat{p}_{i,t}^{**})$ is a solution of the aggregator problems but not to the DSO problem. Suppose $(p_{i,t}^{*}, \hat{p}_{i,t}^{*})$ is a solution to the DSO problem. Then, according to the previous conclusion, $(p_{i,t}^{*}, \hat{p}_{i,t}^{*})$ is also a solution to the aggregator problems. Due to the uniqueness of the aggregator problems, there is $(p_{i,t}^{*}, \hat{p}_{i,t}^{*}) = (p_{i,t}^{**}, \hat{p}_{i,t}^{**})$ and it contradicts to the assumption that $(p_{i,t}^{**}, \hat{p}_{i,t}^{**})$ is not a solution to the DSO problem. Therefore, it can be concluded that any solution to the aggregator problems is also a solution to the DSO problem. Based on the above conclusions, the DSO problem and the aggregator problems do converge.

2.4 Discussion of the DT Method

2.4.1 Regulation Concerns regarding DT

The concern regarding the regulation issues of the DT concept can be explained as follows.

One issue is the non-discrimination requirement by distribution grid code in many European countries [30]. This means that the customers can't have different prices just because of their location. In other words, the customers may receive different prices due to their demand sizes, power band requirement etc., but not due to their location. The DT collected by the DSO from the aggregators is similar to the congestion revenue collected by the independent system operator (ISO) in transmission networks. The concept of the congestion revenue on transmission level is widely accepted in the electricity market with, e.g. nodal price systems [31] or zonal price systems [32]. The congestion revenue will be used to improve the network conditions and reduce the congestion in the future, and thereby benefits the parties who pay this congestion revenue. On the other hand, on distribution level where non-discrimination is required, the aggregators (function as retailors or suppliers) can absorb the discrimination due to DT and socialize the congestion cost among its customers. The aggregators benefit from the flexibility from its customers by optimizing the consumption at the cheapest hours which can be the cause of congestion. Therefore, it is reasonable that the aggregators bear the cost of the congestion due to rearranging the flexible demands. However, there is possibility that the aggregators will tend to contract with customers having low DTs. In chapter 6, a new method called dynamic subsidy will be presented to deal with the non-discrimination requirement. More details about the DS method, including a comparison between the DT and DS method, can be seen from chapter 6.

Another issue is that the total revenue of the DSO is regulated by the regulators [30]. When the DT is considered in addition to the conventional flat tariff structure, the DT should be included in the calculation of the total revenue of the DSO. The DSO uses DT as a tool to handle the potential congestion and cannot pursue maximization of revenue through DT since the total revenue is regulated.

2.4.2 Linear Approximation of Power Flows in Distribution Networks

A distribution network has two distinguishing features, namely unbalanced three-phase loads and a high R/X ratio of the lines, compared to a transmission network. The DT concept is developed for congestion management of medium voltage (MV) distribution networks. In most cases, MV distribution networks are balanced networks. All the loads and the flexible demands are aggregated and considered as a lump load connected to the low voltage (LV) transformers. The LV transformers are considered as load points in the load flow analysis. In future work, the application of the DT method for congestion management of unbalanced distribution networks will be studied.

The high R/X ratio affects the accuracy of the DC OPF model for the DT or DS method, compared to the AC OPF model. Due to the nonlinear and nonconvex feature of the AC OPF model, it is very difficult to find a global optimum. Employing the DC OPF to approximate the AC OPF is a good option; however, the accuracy must be improved before it can be used for distribution networks. It is reported that the total line losses are marginal for many developed countries [33], e.g. China 6%, Denmark 6%, France 7% and the USA 6%. The active power losses in distribution networks will be even smaller. Because the R/X ratio is higher than one, the reactive power losses in distribution networks will be very small as well. Therefore, the main factor that affects the accuracy of the DC OPF is the neglected reactive power consumptions of the loads and the low voltage transformers. For instance, the active power will be 10% less than the apparent power transferred through the lines if the average power factor of the loads and the low voltage transformers is 0.9. One way to handle this issue is that the DSO can set the line loading limits a bit lower than the actual limits, e.g. 10% lower depending on the estimated power factor, to have a safety margin. The other way is to improve the power factor by installing reactive power compensators or having reactive power support from EVs or smart transformers [34].

In addition, the voltage issues are also important aspects of the congestion problems, especially for long distance distribution feeders. Therefore, they should be considered as well. The authors of [35] have proposed a linear approximation method to

calculate the voltages based on the power consumptions at each load point. These linear equations can be combined with the DT model without increasing much of the model complexity and computation time.

2.4.3 Stochastic Nature of the Flexible Demands

The model for determining DT is deterministic and doesn't take into account the stochastic nature of flexible demands. For instance, EVs are modelled by their expected energy demands and the expected arriving and leaving times. The deterministic model has the following advantages: It is easier to understand the concept of the DT method with a simple and clear model; The DSO can have a quick overview of where and how heavy the congestion is in the network based on the average model of the flexible demands; The DSO can choose to use the worst scenario of the flexible demands for the DT method and has a sufficient safety margin in the distribution network.

On the other hand, the DSO may want to manage the uncertainties of the congestion due to the stochastic flexible demands, in addition to the abovementioned average model case and the worst scenario case. It should be pointed out that, in the business model of the DT method for congestion management, the focus is given to DSO side. The DSO determines the DT through an optimal energy planning based on predicted data of the flexible demands and the conventional demands. How the aggregator will interact with its customers in the real-time operations/controls depends on the contract type made between the aggregator and its customers, and it is not a focus of the DT method. However, it is assumed that the aggregators are rational and use optimization methods to make energy planning and control for its customers.

In chapter 4, it will be shown that DTs can be determined using a deterministic method, such that the possibility of congestion is less than a predefined level based on the statistical feature of the predicted data for flexible demands. Since only MV networks are considered and it is assumed that there are many flexible demands connected to a load point (LV transformer), there is enough diversity (randomness) of the stochastic flexible demands at each load point. This feature helps the statistical analysis of the flexible demands at each load point. More aspects about the uncertainty analysis of the DT method will be discussed in chapter 4.

2.5 Case Studies

Case studies were conducted using the Danish driving pattern and the Bus 4 distribution system of the Roy Billinton Test System (RBTS) [36]. In line with the day-ahead market (an introduction can be seen from section B.1), 24 hours of the next day are considered in the hourly based energy planning in the case studies.

2.5.1 Grid Data

The single line diagram of the Bus 4 distribution network is shown in Fig. 2-3. Line segments of the feeder one are labeled in Fig. 2-3, among which L2, L4, L6, L8, L9, L11, and L12 refer to the transformers connecting the corresponding load points (LP1 to LP7). The study is focused on this feeder because it has the most diversity among all the feeders: 5 residential load points with different peak conventional demands and two commercial load points. The detailed data of these load points are listed in Appendix A. The peak conventional demands of residential customers are assumed to occur at 18:00 when people come home and start cooking (shown in Fig. 2-4).

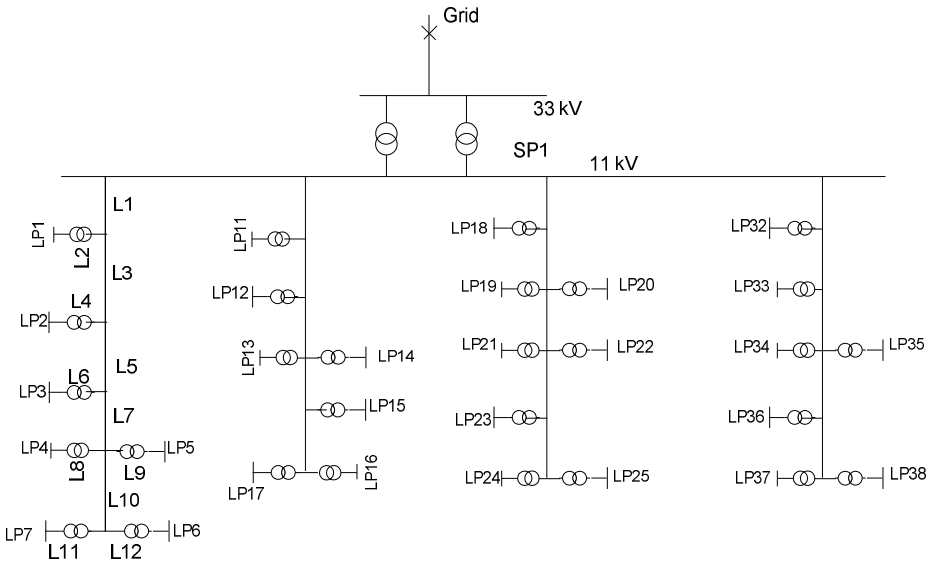

Fig. 2-3. Single line diagram of the distribution network

The key parameters of EVs and HPs, and the EV availability can be seen from Appendix A. There are a large number (200) of households at each residential load point and each household has one EV and one HP. The stochastic feature of the

EVs can be approximated by taking samples from the population. In this study, the Danish National Transport Survey data are used as the population, which have 134,756 survey results [37]. Parameters of HP depend on the household area, which is a random number chosen between 100 and 200 m^2 (see Appendix A for the calculation of the parameters from the household area). The predicted day-ahead system prices are shown in Fig. 2-5 as the 'base price'. The solar radiation impacts can be deemed as negative loads, which are inflexible and are neglected for brevity in this study.

2.5.2 Case Study Results

In the case study, it is assumed that there are two aggregators. The aggregator 'aag1' has contracts with 40 customers per load point while the other has contracts with the rest 160 customers per load point. The line loading limits of all line segments are listed in Table 2-1, which are higher than the peak conventional demands but lower than the peak demands including EVs and HPs.

The simulation was carried out using the General Algebraic Modeling System (GAMS) optimization software [38] although many other tools can be used such as QUADPROG in MATLAB, Gurobi and AMPL. Firstly, the DSO optimization problem was carried out and the results are shown in Fig. 2-4. Because the line loading limits are respected in the optimization, the line loadings of all line segments are lower than the limits.

TABLE 2-1. LINE LOADING LIMIT

line	L2	L3	L4	L8	L9
limit (kW)	1400	7000	1700	1600	1500

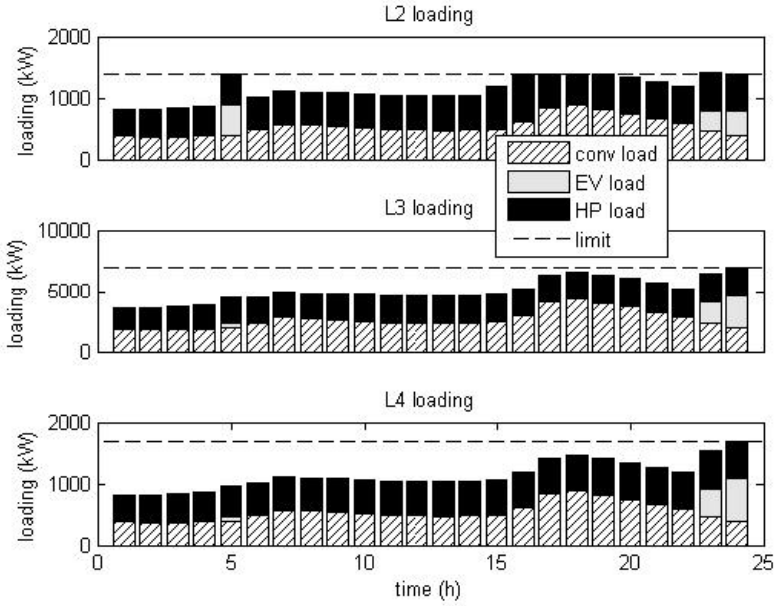

Fig. 2-4. Line loading of the DSO problem

It can be seen from Fig. 2-4 that the line loadings reach (but not exceed) the limits at hour 16-18 (only line L2) and hour 23-24. This means that the corresponding inequality constraints of the optimization problem are 'active' and the Lagrange multipliers of these constraints are positive. Therefore, according to the DT calculation method described in 2.2.3, the locational prices are higher than the base price (shown in Fig. 2-5 and Table 2-2). The prices of LP1 at hour 17-18 are very high and are chopped in Fig. 2-5 (they can be found in Table 2-2) in order to have a better illustration of locational price of other hours. The high prices of LP1 at hour 17-18 can be explained by analyzing the nature of the congestion caused by HPs. HPs are less sensitive to the prices compared to EVs because of the significant thermal leakages of the households; therefore, higher DTs are required to solve the congestion caused by them.

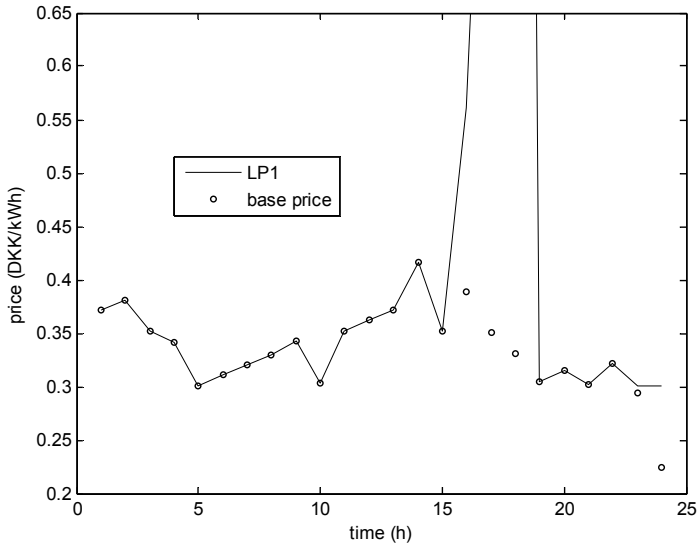

Fig. 2-5. System prices and locational prices at LP1

Secondly, the aggregator optimization was performed. Two aggregators carried out their own optimization problem independently.

In order to clearly show the effect of the DT, two case studies were conducted. In Case One, the DT was not applied; in Case Two, the DT was applied.

As expected, when the DT is not applied, congestion occur at 24:00 and 18:00 (shown in Fig. 2-6). At 24:00, because the system price is the lowest, every EV wants to charge its battery as long as it is available for charging. The simultaneous charging leads to the very high peak. Overloading of line L2 at 18:00, however, is not due to the low price. In fact, it is the peak conventional demand that has consumed most of the capacity of the line and the available capacity is not enough for the HP demands.

TABLE 2-2. LOCATIONAL PRICES, DKK/KWH, DUE TO MULTIPLE CONGESTION ON L2, L3, L4, L8 AND L9 ('-' MEANS EQUAL TO BASE PRICE)

time	5	16	17	18	23	24
base price	0.3012	0.3884	0.3513	0.3313	0.2941	0.2241
LP1	-	0.5611	1.1006	2.4335	0.3012	0.3012
LP2	-	-	-	-	-	0.2940
LP3	-	-	-	-	-	0.2937
LP4	-	-	-	-	0.3006	0.3006
LP5	-	-	-	-	0.3008	0.3008

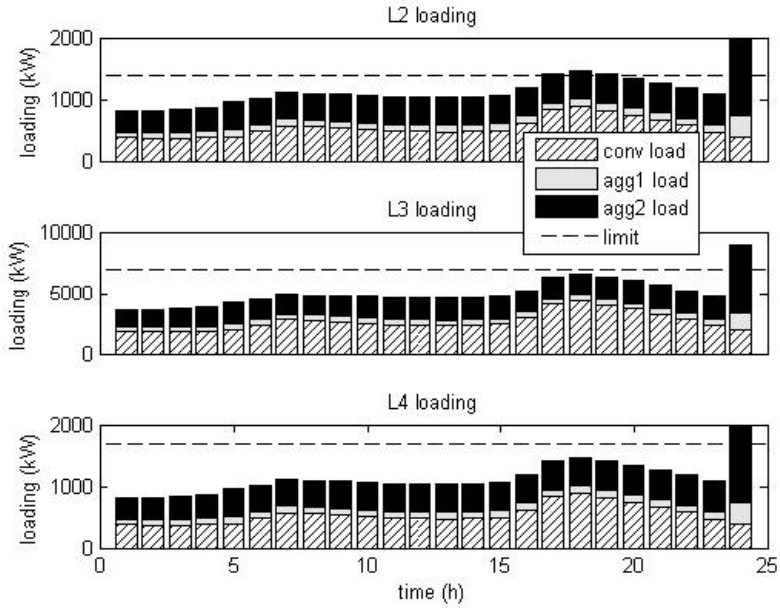

Fig. 2-6. Line loading without DT

When the DT is applied, the congestion is alleviated (shown in Fig. 2-7). Due to the posed DTs, the locational price at load point LP1 at 24:00 is as attractive as the ones at 23:00 and 5:00. Therefore, the EV charging demands are spread at those hours and the resulted peak is not higher than the limits. The previous congestion

of line L2 at 18:00 also disappears due to the DT. The DT at LP1 at 18:00 is so high that the HPs choose to produce more heat before 18:00 and due to the dynamics of the thermal objects (house inside air, house structure), the temperature at 18:00 is maintained between the lower and upper limits. Hence, the HP demands are shifted to the previous hours when the conventional demands are low enough to accommodate them.

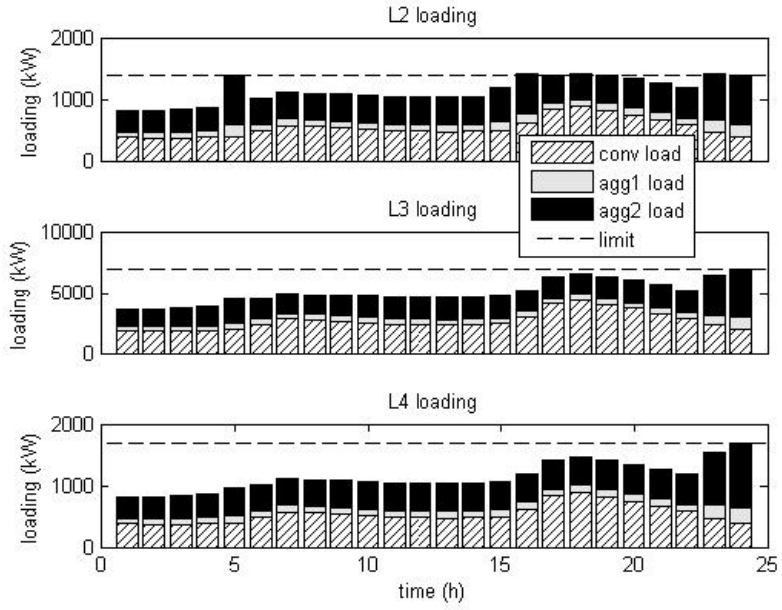

Fig. 2-7. Line loading with DT

In order to illustrate the non-convergence issue that might occur with the linear programming formulation, a simulation was conducted where the price sensitive part was excluded. Without the price-sensitive part, the DSO optimization problem and the aggregator optimization problems are linear programming problems. The locational prices were calculated and shown in Table 2-3. It can be seen that the locational prices of LP1 are the same at time 5, 23 and 24 hour. This will lead to infinite number of solutions of the aggregator problems. As a result, the aggregator may not act as the DSO expects. This is confirmed by the simulation results shown in Fig. 2-8 and Fig. 2-9. In Fig. 2-8, for the DSO optimization, there is no congestion, however, in Fig. 2-9, for the aggregator optimization, congestion occur at line L2; loading of line L3 at 5 hour is different.

TABLE 2-3. LOCATIONAL PRICES, DKK/KWH, WITH MULTIPLE CONGESTION AT L2, L3, L4, L8 AND L9, CALC. WITHOUT QUADRATIC TERMS ('-': EQ. TO BASE PRICE)

time	5	16	17	18	23	24
base price	0.3012	0.3884	0.3513	0.3313	0.2941	0.2241
LP1	-	0.5605	1.0984	2.4267	0.3012	0.3012
LP2	-	-	-	-	-	0.2941
LP3	-	-	-	-	-	0.2941
LP4	-	-	-	-	0.3012	0.3012
LP5	-	-	-	-	0.3012	0.3012

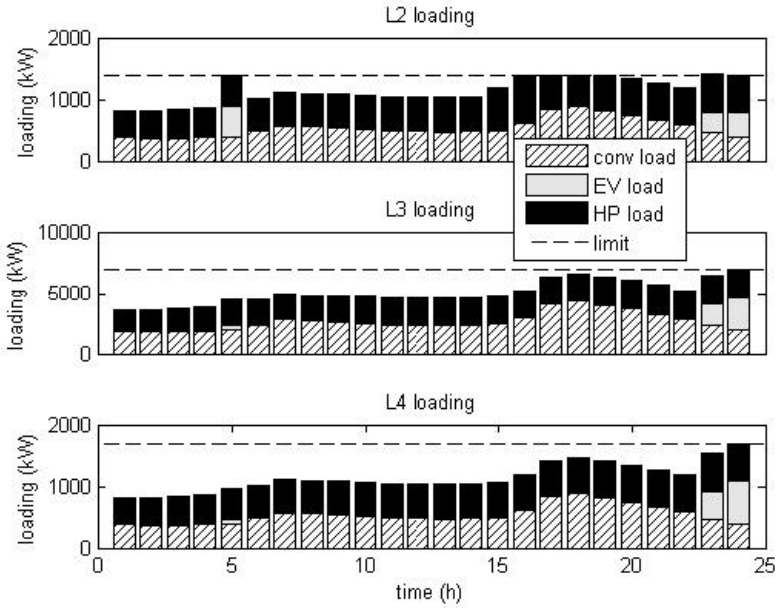

Fig. 2-8. Line loading of the DSO problem excluding quadratic terms

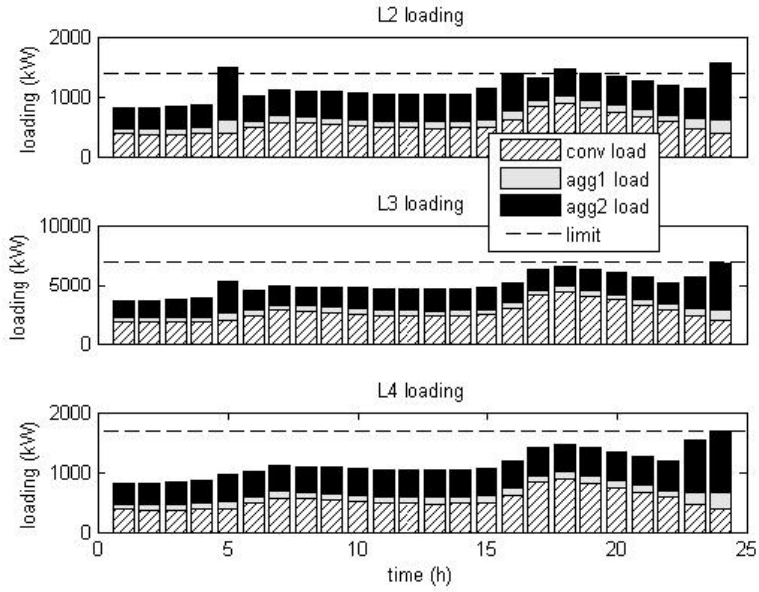

Fig. 2-9. Line loading of the aggregator problems excluding quadratic terms

2.6 Summary

Though the DT concept is efficient in alleviating congestion in distribution networks with high penetration of flexible demands, the formulation of the decentralized aggregator optimization must be carefully handled. With the linear programming formulation of the aggregator optimization, there might be multiple solutions of the decentralized aggregator optimization. The multiple solutions of the aggregator optimization may cause the centralized DSO optimization and the decentralized aggregator optimization not to converge, and the decentralized congestion management to fail.

The multiple solution issue of the aggregator optimization is addressed in this chapter by introducing price sensitivity which leads to strict convex QP formulation for both the DSO optimization and the aggregator optimization. The convergence of the centralized DSO optimization and the decentralized aggregator optimization with the QP formulation is proven which ensures that the aggregators act as the DSO expects. The case study results have demonstrated the convergence of the DSO optimization and the aggregator optimization with the strict convex QP formulation, and the efficacy of the DT through QP for congestion management.

CHAPTER 3.

OPTIMAL RECONFIGURATION BASED DT[3]

This chapter is to investigate the possibilities of combining the DT method with direct control methods, such as feeder reconfiguration, for a more efficient congestion management on distribution networks. The other direct control methods, e.g. control of online tap changer of the transformers and the reactive power compensators, can also be combined with the DT method in a similar manner; however, they will not be covered in this thesis.

3.1 Introduction

Feeder reconfiguration (FR) has been used for reducing resistive line losses in distribution networks for a long time [39]. The DSOs, who have the responsibility of operating the distribution network in an optimal way, will search the best operation topology of the distribution network that can minimize the line losses. Many methods have been developed for searching the optimal operation topology in the last few decades, including exact optimization methods [40]–[42], heuristic methods [39], [43] and their combinations.

Meanwhile, the congestion problems due to the physical limits of the distribution network, caused by increasing penetration of DERs, such as EVs and HPs, have become a major concern of the DSOs. Different methods have been proposed in recent years for congestion management within distribution networks. DT is one of such methods that can solve the congestion within distribution networks in a decentralized manner. In the DT framework for congestion management, the DSO will first acquire the energy requirement information of the flexible demands in the distribution network; then the DSO will calculate the DT through an optimal energy

[3] This chapter is based on paper: S. Huang, Q. Wu, C. Lin and Z. Liu, "Optimal reconfiguration-based dynamic tariff for congestion management and line loss reduction in distribution networks", IEEE Tr. Smart Grid, vol: 7, issue: 3, pages: 1295-1303, May 2016.

planning taking into account the network constraints; in the end, the DT will be sent to the aggregators, who make the optimal energy planning of flexible demands on behalf of the owners and submit the bids to the spot market. It is proven in chapter 2 that the energy planning at the aggregator side without the knowledge of the network constraints converges to the energy planning at the DSO side because the DT, as a price control signal linking both sides, contains the network congestion information.

However, the combination of the FR and the DT framework for congestion management and line loss reduction has not been studied yet. Given the DT framework, the FR can be used ex post, i.e. handle the potential congestion that have not been solved by the DT method. A superior way of integrating the FR into the DT framework is to take into account the FR during the process of calculating DT. The advantages of combining the FR and the DT framework include: combined optimization of the flexible demands and the network topology can achieve the best solution for congestion management in distribution networks with minimized energy cost; DT can be reduced if the congestion is alleviated by the FR during the calculation of DT; line losses can be reduced on top of the congestion management. Motivated by this idea, the optimal reconfiguration based DT is proposed in this chapter for congestion management and line loss reduction within distribution networks.

The chapter will first describe the optimal reconfiguration based DT for congestion management within distribution networks. Next, the optimal reconfiguration based DT is extended to take into account line loss reduction. At last, case studies are presented and discussed.

3.2 Optimal Reconfiguration Based DT for Congestion Management

3.2.1 Distribution Network Reconfiguration Modeling

According to the DT calculation method presented in chapter 2, the exact optimization method is required in order to determine the DTs. The exact optimization method can ensure the consistency among the aggregators who have freedom of choosing different optimization tools in the decentralized congestion management framework. Hence, it is very desirable that the additional network reconfiguration constraints can be modelled algebraically through a group of equations and/or inequalities. It will be better to prevent the nonlinearity of constraints considering the complexity of integer programming caused by multiple planning periods (e.g. for 24 planning periods/hours, the total possible combinations are the number of combinations of the switch status to the power of 24).

Medium voltage (MV) distribution networks usually have a meshed structure, but operate radially in most cases for safety reasons. The radial condition of the network is equivalent to a tree graph in the graph theory. A spanning tree is defined as a tree that consists of all the vertexes of a graph. There are a number of equivalent conditions that can assure a spanning tree in a given connected graph with n vertexes. For instance, any of the following conditions is an equivalent condition [44]:

- It has $n-1$ edges and it is connected;
- It has $n-1$ edges and it has no loop;
- There is only one path from one vertex to another.

Based on the above equivalent conditions of a spanning tree, a number of modelling methods for network reconfiguration have been developed in [40]–[42], [45]. Among them, the method in [45] is the most efficient one in terms of reduced number of constraints, and is employed in this chapter.

Considering the fact that not every line segment (or branch) is equipped with sectionalizing switches, the electric distribution network can be abstracted to a connected graph, where several electric nodes are deemed as one graphic node. This is beneficial in terms of reducing the number of variables in the optimization problem. The process is illustrated in Fig. 3-1, where (a) is a portion of the original electric network, (b) is the equivalent graph of the portion and (c) is the final graph. The positive direction of the active power is defined in the graph such that the sign of the power flow solution (P or K) is meaningful, i.e. a positive sign means that the power is transported along the direction while a negative sign means that it is done backwards.

The network reconfiguration constraints (radial condition) can be formulated as the follows [45] with consideration of multiple planning periods.

$$\sum_{(jk)\in\mathcal{E}^s} x_{jk,t} = n_v - 1, \forall t \in \mathcal{T} \tag{3.1}$$

$$CK_t = \mathbf{1}, \forall\, t \in \mathcal{T} \tag{3.2}$$

$$\left|\{K_t\}_{jk}\right| \le M x_{jk,t}, \forall (jk) \in \mathcal{E}^s, t \in \mathcal{T} \tag{3.3}$$

$$x_{jk,t} \in \{0,1\}, \forall (jk) \in \mathcal{E}^s, t \in \mathcal{T} \tag{3.4}$$

In the above equations, $\mathcal{E}^s$ is the set of lines with sectional switches, $\mathcal{T}$ is the set of planning periods, decision variable $x_{jk,t}$ represents the status of the switch (jk) at planning period t, n_v is the number of the total vertexes/ graphic nodes, vector K_t represents fictitious active power flows, C is the reduced incidence matrix of graphic nodes. Parameter M is a sufficiently large number; when x is zero, the corresponding element of K is forced to be zero. Matrix C is obtained in this way: the element is 1 if the positive direction of the edge enters into a node (junction); it is -1 if the positive direction goes out of a node; and it is 0 if the edge is not associated with a node (see Fig. 3-1(c)).

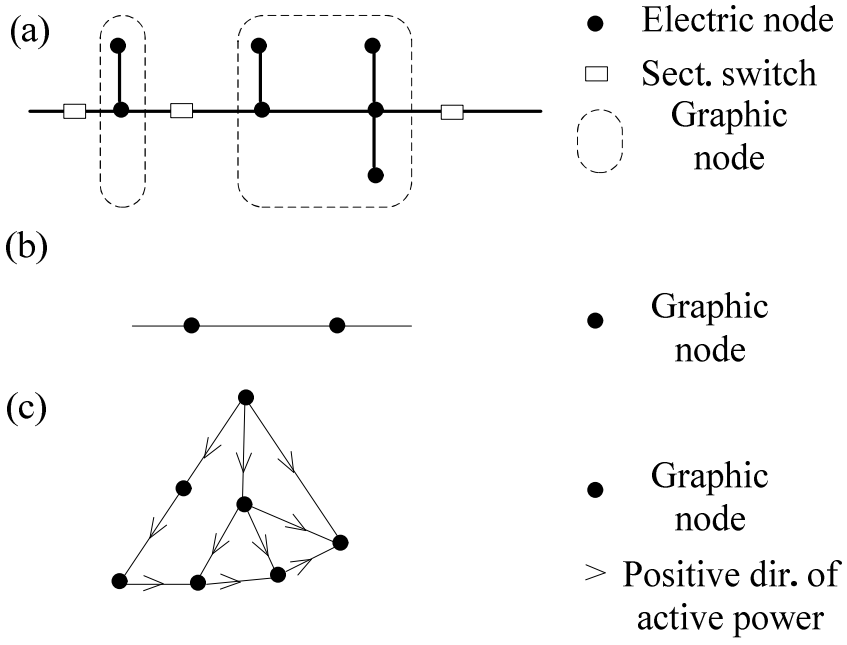

Fig. 3-1. From electric network to an abstract graph (a) a portion of the original electric network (b) the equivalent graph of the portion (c) an example of the final abstract graph

Constraint (3.1) is to assure the total edges of the resulting graph (after reconfiguration) are the total vertexes n_v minus one. This ensures that there are no loops in a fully connected graph. Constraints (3.2)-(3.3) are to force the resulting graph being connected. The connection of the resulting graph is assured by supplying fictitious positive active power (=1) to each node from the substation.

The substation node is not part of the constraints because the active power supplied from the bulk grid is assumed to be unlimited. If there are two or more substation nodes in the distribution network, the model can be slightly modified to cope with those situations.

According to [45], constraints (3.2)-(3.3) can be omitted since they are implied in the 'real' power flow constraints if the active power demand of each node is positive and there is no DG in the network. In this chapter, these constraints are explicitly kept in order to have generality.

3.2.2 DSO Optimal Energy Planning with Reconfiguration

It is obvious that the combined optimization of flexible demand and reconfiguration can achieve better solution than the optimization of flexible demand alone or reconfiguration alone. The key feature of the decentralized congestion management through DT is that the optimal energy planning made at the DSO side can be realized at the aggregator side with their own optimal planning independently. Hence it is an obligation of the DSO that they should make the best solution for their customers with whatever resources they have, which in principle are all paid by the customers.

On the other hand, the cost of the combined optimization is the increased complexity and computation burden. The increased complexity and computation burden can be alleviated by formulating the optimization with a good structure and condition. In this sense, the DC power flow is employed as in [14], [15]. However, the power transfer distribution factor (a matrix describing the coefficient of line power flow with respect to a unit injection at each node) cannot be used because it is no longer a given parameter in the optimal reconfiguration problem. Instead, the reduced incidence matrix is employed to establish a group of load flow equations, all in linear forms.

Thus, the optimal energy planning of EVs, which represent the flexible demands in this chapter, with reconfiguration is formulated below.

$$\min_{p_{i,t},P_t,x_{jk,t}} \quad g(p_{i,t}) \tag{3.5}$$

subject to,

$$BP_t = p_t^c + \sum_{i \in \mathcal{B}} E_i p_{i,t}, \forall t \in \mathcal{T}, (\rho_t) \tag{3.6}$$

$$-F_t \le P_t \le F_t, \forall t \in \mathcal{T}, (\lambda_t^-, \lambda_t^+) \tag{3.7}$$

$$\left| \{P_t\}_{jk} \right| \le M x_{jk,t}, \forall (jk) \in \mathcal{E}^s, \forall t \in \mathcal{T}, (\psi_{jk,t}^-, \psi_{jk,t}^+) \tag{3.8}$$

$$e_i^{\min} \le \sum_{t\_ \le t} (p_{i,t\_} - d_{i,t\_}) + e_{i,0} \le e_i^{\max}, \forall t \in \mathcal{T}, i \in \mathcal{B}, (\mu_{i,t}^-, \mu_{i,t}^+) \tag{3.9}$$

$$p_{i,t}^{\min} \le p_{i,t} \le p_{i,t}^{\max}, \forall i \in \mathcal{B}, t \in \mathcal{T}, (\varsigma_{i,t}^-, \varsigma_{i,t}^+) \tag{3.10}$$

and (3.1)-(3.4).

In the above equations, cost function g depends on the energy planning, vector $p_{i,t}$ is the charging power of EVs, vector P_t is the power flow, B is the reduced incidence matrix regarding electric nodes, E is the matrix mapping individual houses to the node, vector p_t^c represents the total conventional loads on each node, d is the discharging power of EVs, $e_i^{\max}$ / $e_i^{\min}$ are the limits of SOC, $\mathcal{B}$ is the set of aggregators, and F is the line loading limit.

Constraint (3.6) is the DC load flow equation, which in this case corresponds to KCL only (there are no loops when the network is operating). Constraint (3.7) expresses the line loading limit. Constraint (3.8) forces the transferred active power to be zero if the corresponding switch is open. Constraints (3.9)-(3.10) are the EV charging limits.

3.2.3 Optimal Reconfiguration Based DT

It can be seen that (3.1)-(3.10) form a Mixed Integer Quadratic Programming (MIQP), where the quadratic terms are introduced for the same reason discussed in Chapter 2. In general, there are no dual variables (or Lagrange multiplier) for the MIQP as the case that there are only continuous variables [46]. Therefore, it is required to make an assumption to determine the reconfiguration based DT, which shall serve as a control signal and ensure the energy planning at the aggregator side converges with the one at the DSO side. It is assumed that a very small change at the right side of the constraints will not lead to a change of the discrete variables.

Accordingly, the Lagrange multipliers of (3.1)-(3.3) are zero because they can only influence the objective function through discrete variables. The above assumption is consistent with those in market clearing methods of US ISOs (MILP SCUC models), where binary/integer variables are involved.

Suppose an optimal solution $(p_{i,t}^{*}, P_t^{*}, x_{jk,t}^{*})$ is obtained through a commercial optimization tool, e.g. MINLP in MATLAB (R2014a) [47] or the MIQCP solver in GAMS/CPLEX [38] (both tools use cut and/or branch and bound algorithm; a near optimal solution with a small relative gap to the optimal solution, e.g. 1%, is allowed if the convergence becomes too slow due to the large scale of the MIP problem). The Lagrange multiplier of (3.6)-(3.10) can be determined by solving the following linear equations (derived from the KKT optimal conditions by fixing $x_{jk,t}^{*}$ according to the assumption).

$$\frac{\partial g(p_{i,t}^{*})}{\partial p_{i,t}} + E_i^{T}\rho_t - \sum_{t\_\le t}(\mu_{i,t\_}^{+} - \mu_{i,t\_}^{-}) - (\varsigma_{i,t}^{+} - \varsigma_{i,t}^{-}) = 0, \quad \forall i \in \mathcal{B}, t \in \mathcal{T} \tag{3.11}$$

$$\{B^{T}\rho_t + \lambda_t^{+} - \lambda_t^{-}\}_{jk} + \psi_{jk,t}^{+} - \psi_{jk,t}^{-} = 0, \quad \forall (jk) \in \mathcal{E}^{s}, t \in \mathcal{T} \tag{3.12}$$

$$\{B^{T}\rho_t + \lambda_t^{+} - \lambda_t^{-}\}_{jk} = 0, \forall (jk) \in \mathcal{E} \setminus \mathcal{E}^{s}, t \in \mathcal{T} \tag{3.13}$$

Set $\mathcal{E}$is the set of all lines. The element of $\lambda_t^{+}, \lambda_t^{-}, \psi_{jk,t}^{+}, \psi_{jk,t}^{-}, \mu_{i,t}^{+}, \mu_{i,t}^{-}, \varsigma_{i,t}^{+}, \varsigma_{i,t}^{+}$ is zero if the associated inequality (3.7)-(3.10) does not bind. There is a feasible solution to (3.11)-(3.13) since the optimal solution $(p_{i,t}^{*}, P_t^{*}, x_{jk,t}^{*})$ exists by assumption.

According to the decentralized congestion management framework, the optimization problem at the aggregator side can be formulated as (for aggregator i),

$$\min_{p_{i,t}} \; g(p_{i,t}) + (c_t^{DT})^{T} E_i p_{i,t} \tag{3.14}$$

subject to,

$$e_i^{\min} \le \sum_{t\_\le t} (p_{i,t\_} - d_{i,t\_}) + e_{i,0} \le e_i^{\max}, \forall t \in \mathcal{T}, (\mu_{i,t}^-, \mu_{i,t}^+) \tag{3.15}$$

$$p_{i,t}^{\min} \le p_{i,t} \le p_{i,t}^{\max}, \forall t \in \mathcal{T}, (\varsigma_{i,t}^-, \varsigma_{i,t}^+). \tag{3.16}$$

Comparing the KKT optimal conditions of the optimal energy planning at the aggregator side with (3.11)-(3.13), it can be seen that ρ_t is the DT (c_t^{DT}) that can link the optimal energy plans at both sides. It is proven in chapter 2 that the optimal energy plan $p_{i,t}^*$ at the DSO side can be achieved at the aggregator side through solving (3.14)-(3.16) independently, assuming that $g()$ is quadratic and strictly convex.

Moreover, it can be observed from (3.12) and (3.13) that the DT contains both the congestion cost due to the line loading limit and the marginal cost of the topology requirement of the reconfiguration. It can be explained by the fact that the optimal energy plan can be achieved at the aggregator side without knowledge of the line loading limits or knowledge of the topology requirement. Therefore, the information of both costs must be contained in the DT.

3.2.4 Minimization of Switching Cost

If the cost of the switching operations is concerned by the DSO, the following optimization problem can be formulated, where the switching operation cost is included in the objective function.

$$\min_{p_{i,t}, P_l, x_{jk,t}, y_{jk,t}} \quad g(p_{i,t}) + \sum_{jk \in \mathcal{E}^s, t \in \mathcal{T}} c_{jk}^s y_{jk,t} \tag{3.17}$$

subject to,

(3.1)-(3.4), (3.6)-(3.10) and,

$$\left| x_{jk,t} - x_{jk,t-1} \right| \le y_{jk,t}, \forall (jk) \in \mathcal{E}^s, t \in \mathcal{T} \setminus \{1\}, \tag{3.18}$$

$$\left| x_{jk,t} - x_{jk,0} \right| \le y_{jk,t}, \forall (jk) \in \mathcal{E}^s, t \in \{1\}, \tag{3.19}$$

where c_{jk}^{s} is the switching cost and the binary variable $y_{jk,t}$ represents the switching operation (0 means no switching, 1 means a switching operation).

Constraints (3.18)-(3.19) are to count the number of switching operations (open/close). Due to the fact that the objective is to minimize the cost, constraints (3.18)-(3.19) always bind at one side (notice that an inequality including absolute operation is equivalent to two linear inequalities).

For conventional circuit breakers (CB), such as vacuum or gas insulated CB, the average switching cost c_{jk}^{s} can be estimated by dividing the total investment and installation cost by the predicted total number of normal operations according to the electrical and mechanical endurance. Due to the limited number of normal operations, the average switching cost is usually prohibitive for the reconfiguration. More research on improving the endurance of CB is required for enabling the reconfiguration applications [48], [49]. The use of power electronics in the power systems offers a good solution for the above issue, e.g. solid state CB [50], [51]. In such cases, the average switching cost is reasonably small and can be estimated from the average turn on and off losses of the power electronic devices.

Suppose $(p_{i,t}^{**}, P_t^{**}, x_{jk,t}^{**}, y_{jk,t}^{**})$ is a solution for the above MIP problem. Based on the same assumption made in section 3.2.3, it can be observed from (3.17)-(3.19) that the terms associated with $y_{jk,t}$ can be separated from the terms associated with $p_{i,t}$ and P_t, since $x_{jk,t}$ is fixed at $x_{jk,t}^{**}$. It can be inferred that the terms associated with $y_{jk,t}$ do not affect the calculation of DT (notice that the aggregator side optimization is the same as in 3.2.3, i.e. (3.14)-(3.16)). The DT (ρ_t) can be found by solving (3.11)-(3.13) at the new optimal point $(p_{i,t}^{**}, P_t^{**}, x_{jk,t}^{**})$. Similarly, the DT contains the information of both the line loading limit and the topology requirement as in section 3.2.3; meanwhile the information of the reduced switching cost is embedded in the topology information.

3.3 Optimal Reconfiguration Based DT with Line Loss Reduction

Both reconfiguration of distribution network and rescheduling of flexible demands for line loss reduction are interesting topics and they have been widely studied [39], [42], [52]–[54]. It is natural to look into the possibility of combining these two

methods and achieving the best solution. Moreover, it will be demonstrated in this section that the combined objective of minimizing energy cost and line loss cost can be realized in the decentralized management framework through the DT concept.

The main goal of the DSO energy planning for the flexible demands is to meet the energy requirements of their customers with the minimal energy cost and meanwhile respect the network constraints. The cost of line losses of the distribution network will be paid eventually by the customers through grid tariffs since the DSO does not make any profit and certainly does not bear any loss. Hence the line loss cost can be put together with the energy cost, and the DSO can form a single objective function of the energy planning. The complete optimization problem at the DSO side can be formulated as below.

$$\min_{p_{i,t},P_t,x_{jk,t}} \quad g(p_{i,t})+h(P_t) \tag{3.20}$$

subject to,

(3.1)-(3.4), (3.6)-(3.10)

The cost function of line losses $h(P_t)$ can be estimated with a linear method [55], a piece-wise linear method [56] or second order polynomials, such as $h(P_t)\approx\sum_{t\in\mathcal{T}}c_t\sum_{jk\in\mathcal{E}}\frac{r_{jk}}{V_n^2}P_{jk,t}{}^2$, where c_t is the predicted baseline energy prices, $P_{jk,t}$ is an element of vector P_t corresponding to edge (jk), V_n is the average voltage level.

Suppose the optimal solution of the above problem is found as $(p_{i,t}{}^{***},P_t^{***},x_{jk,t}{}^{***})$. The associated linear equations for determining the DT are formulated below.

$$\frac{\partial g(p_{i,t}{}^{***})}{\partial p_{i,t}}+E_i{}^T\rho_t-\sum_{t\_\le t}(\mu_{i,t\_}^{+}-\mu_{i,t\_}^{-})-(\varsigma_{i,t}^{+}-\varsigma_{i,t}^{-})=0, \tag{3.21}$$
$$\forall \mathrm{t}\in\mathcal{T},i\in\mathcal{B}$$

$$\{-\frac{\partial h(P_t^{***})}{\partial P_t} + B^T \rho_t + \lambda_t^+ - \lambda_t^-\}_{jk} + \psi_{jk,t}^+ - \psi_{jk,t}^- = 0, \quad \forall (jk) \in \mathcal{E}^s, t \in \mathcal{T} \tag{3.22}$$

$$\{-\frac{\partial h(P_t^{***})}{\partial P_t} + B^T \rho_t + \lambda_t^+ - \lambda_t^-\}_{jk} = 0, \quad \forall (jk) \in \mathcal{E} \setminus \mathcal{E}^s, t \in \mathcal{T} \tag{3.23}$$

Similar to section 3.2.3, the elements of the Lagrange multiplier vectors are zero if the corresponding inequality (3.7)-(3.10) does not bind at the optimal point $(p_{i,t}^{***}, P_t^{***}, x_{jk,t}^{***})$. Equations (3.21)-(3.23) can be solved and the DT is found to be ρ_t. From (3.22)-(3.23), it can be seen that the information of the line loading limit, the topology requirement and the marginal cost of line losses are all included in the DT. If there is no congestion in the network, i.e. λ_t^+, λ_t^- are zero, the DT contains only the line loss information and topology requirement (see (3.22)-(3.23)). Therefore, it can be served as a line loss control signal by the DSO.

After obtaining the DT, the DSO will send them to each aggregator, and the aggregator will use (3.14)-(3.16) to determine its own optimal energy plan, which should be $p_{i,t}^{***}$ as the DSO expects. Thus, the objective of congestion management, overall energy cost reduction and line loss reduction can be achieved in a decentralized manner.

3.4 Case studies

In order to verify the methods developed in section 3.2 and 3.3, three case studies were conducted and described in this section using the Danish driving pattern [37] and the Bus 4 distribution system of the RBTS [36].

3.4.1 Grid Data and Simulation Parameters

The single line diagram of the Bus 4 distribution network of the RBTS with marked sectionalizing CBs is shown in Fig. 3-2 (a). Its equivalent graphic diagram is shown in Fig. 3-2 (b), where the dotted lines indicate that the corresponding CBs are open. This provides the original tree-like operation topology of the meshed distribution network.

Line segments of the feeder one to four are labeled in Fig. 3-2 (a), among which L2, L4, L6, L8, L9, L11, and L12 refer to the transformers connecting the corresponding load points LP1 to LP7 (other transformer branches are not labeled for simplicity). The feeders without residential customers are not shown in the figure since the EVs are assumed to be passenger cars and charged with household facilities. The detailed data of the load points (residential and commercial customers) can be seen in Appendix A. The lengths of the line segments on the four feeders and line loading limits are listed in Table 3-1.

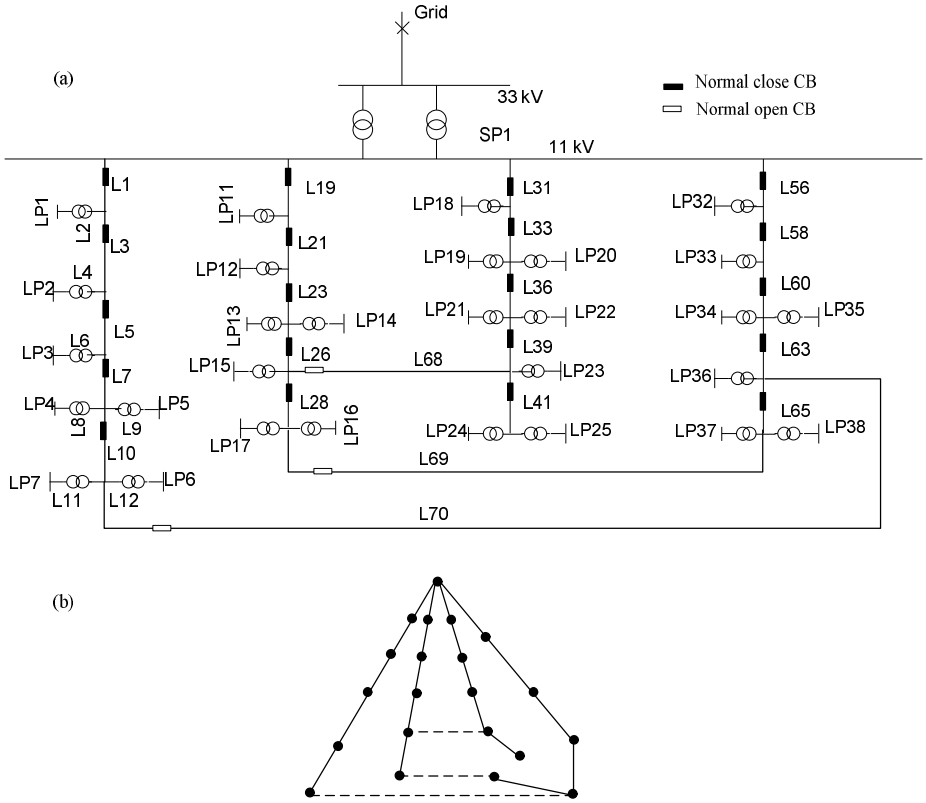

Fig. 3-2. (a) Single line diagram of the distribution network. (b) The equivalent graphic diagram (dotted lines are equipped with normal open CBs)

The key parameters of EVs and their availability can be seen from Appendix A. In the case studies below, two aggregators are assumed to manage the EVs in the distribution network independently, where the aggregator 'agg1' has contracts with 80 customers per load point while the other has contracts with the rest 120 customers per load point. The high availability and penetration level of the EVs provide

enough flexibility for the DSO to manage the congestion and the line losses of the distribution network.

The predicted day-ahead system prices can be seen from Appendix A, which serve as the baseline prices for the optimal energy planning at the DSO side. The system prices are employed for calculating the cost of the line losses as well.

TABLE 3-1. KEY PARAMETERS FOR THE SIMULATION

Parameter	value
Resistance of the feeders	0.1 ohm/km
Len. of line seg.: L2 6 10 21 28 41 58 68 69 70	0.6 km
Len. of line seg.: L1 4 7 9 12 19 56 60 63 65	0.75 km
Len. of line seg.: L3 5 8 11 23 26 31 33 36 39	0.8 km
Line loading limit: L1	8000 kW
Line loading limit: L3 19 51 56	6100 kW
Switching cost	0.5 DKK/switching

3.4.2 Case Study Results

3.4.2.1 Case One

In this case study, the feeder reconfiguration and flexible demand reallocation is performed for congestion management and energy cost reduction (without considering switching times and line losses). The resulting line loadings of L3, L19, L31 and L56 are shown in Fig. 3-3. It can be seen that the line loadings reach the limits at 't24'; therefore, the locational prices of the load points under these line segments are expected higher than the baseline prices (see Table 3-2) while LP1 has a locational price equal to the baseline price since L1 is not congested.

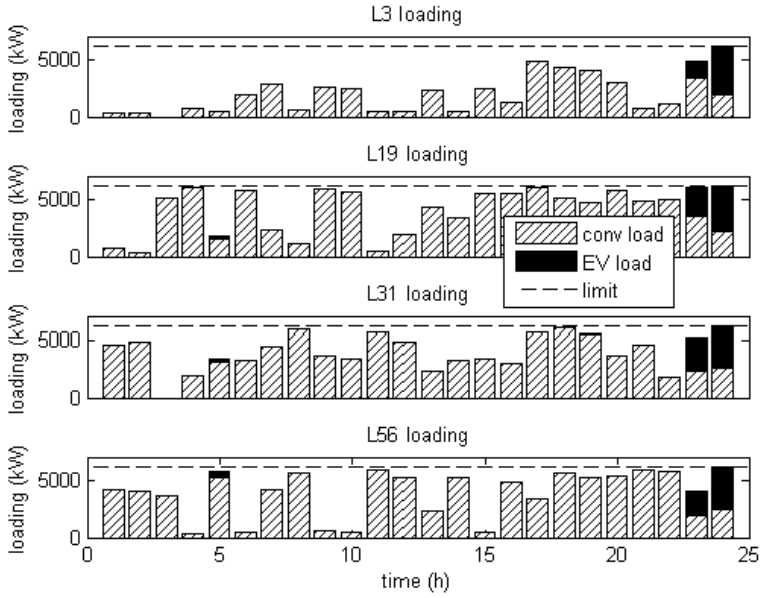

Fig. 3-3. Line loadings with the optimal topology in Case One

The optimal topology schedule is shown in Fig. 3-4. The topology changes at every planning period because there is no limitation of the switching operations and the solver of the optimization tool returns an arbitrary solution (the integer part) of the many alternative solutions (the number of alternative topologies is huge at e.g. the non-congestion periods).

As a comparison, the optimal energy planning with the original topology is obtained and the line loadings are shown in Fig. 3-5. The locational prices with the original topology are listed in Table 3-2. It can be seen that the congestion under the optimal topology is further alleviated and the locational prices are reduced in comparison to the congestion and locational prices with the original topology (zero DT at 't23' with the optimal topology indicates no congestion while positive DT at 't23' with the original one suggests the potential congestion; DT at 't24' is reduced under the optimal topology versus the original one).

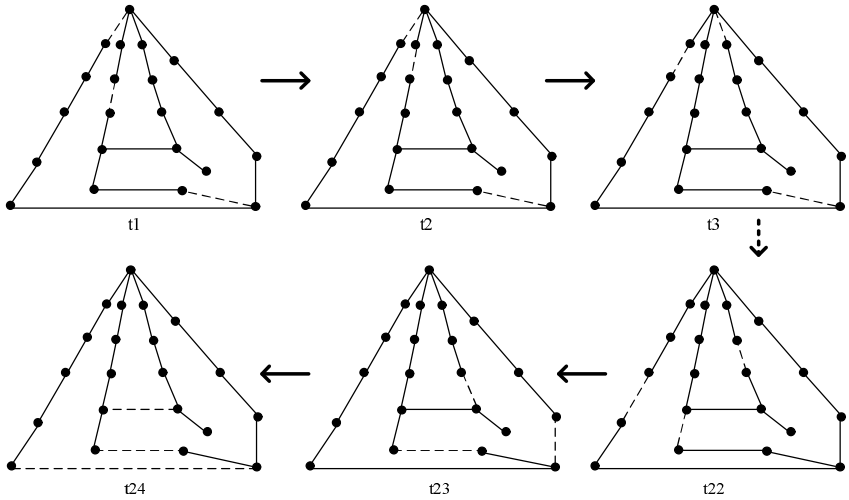

Fig. 3-4. The optimal topology schedule of the planning periods in Case One

TABLE 3-2. LOCATIONAL PRICE, DKK/KWH, OF CASE ONE (DT = LOCATIONAL PRICE - BASELINE PRICE; '-' MEANS THE LOCATIONAL PRICE EQUALS TO THE BASELINE PRICE)

	optimal topology			*original topology*	
time	t5	t23	t24	t23	t24
baseline	0.3012	0.2941	0.2241	0.2941	0.2241
LP1	-	-	-	-	-
LP2-7	-	-	0.2938	-	0.2938
LP11-17	-	-	0.2940	-	0.2940
LP18-25	-	-	0.2942	0.3010	0.3009
LP32-38	-	-	0.2942	0.3008	0.3008

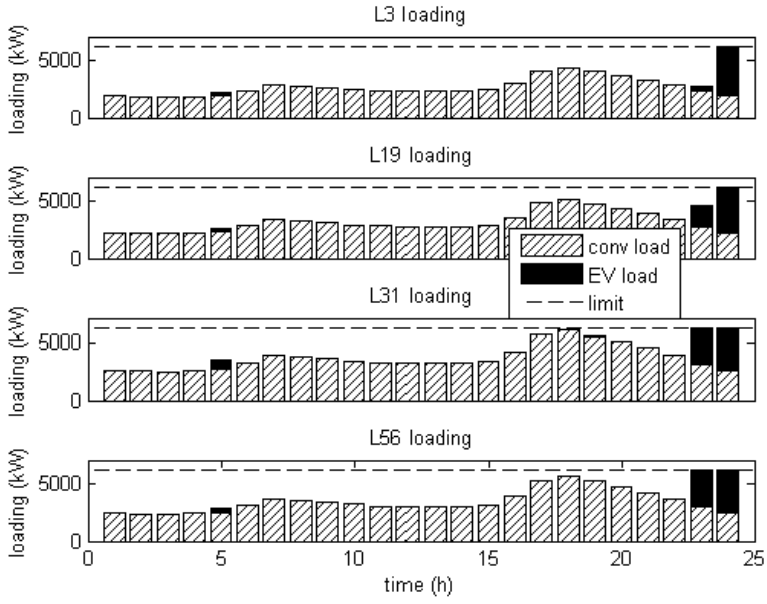

Fig. 3-5. Line loadings with the original topology in Case One

3.4.2.2 Case Two

In Case Two, the cost of switching operations is taken into account in the objective function. As a result, the switching operations are reduced to a minimum, which are twice (a switch-on operation and a switch-off operation) as shown in Fig. 3-7. The line loadings are shown in Fig. 3-6 and the locational prices are listed in Table 3-2. Comparing to the results of Case One, the solution of the Case Two is better than the one of the original topology in Case One in terms of the reduced congestion and reduced locational prices, but not as good as the one with the optimal topology in Case One.

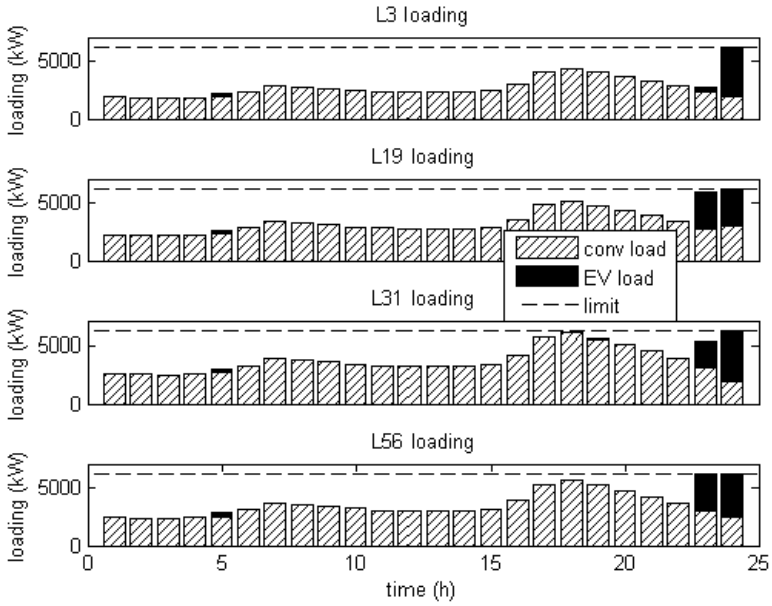

Fig. 3-6. Line loadings under reduced switching operations

The line losses and the cost of the three case studies are listed in Table 3-4. It can be seen that Case Three has the minimum total line losses and the cost of the line losses.

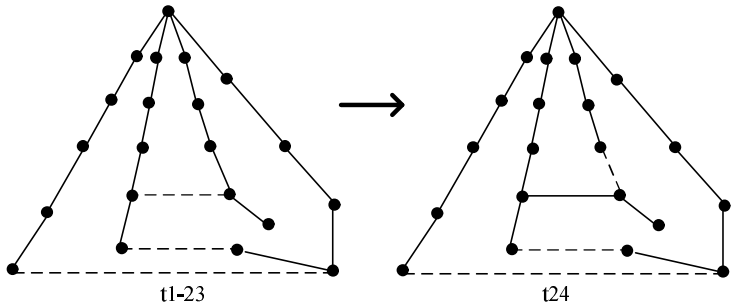

Fig. 3-7. The optimal topology schedule for minimum energy cost and reduced switching operations

TABLE 3-3. LOCATIONAL PRICE, DKK/KWH OF CASE TWO AND THREE (DT = LOCATIONAL PRICE - BASELINE PRICE; '-' MEANS THE LOCATIONAL PRICE EQUALS TO THE BASELINE PRICE)

	Case Two		*Case Three*		
time	t23	t24	t5	t23	t24
baseline	0.2941	0.2241	0.3012	0.2941	0.2241
LP1	-	-	0.3022	0.2953	0.2264
LP2	-	0.2937	0.3031	0.2964	0.2953
LP3	-	0.2937	0.3037	0.2972	0.2967
LP4-5	-	0.2937	0.3042	0.2979	0.2976
LP6-7	-	0.2937	0.3043	0.2980	0.2976
LP11	-	0.2942	0.3020	0.2957	0.2959
LP12	-	0.2942	0.3028	0.2975	0.2974
LP13-14	-	0.2942	0.3034	0.2988	0.2987
LP15	-	0.2942	0.3038	0.2996	0.2992
LP16-17	-	0.2942	0.3039	0.2997	0.2993
LP18	-	0.2939	0.3024	0.2963	0.2965
LP19-20	-	0.2939	0.3034	0.2980	0.2980
LP21-22	-	0.2939	0.3041	0.2989	0.2990
LP23	-	0.2942	0.3044	0.2999	0.2995
LP24-25	-	0.2942	0.3045	0.3000	0.2996
LP32	0.3008	0.3008	0.3024	0.3004	0.3007
LP33	0.3008	0.3008	0.3031	0.3018	0.3019
LP34-35	0.3008	0.3008	0.3039	0.3032	0.3032
LP36	0.3008	0.3008	0.3043	0.3040	0.3039
LP37-38	0.3008	0.3008	0.3046	0.3044	0.3042

3.4.2.3 Case Three

In this case study, the DT concept for congestion management and line loss reduction in a decentralized manner was tested. Firstly, the optimal energy plan taking into account the cost of line losses (modelled by a quadratic approximation) was obtained at the DSO side with respect to the line loading limits and network topology requirements. The resulting line loadings and the optimal topology schedule are shown in Fig. 3-8 and Fig. 3-10, respectively. The DTs were then calculated which are listed in. Due to the consideration of line losses, DTs are not zero even though there is no congestion, e.g. at 't5'. At last, the aggregators ('agg1' and 'agg2') perform their own energy planning based on the DTs received from the DSO. The line loadings due to the energy plan realized at the aggregator side are shown in Fig. 3-9. It can be seen that the total line loading of each line segment is the same as the one at the DSO side energy planning (Fig. 3-8), which means the DTs are effective in terms of alleviating the congestion and reducing the line losses in a decentralized manner.

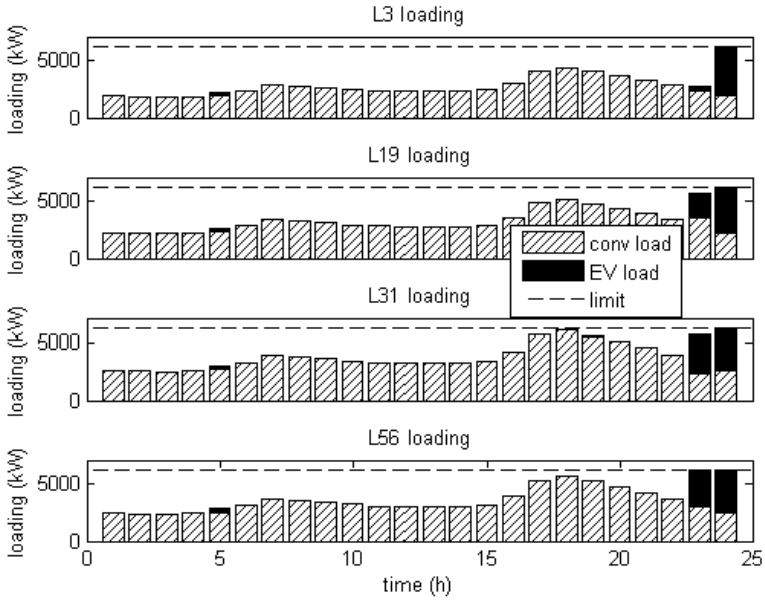

Fig. 3-8. Line loadings under reduced total line loss cost

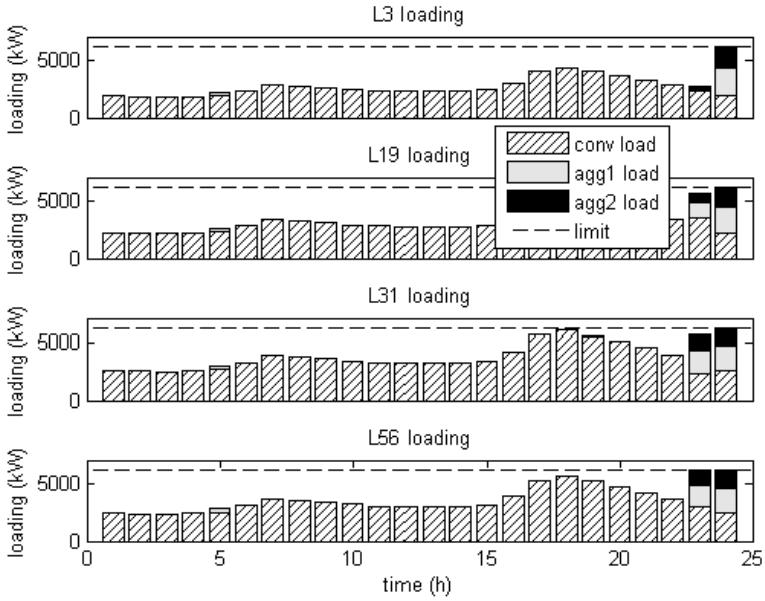

Fig. 3-9. The line loadings realized in the decentralized manner where the two aggregators make their own optimal energy plans independently

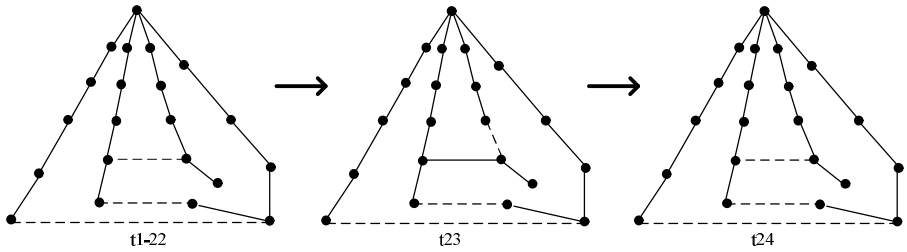

Fig. 3-10. The optimal topology schedule for reduced energy cost and line loss cost

TABLE 3-4. LINE LOSS COMPARISON OF THE THREE CASE STUDIES

	Case One	*Case Two*	*Case Thr.*
Total line losses (kWh)	2759.29	1961.39	1960.73
Cost of line losses (DKK)	901.642	627.01	626.24

3.5 Summary

The optimal reconfiguration based DT method is proposed in this chapter. The method is derived from the DT method by integrating the FR into the formulation of the optimal energy planning problem at the DSO side for congestion management. The combined optimization of the flexible demands and the network topology can achieve congestion management with minimum energy cost and reduced DT. The switching cost can be taken into account in the proposed DT framework if it is concerned by the DSO. By including the line loss cost in the energy planning at the DSO side, the calculated DT can contain the line loss information in addition to the congestion information, and therefore realize the line loss reduction in a decentralized manner through DT. The case studies have validated the efficacy of the optimal reconfiguration based DT method for both congestion management and line loss reduction in distribution networks with high penetration of EVs.

CHAPTER 4.

UNCERTAINTY MANAGEMENT OF DT METHOD[4]

This chapter is to provide a method to handle the uncertainties related to the DT method for congestion management.

4.1 Introduction

In previous two chapters, the DT concept and its application for congestion management and line loss reduction have been introduced. However, the uncertainty within the DT framework and the corresponding optimization under uncertainty has not been studied yet. The uncertainty comes from the following aspects.

Firstly, the uncertainty lies in the nature of the decentralized control structure of the DT method. The DSO employs price signals instead of direct command to control the energy planning of each aggregator, which makes it a decentralized control method. In the previous studies [14], [15], and chapter 2 and 3, an assumption was made that the parameters used by the DSO were the same as used by the aggregators. However, this might not be the case in practice and it may compromise the decentralized control concept by forcing the aggregators to report parameters to the DSO. Recognizing the importance of relaxing the link between the DSO and the aggregators, a different, but more practical assumption is made in this chapter, i.e. the DSO predicts the energy requirements of the flexible demands as the aggregators will not share this information with the DSO for protecting privacy of their customers. The prediction leads to a certain level of uncertainty of the DT method for congestion management. Secondly, there is uncertainty between the day-ahead

[4] This chapter is based on paper: S. Huang, Q. Wu, C. Lin, X. Zhao and H. Zhao, "Uncertainty Management of Dynamic Tariff Method for Congestion Management in Distribution Networks", IEEE Tr. Power System, Vol. 31, pp 4340 – 4347, Nov. 2016.

energy planning and the real-time operation condition. For instance, the components of the power system or DER can fail with a certain level of probability. The forecast error of the energy production or consumption of the DER is another example.

By knowing the sources of the uncertainty and quantifying the uncertainty, it is possible to enhance the robustness of the DT method for congestion management through uncertainty management, which is the main contribution of this chapter. The robustness is defined in this chapter as the guarantee that the congestion probability is under a certain level with a given confidence level. Uncertainty management has been previously employed in other optimal scheduling problems in distribution networks, such as EV scheduling in [57] where a stochastic load profile is considered, and DG scheduling in [58] where stochastic productions of DERs are treated. However, unlike the DT method, both of them are using direct control methods without employing the DSO-Aggregator business model and the price incentives.

This chapter will first briefly present the DT method for congestion management in distribution networks with high penetration of EVs, adapted from chapter 2. Next, the uncertainty sources of the decentralized control of the DT method are analyzed. The robustness enhancement of the DT method through uncertainty management is then proposed. At last, two case studies regarding robustness enhancement are described and discussed.

4.2 DT Method and Its Uncertainty

4.2.1 Quadratic Programming Based DT Method

In chapter 2, a quadratic programing formulation was proposed for the DT method. The DT is determined by the DSO through an optimal energy planning of the flexible demands. In chapter 2, the optimization model is given based on the flexible demands of both EVs and HPs. In order to simplify the analysis of the uncertainties, EV is chosen to represent the flexible demands in this chapter. In the follows, the optimization model for the DT method presented in chapter 2 is tailored for the EV case of this chapter. In chapter 2, it is assumed that the aggregators are willing to share the flexible demand information (energy requirement, availability, etc.) with the DSO; therefore, the DSO can have detailed information for modelling the optimal EV and HP planning. However, in this chapter, the DSO will forecast the flexible demands by itself. The DSO will forecast the parameters, such as mean and

variation, of the statistic distribution of the flexible demands. Then a sampling/Monte Carlo process is employed to provide data for modelling the optimal EV and HP planning. Because there are a large number (e.g., 200) of flexible demands of each load point (refers to low voltage transformer; the network below the transformer is not modelled), the sampling process can provide a good representation of the actual flexible demands.

The optimal energy planning at the DSO is,

$$\min_{p_{i,t}} \quad \sum_{i\in\mathcal{B},t\in\mathcal{T}} \frac{1}{2} {p_{i,t}}^T B_{i,t} p_{i,t} + (c_t 1)^T p_{i,t}\,, \tag{4.1}$$

subject to,

$$\sum_{i\in\mathcal{B}} DE_i (p_{i,t} + p_{i,t}^c) \le F_t, \forall t \in \mathcal{T}, (\lambda_t)\,, \tag{4.2}$$

$$\sum_{t\in\mathcal{T}} p_{i,t} \ge d_i, \forall i \in \mathcal{B}\,, \tag{4.3}$$

$$0 \le p_{i,t} \le a_{i,t} p_i^{\max}, \forall i \in \mathcal{B}, t \in \mathcal{T}\,, \tag{4.4}$$

where $\mathcal{B}$ is the set of the aggregators, $\mathcal{T}$ is the set of the planning periods, $p_{i,t}$ is the charging power of EVs, $p_{i,t}^c$ is other fixed load of the household, d_i is the energy requirement of the EVs, $p_i^{\max}$ is the maximum charging power, $a_{i,t}$ is the availability of the EVs, F_t is the line flow limits, c_t is the baseline energy price, D is PTDF, E maps the household to load point, and $B_{i,t}$ is a diagonal matrix of the price sensitivity coefficients (see chapter 2 for the definition).

In the energy planning, the line loading limit is ensured by constraint (4.2), energy demand requirement of EVs is fulfilled by constraint (4.3) and the allowed charging power of EVs is represented by (4.4).

The calculated DT through the above optimization by the DSO, denoted as r_t, is equal to $D^T \lambda_t$. It will be sent to the aggregators, who then make the energy planning of the flexible demands on behalf of the owners. The energy planning of different

aggregators is independent and without the information of the network constraints. Aggregator i can employ the following optimization to make the energy planning.

$$\min_{p_{i,t}} \quad \sum_{t\in\mathcal{T}} \frac{1}{2} {p_{i,t}}^T B_{i,t} p_{i,t} + (c_t \mathbf{1} + {E_i}^T r_t)^T p_{i,t} \tag{4.5}$$

subject to,

$$\sum_{t\in\mathcal{T}} p_{i,t} \geq d_i \tag{4.6}$$

$$0 \leq p_{i,t} \leq {a_{i,t}}^T p_i^{\max} \quad \forall t \in \mathcal{T} \tag{4.7}$$

In chapter 2, it is proven that the convergence of the aggregator energy planning and the DSO one can be assured, i.e. the results and the line loading profiles resulting from the energy planning at the aggregator side will be same as those at the DSO side. As such, the DT method for the congestion management is realized in a decentralized manner. A strong assumption made in chapter 2 is that the parameters of the optimization problem at the DSO side are same as those at the aggregator side. However, it is not necessarily true. In the following sub section, the source of parameter differences and the resulting uncertainty of the decentralized control of the DT method will be studied.

4.2.2 Uncertainty of the Decentralized Control

Table 4-1 gives one possible scenario of the information sources where the DSO and aggregators may have the required parameters ready for their energy planning respectively, which will be the assumption made for the study of the following sections. In this scenario, parameter $B_{i,t}$ is mainly to resolve the multiple-response issue in linear program and therefore the DSO should share it with the aggregators. Although the aggregators should have the freedom to choose their own energy price prediction resources, it is suggested that they (include DSO) all use the same source, since the DT method works through the total price (DT + energy price) as the price signal to control the behavior of the flexible demands. However, small discrepancy due to e.g. numerical errors of computers or modifications according to their own preferences is allowed as shown by case studies in [59]. The only uncertainty sources lie in the parameters d_i and $a_{i,t}$, i.e. the driving patterns of EVs, where the DSO can only predict the driving pattern while the aggregators can have the de-

tailed data from their customers. Since the study is focused on the difference between the DSO plan and the actual plans made by the aggregators that will be submitted to the day-ahead market, the data that the aggregators employ to determine the optimal energy plans will be deemed as accurate.

TABLE 4-1. INFORMATION SOURCE OF DSO AND AGGREGATOR

Para.	DSO	Aggregator
$B_{i,t}$	Predicted by DSO	From DSO
c_t	Predicted by DSO or third party	From DSO or choose the same third party as the DSO do
D, F_t	Determined by DSO	Not needed
E_i, $p_i^{\max}$	From customers' subscription	From customers' subscription
d_i, $a_{i,t}$	Predicted by DSO	From the customers' reports

It is important to know the distribution of the prediction error of predicted parameters d_i and $a_{i,t}$ in order to analyze the accuracy of the DSO's energy plan (compared to the energy plans of the aggregators) and then enhance the robustness of the DT method. In [37], the driving pattern (driving distance and availability) of a large number of drivers has been surveyed. The study is based on Denmark and it can help illustrate the discussion of parameter randomness in this section and the methodology of robust enhancement in the following sections without affecting the generality of the discussion.

In Denmark, a large portion of the drivers (about 40% on weekdays, about 50% on weekends) do not drive at all according to the daily observations (interviews). The percentage of the drivers who drive on a particular day diminishes as the driving distance goes up. The average driving distance is about 30 km while it varies from weekdays to weekends. From the statistics point of view, the prediction error (parameter used by the DSO minus the one used by the aggregator) of the predicted driving distance of each EV can be considered to have a normal distribution with variance σ^2 as shown in Fig. 4-1. The chance of the error bigger (or less) than a predefined number can be calculated from the normal distribution table, e.g. the probability of the error that is positive and bigger than 2σ is only 2.5% (the shadow part of Fig. 4-1).

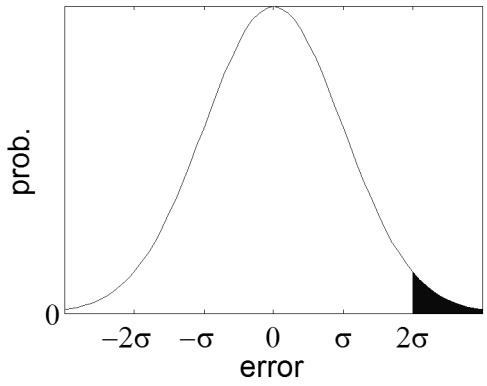

Fig. 4-1. Normal distribution of the prediction error

The energy demand of an EV has a linear relationship with the driving distance, which is defined as the parameter "energy consumption per km" (Table 4-2). Therefore, the prediction error of the energy demands d_i also has a normal distribution.

The parameter $a_{i,t}$ is also influenced by the randomness of the driving pattern. The availability of an EV can be modeled through two random variables, namely arriving (home) time and leaving (home) time. For example, in Fig. 4-2, $y$is the arriving time while x is the leaving time. The availability $a_{i,t}$ (j-th element) can be determined by the following rules.

$$\{a_{i,t}\}_j = \begin{cases} 1 & t \le \lfloor x \rfloor, or, t \ge \lceil y \rceil \\ 0 & \lceil x \rceil \le t \le \lfloor y \rfloor \\ x - \lfloor x \rfloor & t = \lfloor x \rfloor, t \ne \lfloor y \rfloor \\ \lceil y \rceil - y & t = \lfloor y \rfloor, t \ne \lfloor x \rfloor \\ x - \lfloor x \rfloor + \lceil y \rceil - y & t = \lfloor x \rfloor = \lfloor y \rfloor \end{cases} \quad ,t \in \mathcal{T} \tag{4.8}$$

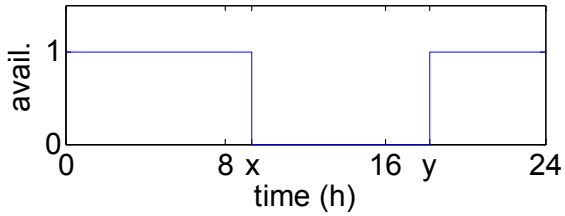

Fig. 4-2. Illustration of the modeling of the availability, x is the leaving time and $y$is the arriving time

The prediction error of the predicted arriving time has a normal distribution, so does the prediction error of the predicted leaving time.

4.3 Robustness Enhancement of The DT Method through Uncertainty Management

The criterion of the robustness enhancement for the DT method is defined as: The probability of the line overloading ε(percentage) is no bigger than a predefined number, e.g. $1-\eta$ with ηbeing a confidence level, under the uncertainty of the parameters. The task of the robustness enhancement is to find such DT that the above criterion is fulfilled.

4.3.1 Problem Formulation

According to the concept described in chapter 2, DT should be able to serve as a proper price signal such that the optimal energy plans made by the aggregators based on the received DT will result no (or alleviated) congestion on the distribution network. The method to determine such DT presented in chapter 2 has been tailored as (4.1)-(4.4), which is based on a deterministic optimization. However, it is not suitable for determining a DT with uncertainty constraints (such as (4.13)) presented, because of the following two facts: 1) The Lagrange multiplier of uncertainty constraints is very difficult to find; 2) The Lagrange multiplier with uncertainty constraints presented is no longer the marginal price of the congestion cost.

A method that can determine the DT without using Lagrange multiplier can be written as a two-level optimization,

$$\min_{r_t} \sum_{t\in\mathcal{T}} \|r_t\|_1 \tag{4.9}$$

subject to,

$$\sum_{i\in\mathcal{B}} DE_t(p_{i,t}+p_{i,t}^c) \le F_t, \forall t\in\mathcal{T}, \tag{4.10}$$

$$r_t \ge 0, \forall t\in\mathcal{T}, \tag{4.11}$$

$$p_{i,t} \in \arg\min \{(4.5): (4.6)\text{-}(4.7)\}, \forall i\in\mathcal{B}. \tag{4.12}$$

In the above two-level optimization, variable $p_{i,t}$ is the unique minimizer of the inner optimization, which is a strictly convex optimization. The parameters d_i and $a_{i,t}$ in (4.6)-(4.7) are deemed as random parameters; therefore constraint (4.10) cannot be fulfilled with certainty. A chance constrained two-level optimization can be formed as,

(4.9) ,

subject to,

$$prob.\{\sum_{i\in\mathcal{B}} DE_t(p_{i,t}+p_{i,t}^c) \le (1+\varepsilon)F_t, \forall t\in\mathcal{T}\} \ge \eta, \tag{4.13}$$

and (4.11)-(4.12),

where $\eta$is the confidence level and has a typical value of 0.9, 0.95 or 0.99, and ε is the predefined allowed overloading percentage.

The above chance constrained two-level optimization is very difficult to solve directly. An alternative method is developed in this chapter to solve it, i.e. an iteration method based on the probability analysis, the deterministic method to determine DT presented in section 4.2.1 and the sensitivity analysis proposed in [59]. The main idea of the iteration method is explained as follows.

Firstly, the chance constraint (4.13) is reformed to be deterministic. Meanwhile, the parameter εbecomes a control variable which will take different value in each

iteration step according to the results of the previous iteration step. Random parameters d_i and $a_{i,t}$ are replaced with their expected values, i.e. $\overline{d}_i$ and $\overline{a}_{i,t}$, respectively.

Secondly, the two-level optimization is reformed as the standard form descripted in section 4.2.1 ((4.1)-(4.4)) in order to determine an iterative DT, denoted as $r_t^{(k)}$. The idea is based on the theory proven in chapter 2: The solution at the aggregator side ((4.5)-(4.7)) is the same as the solution at the DSO side ((4.1)-(4.4)) if $r_t = D^T \lambda_t$ holds. Thus, the optimization to determine the iterative DT can be written as,

$$(4.1)\,,$$

subject to,

$$\sum_{i\in\mathcal{B}} DE_i(p_{i,t}+p_{i,t}^c) \le (1+\varepsilon_t^{(k)})F_t, \forall t\in\mathcal{T}, (\lambda_t^{(k)})\,, \tag{4.14}$$

$$\sum_{t\in\mathcal{T}} p_{i,t} \ge \overline{d}_i, \forall i\in\mathcal{B}\,, \tag{4.15}$$

$$0 \le p_{i,t} \le \overline{a}_{i,t} p_i^{\max}, \forall i\in\mathcal{B}, t\in\mathcal{T}\,, \tag{4.16}$$

where $k$represents the iteration step and $\varepsilon_t^{(k)}$ is the control parameter representing the overloading level at k-th iteration step.

Thirdly, the chance constraint (4.13) will be verified through probability calculation based on the uncertainty analysis described in section 4.2.2 and the sensitivity analysis of the optimization (4.5)-(4.7) with updated DT, i.e. $r_t^{(k)} = D^T \lambda_t^{(k)}$, which will be elaborated in section 4.3.2. If (4.13) is fulfilled, then we find the final DT; otherwise the control parameter $\varepsilon_t^{(k)}$ will be updated and perform the next iteration. The detailed procedure of the iteration method will be described in section 4.3.3.

4.3.2 Probability Calculation

Probability calculation is an important step in the uncertainty management. It is carried out through uncertainty analysis of the parameters and the sensitivity analysis of the optimal solution of the energy planning at the aggregator side.

4.3.2.1 Sensitivity analysis

The sensitivity analysis is to determine the changes of the optimal solution due to the changes of the parameters and it shall be done for a specific optimal solution [59]. The optimization (4.5)-(4.7) (the optimization at the aggregator side) can be rewritten with updated parameters as,

$$\min_{p_{i,t}} \quad \sum_{t\in\mathcal{T}} \frac{1}{2} {p_{i,t}}^T B_{i,t} p_{i,t} + (c_t 1 + {E_i}^T r_t^{(k)})^T p_{i,t} \tag{4.17}$$

subject to,

$$\sum_{t\in\mathcal{T}} p_{i,t} \geq \bar{d}_i, \tag{4.18}$$

$$0 \leq p_{i,t} \leq \bar{a}_{i,t}{}^T p_i^{\max} \quad \forall t \in \mathcal{T}. \tag{4.19}$$

Assume that the optimal solution of the above deterministic optimization problem is $(p_{i,1}^*, p_{i,2}^*, p_{i,3}^*, ..., p_{i,n_T}^*)^{(k)}$, which should be also the optimal solution of (4.1) subject to (4.14)-(4.16). Now assume that the parameters d_i and $a_{i,t}$ at the right side of (4.18)-(4.19) can vary according to their statistic distributions with their centers $\bar{d}_i$ and $\bar{a}_{i,t}$ respectively, note that $d_i = \bar{d}_i + \Delta d_i$ and $a_{i,t} = \bar{a}_{i,t} + \Delta a_{i,t}$. It therefore can be determined how the optimal solution will change according to the changes of the parameters d_i and $a_{i,t}$, i.e. Δd_i and $\Delta a_{i,t}$, near the optimal point $(p_{i,1}^*, p_{i,2}^*, p_{i,3}^*, ..., p_{i,n_T}^*)^{(k)}$ through the sensitivity analysis method presented in [59].

According to [59], the optimization problem (4.17)-(4.19) should be rewritten as a standard form as below (i is fixed) with inactive constraints removed,

$$\min_{p} \quad \frac{1}{2} p^T B p + g^T p \tag{4.20}$$

subject to,

$$Ap = b \tag{4.21}$$

where p is $\left[{p_{i,1}}^T, {p_{i,2}}^T, {p_{i,3}}^T, ..., {p_{i,n_T}}^T \right]^T$,

$$B \text{ is} \begin{bmatrix} B_{i,1} & & & & \\ & B_{i,2} & & & \\ & & B_{i,3} & & \\ & & & \dots & \\ & & & & B_{i,n_T} \end{bmatrix},$$

$$g \text{ is} \begin{bmatrix} c_1 1 + E_i^T r_1^{(k)} \\ c_2 1 + E_i^T r_2^{(k)} \\ c_3 1 + E_i^T r_3^{(k)} \\ \dots \\ c_{n_T} 1 + E_i^T r_{n_T}^{(k)} \end{bmatrix}^T,$$

A and $b$are coefficients of the active constraints in (4.18)-(4.19), n_T is the number of planning periods.

The optimal solution changes over the changes of the vector $b$can be obtained as,

$$\frac{\partial p}{\partial b} = B^{-1} A^T (A B^{-1} A^T)^{-1}. \tag{4.22}$$

The line loading change at a particular hour t is the summation of the changes of the EV charging power p , which can be written as,

$$\sum_{i \in \mathcal{B}} DE_i (\Delta p_{i,t}) = \sum_{i \in \mathcal{B}} DE_i \frac{\partial p_{i,t}}{\partial b} \Delta b, \tag{4.23}$$

where $\frac{\partial p_{i,t}}{\partial b}$ can be retrieved from matrix $\frac{\partial p}{\partial b}$ by taking the corresponding rows.

4.3.2.2 Chance of overloading due to energy demand

Since the change of the energy demand d_i results the change of $b$vector of (4.21), the sensitivity of the change of the line loading over the change of the energy demand can be calculated through (4.22) and (4.23). Moreover, the probability of a predefined overloading ε, e.g. line overloading 5% (5% more than the line loading limit), due to the prediction error of the energy demand, denoted as Δd_i , can be

calculated through combining the statistic distribution of the prediction error into the calculation. Specifically, the probability can be determined by (for given t),

$$\rho_d = prob.\left\{\sum_{i\in\mathcal{B}} \alpha_i^T \Delta d_i \geq \varepsilon F_t\right\}, \tag{4.24}$$

where α_i is the sensitivity coefficients corresponding to Δd_i and can be retrieved from the result of (4.23).

4.3.2.3 Chance of overloading due to availability

Similarly, the prediction error of the availability $a_{i,t}$ can be determined through (4.8) and the changes of the line loading can be determined through (4.22) and (4.23). The probability of a predefined overloading ε due to the prediction error of the availability, denoted as $\Delta a_{i,t}$, can be calculated by (for given t),

$$\rho_a = prob.\left\{\sum_{i\in\mathcal{B},t'\in\mathcal{T}} \beta_{i,t'}^T \Delta a_{i,t'} \geq \varepsilon F_t\right\}, \tag{4.25}$$

where $\beta_{i,t}$ is the sensitivity coefficient corresponding to $\Delta a_{i,t}$ and can be retrieved from (4.23).

Combining (4.24) and (4.25), the probability of a predefined overloading ε due to EV parameters can be obtained as (for given t),

$$\rho = prob.\left\{\sum_{i\in\mathcal{B}} \alpha_i^T \Delta d_i + \sum_{i\in\mathcal{B},t'\in\mathcal{T}} \beta_{i,t'}^T \Delta a_{i,t'} \geq \varepsilon F_t\right\}. \tag{4.26}$$

The distribution $\sum_{i\in\mathcal{B}} \alpha_i^T \Delta d_i + \sum_{i\in\mathcal{B},t'\in\mathcal{T}} \beta_{i,t'}^T \Delta a_{i,t'}$, denoted by Γ, is a normal distribution since each element of Δd_i and $\Delta a_{i,t}$ is a normal distributed random variable and Γ is a linear combination of them. It is assumed that Δd_i and $\Delta a_{i,t}$ are independent random variables since the mathematical complexity incurred from the dependency of these random variables is not a focus of this chapter. The variance of the joint distribution Γ is a linear combination of the variance of each random variable.

4.3.3 Procedure of Robustness Enhancement

In order to achieve robustness enhancement, a procedure is designed and illustrated in Fig. 4-3. The procedure that the DSO should follow is:

1) Forecast the day-ahead energy prices.
2) Forecast the driving behaviors of EVs, including driving distance, arriving time and leaving time.
3) Set the initial line loading limit to be 100%, i.e. $\varepsilon_t^{(0)} = 0$ in (4.14).
4) Perform the optimal energy planning at the DSO side through QP and calculate the DT, i.e. solve (4.1) subject to (4.14)-(4.16).
5) Perform the sensitivity analysis of the energy planning at the aggregator side, i.e. (4.17)-(4.19). Determine α_i and $\beta_{i,t}$ in (4.26).
6) Perform the probability calculation, i.e. determine the value ρ of (4.26).
7) Check whether the probability ρ is no bigger than 1-η. If yes, publish the final DT and terminate the algorithm; otherwise,
8) Calculate the new line loading limit, which is achieved by pushing down the limit with a small step. The step size can be a fixed small number, e.g. 0.5%, or estimated by the Newton-Raphson method noticing the fact that the sensitivity matrix is the Jacobian matrix.
9) Go back to step 4.

The above algorithm for uncertainty management has a heuristic feature. It can find a feasible solution that makes sure the congestion probability below a certain critical value. If there are more than one congested lines, step 8 should handle multiple lines, i.e. push down the line loading limits for multiple lines. The theory and the algorithm themselves do not assume only one congested line.

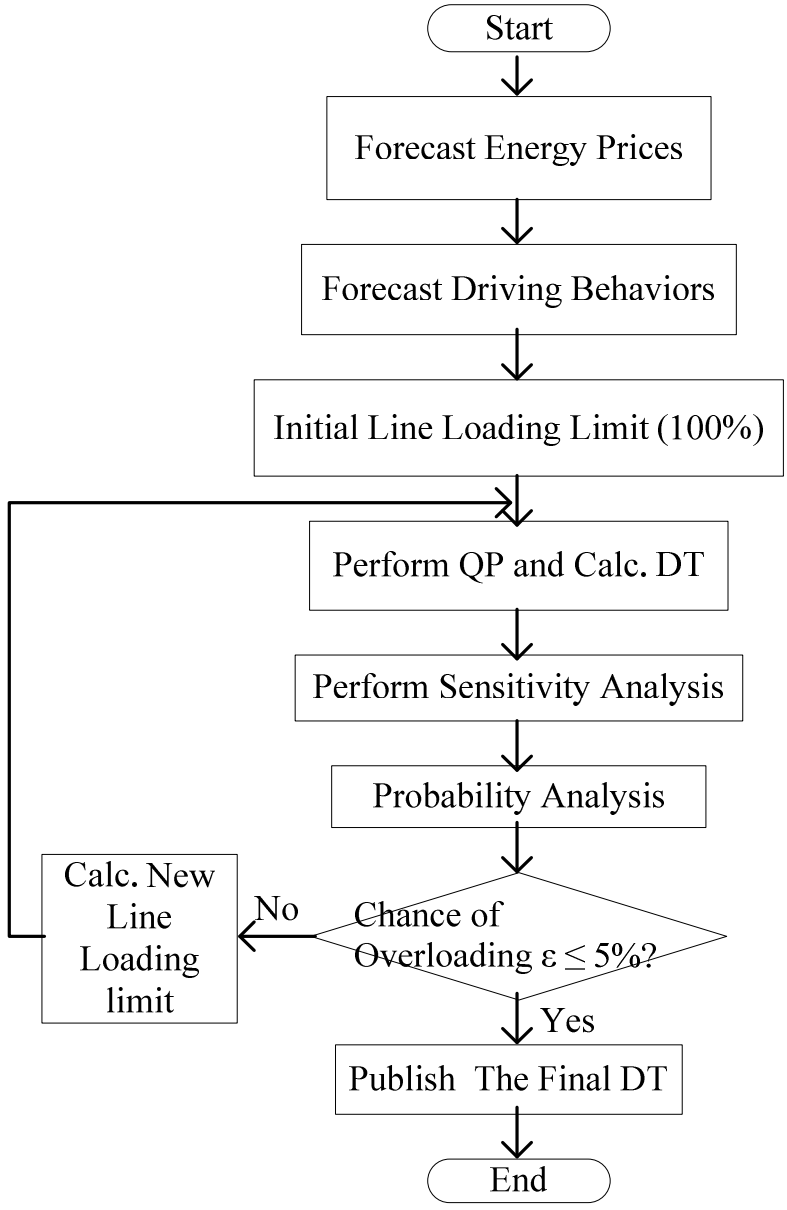

Fig. 4-3. Flowchart illustrating the procedure of robustness enhancement

4.4 Case Studies

Case studies were conducted using the Danish driving pattern and the Bus 4 distribution system of the RBTS [36] to demonstrate the robustness enhancement of the DT method through uncertainty management. The details of the case studies are presented in this section.

4.4.1 Grid Data

The single line diagram of the Bus 4 distribution network is shown in Fig.4-4. Line segments of the feeder one are labeled in Fig.4-4, among which L2, L4, L6, L8, L9, L11, and L12 refer to the transformers connecting the corresponding load points (LP1 to LP7). Each of the residential load points (LP1-5) has 200 customers while each of the commercial load points (LP6-7) has 10 customers. Detailed data about the load points can be seen in Appendix A. The peak conventional demands of residential customers are assumed to occur at 18:00 when people come home and start cooking (shown in Fig. 4-5).

The key parameters of the simulations are listed in Table 4-2. The EV availability information can be seen from Appendix A. Assume that there are two aggregators (agg1 and agg2); one has 40 customers per load point and the other has 160 customers per load point.

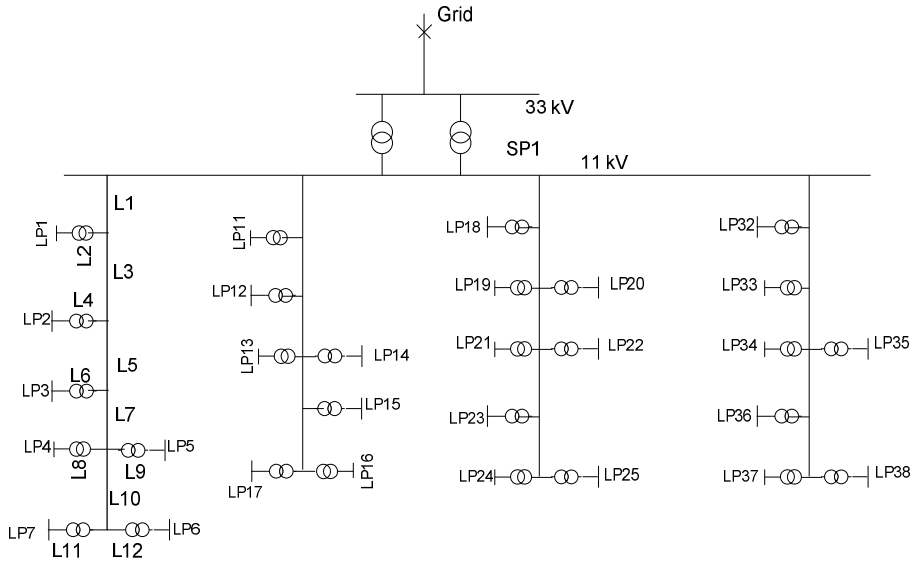

Fig. 4-4. Single line diagram of the distribution network

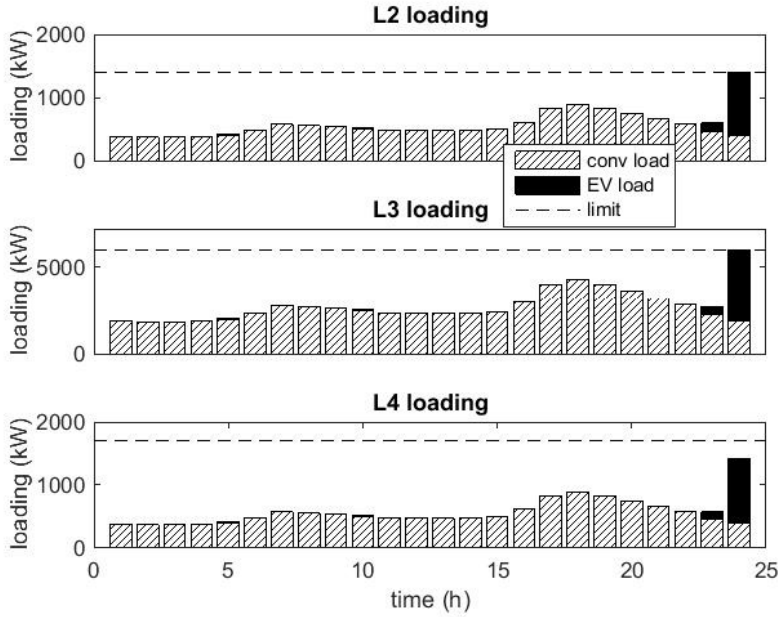

Fig. 4-5. Line loading of the initial energy planning at DSO side

TABLE 4-2. KEY PARAMETERS FOR THE SIMULATION

Parameter	**value**
EV battery size	25 kWh
Peak charging power	11 kW (3 phase)
Energy consumption per km, ϕ	150 Wh/km
expected driving distance	40 km
expected leaving time	Hour 8
expected arriving time	Hour 18
σ of predicted driving distance, σ_d	20 km
σ of predicted leaving time	60 minute
σ of predicted arriving time	60 minute
Line loading limit: L2	1400 kW
Line loading limit: L3	6000 kW
Line loading limit: L4	1700 kW

4.4.2 Results of The Robustness Enhancement

4.4.2.1 Case One

According to the procedures proposed in section 4.3.3, the basic energy prices are firstly predicted. The predicted energy prices can be seen from Appendix A. In this chapter, the prediction of the energy price is assumed to be shared by the DSO and the aggregators. Then the driving behaviors including driving distance, arriving time and leaving time are predicted as list in Table 4-2. The energy planning at the DSO side is performed with initial values, i.e. let $\varepsilon_t^{(0)} = 0$ in (4.14), and the results are plotted in Fig. 4-5.

Then the sensitivity analysis of the line loading change to the change of energy demand, arriving time and leaving time is performed at the optimal point. Part of the results (only regarding L3) is shown in Table 4-3. It can be seen that the line loadings (L3) at hour 23 and 24 are sensitive to energy demand of EVs (the results are synthesized from the individual sensitivity of each EV, because it is not necessary to show the results of a thousand EVs), while it is less sensitive at hour 5, 6, 10 and 19. The change of energy demand will not affect the line loadings at other hours since the sensitivity coefficient is zero. For the change of the arriving time, it will only influence the line loading at hour 24 and the influence is insignificant (one minute change of the arriving time will only lead to 3.2 kW change of the line loading). The reason can be explained by the fact that the expected arriving time (see Table 4-2) is far away from the congestion hour, namely hour 24. The same reason explains that the change of the leaving time has insignificant influence to the line loading change.

TABLE 4-3. SENSITIVITY OF L3 LOADING CHANGE TO THE CHANGE OF ENERGY DEMAND, ARRIVING TIME AND LEAVING TIME (DATA OF OTHER HOURS IS ZERO)

Hour	Energy Demand (kW/kWh)	Arriving Time (kW/min)	Leaving Time (kW/min)
5	32	0	0
6	8	0	0
10	16	0	0
19	8	0	0
23	352	0	0
24	384	3.2	0

The next step is to carry out the probability analysis. Take L3 as an example (both L2 and L3 are critical which can be observed from Fig. 4-5; however, L2 can be analyzed through the same method as for L3). The line loading limit is 6000 kW

and the probability of the overloading 5%, i.e. 5% of the original limit or 300 kW, will be estimated. The critical hour (congestion hour) is hour 24 and the sensitivities associated with arriving time and leaving time are negligible according to Table 4-3. The standard deviation of Γ can be determined as $\sqrt{\alpha_1^T \alpha_1 + \alpha_2^T \alpha_2}\phi\sigma_d = 43.26\,(\text{kW})$. Therefore, the probability of Γ bigger than 300 kW is very low (less than 0.1%). According the procedure, the algorithm can be terminated with the final DT (the 1st iteration column of Table 4-4).

TABLE 4-4. RESULTS OF EACH ITERATION

	1st iter	**2nd iter**	**3rd iter**	**4th iter**
DT at LP1, Hour 24 (DKK/kWh)	0.0519	0.0519	0.0519	0.0519
DT at LP2-5, Hour 24 (DKK/kWh)	0.0511	0.0514	0.0518	0.0521
Prob. of over-loading 5%	<0.1%	-	-	-
Prob. of over-loading	50%	24.5%	8.2%	2.1%
L3 loading limitation (kW)	6000	5970	5940	5910

4.4.2.2 Case Two

However, if the DSO is more conservative, e.g. the DSO sets its goal to be that the probability of overloading (0%) is no bigger than 5%, the algorithm needs to continue to the second iteration because after the first iteration, the probability of overloading is 50%. The new line loading limit of L3 at the critical hour is reduced by 0.5% (a fixed small step), i.e. the new line loading limit is 5970 kW. The procedure is repeated from step 4. The sensitivity and the standard deviation of Γ are almost not changed from the first iteration. The probability of $-30+\Gamma \geq 0$ (noted that the line loading limit is reduced by 30 kW in the optimal energy planning) is 24.5%. The algorithm needs to continue to the third and fourth iteration. After the fourth iteration, the probability is reduced to 2.1 % and the algorithm can be terminated with the final DT (the 4th iteration column of Table 4-4).

The results of Case One and Case Two are listed in Table 4-4. As the L3 loading limitation sets to be lower and lower in the optimal energy planning at the DSO

side, the DTs at LP2-5 go up gradually (DT at LP1 is not changed because the enhancement regarding L2 overloading has not been carried out yet; it can be done by following the same procedure for L3), which is reasonable because it needs to shift more power consumption to other hours. It can be seen from the final energy planning results shown in Fig. 4-6 that 90 kW is shifted from hour 24 to hour 23 comparing to the original planning (Fig. 4-5). The benefit is that the probability of L3 overloading (the physical limitation is still 6000 kW) is only 2.1%, which is the confidence that the DSO has on the DT method for congestion management.

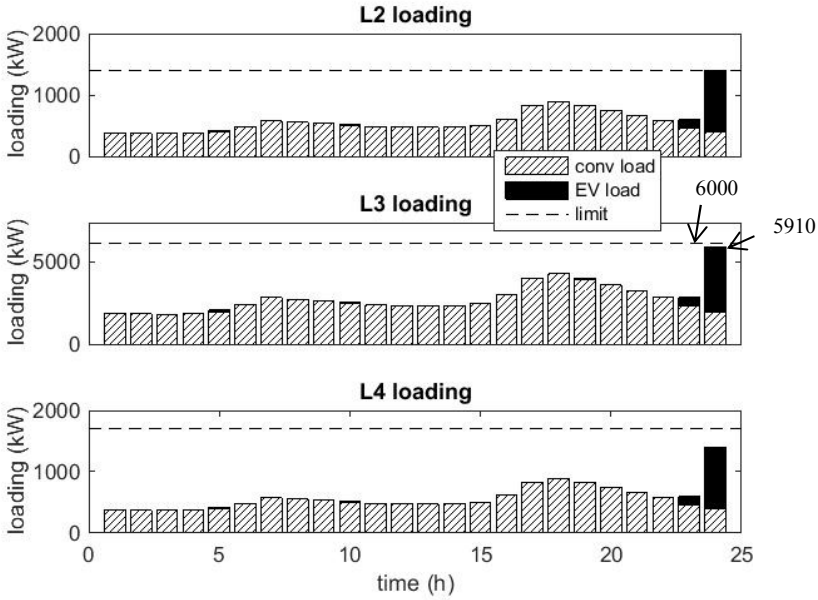

Fig. 4-6. The final energy planning results at the DSO side

4.5 Summary

This chapter presents the uncertainty management of the DT method with the presence of stochastic parameters of the flexible demands. The uncertainty comes from the fact that the DSO needs to forecast the behavior and energy requirement of the flexible demands since the DT method has a decentralized control architecture, where the aggregators make day-ahead energy plans independently without considering network constraints. With the uncertainty management, the robustness of

the DT method is enhanced that the probability of congestion (or an allowed congestion level) resulting from the DT method is under a predefined level.

The main limitation of the proposed uncertainty management method lies on the sensitivity analysis carried out in each iteration step, which has an assumption that the changes of the parameters are reasonably small. Therefore, the forecast errors should not be too big; otherwise, the accuracy of the sensitivity analysis will be compromised.

CHAPTER 5.

CONVEX RELAXATION OF AC OPF[5]

In all previous chapters, the DC OPF is employed to determine the DT where voltage constraints are neglected. This chapter will present a method to solve AC OPF through exact convex relaxation and its application for EV energy planning and DT determination where voltage constraints are included.

5.1 Introduction

Optimal power flow (OPF) is a very important optimization problem widely used in power system applications, such as congestion management, economic operation and control. The OPF considers the economic aspect of the power system components, and models the system at the steady state. There are two types of OPF, namely AC OPF [60] and DC OPF [61], resulting from AC and DC power flow models.

The DC OPF is a linear problem, and can be solved very efficiently and robustly by many commercial optimization solvers such as GAMS/CPLEX [38]. However, the solution of the DC OPF is only an approximation of the power system status. The accuracy will be poor if the R/X ratio is high in the studied system. Furthermore, even if the R/X ratio is low, if voltage constraints are an issue or if power factors are poor, congestion may be misestimated and the solutions from a DC optimization may be far from feasible.

The AC OPF is non-convex in its original form and is an NP-hard problem. General-purpose nonlinear programming (NLP) solvers can be used to solve the AC OPF. A number of dedicated methods were developed to solve the AC OPF problems in the last two decades, such as the trust region interior point algorithm [62],

[5] This chapter is based on paper: S. Huang, Q. Wu, J. Wang and H. Zhao, "A Sufficient Condition on Convex Relaxation of AC Optimal Power Flow in Distribution Networks", IEEE Tr. Power System, epub ahead.

[63], Lagrangian method [64], and primal-dual interior point method [65]. However, these methods normally obtain a locally optimal solution and it is not possible to know how far it is from the global optimum.

The convex relaxation method for solving the AC OPF was first presented in [66] as a second-order cone programming (SOCP) for radial networks and in [67] as a semidefinite programming (SDP) for meshed networks. For meshed networks, [68] has analyzed the exactness of the convex relaxation. However, the analysis is limited to pure resistive networks.

For radial networks, [69]–[71] have proposed several sufficient conditions for the convex relaxation to be exact. In [69], [70], it is proposed that if just one of any two connected nodes has a lower active power bound and no node has a lower reactive power bound, the convex relaxation is exact. However, these sufficient conditions may not be practical. In [71], the authors propose that if the upper bounds of the active and reactive power are not too large, the convex relaxation will be exact. The conclusion of [71] is promising as it allows a certain amount of feed-in power from renewables; however, the constraints of the AC OPF formulation in [71] miss the thermal and line capacity limits. The line capacity limit may lead to inexactness of the convex relaxation of the AC OPF as shown in [72]. Besides, the thermal and line capacity limits are necessary in many practical applications with renewable energy or flexible demands present, such as the congestion management applications in [19] and chapter 2. The details of the convex relaxation for the AC OPF can be found in [73], [74].

This chapter will propose a sufficient condition such that the convex relaxation of the AC OPF with all practical constraints is exact for radial networks, after the introduction of the basic idea of the convex relaxation and the discussion of the convexity of the sub-injection region. Next, the models for applications based on the convex relaxed AC OPF, such as optimal EV energy planning and DT calculations, will be presented. Then, case studies for the above applications are carried out and presented.

5.2 Convexity and Convex Relaxation of AC OPF in Distribution Networks

5.2.1 Convex Relaxation

A few assumptions are made for the convexity analysis and convex relaxation of AC OPF in distribution networks. Only radial networks are considered, i.e. the network $(\mathcal{N}, \mathcal{E})$ is a tree. Node 0 is chosen to be the slack node, which means voltage

$\mathbf{v}_0$ is fixed and given (normally 1 p.u.). In this chapter, $\mathbf{v}$ represents square magnitude of the original voltage v, while $\mathbf{i}$ represents square magnitude of the original current i, for the sake of using branch flow model. Node 0 is also the root of the tree graph and the direction of each edge is pointed towards the root, e.g. node j of edge (i, j) is the parent node of node i. In all practical applications in distribution networks, the (square) voltage limits of each node are $1 \pm \alpha\%$ p.u., where α can be a number between 8 and 21 (corresponding to the original voltage limits 1 +/- 0.04 p.u. and 1 +/- 0.1 p.u. respectively) depending on the standards. Therefore, it is reasonable to assume that $\overline{\mathbf{v}} > \mathbf{v}_0$ and $\underline{\mathbf{v}} < \mathbf{v}_0$ (assume that $\mathbf{v}_0$ =1 p.u. in this chapter).

The original AC OPF can be written as (5.1)-(5.9). The cost function f_0 of s_0 is listed separately in the objective function because there is a special requirement for f_0 (see the discussion in section 5.3.1). Constraints (5.2)-(5.5) describe the line flow through a branch flow model. Constraints (5.6)-(5.7) are the thermal and line capacity limits. Constraint (5.8) is the limit of the generator output or the demand, and (5.9) is the voltage limits.

OPF:
$$\min_{s,S,\mathbf{v},\mathbf{i},s_0} f_0(\mathrm{Re}(s_0)) + f_1(\mathrm{Re}(s)), \tag{5.1}$$

s.t.
$$S_{ij} = s_i + \sum_{h:h\to i} (S_{hi} - z_{hi}\mathbf{i}_{hi}), \forall (i,j) \in \mathcal{E}, \tag{5.2}$$

$$0 = s_0 + \sum_{h:h\to 0} (S_{h0} - z_{h0}\mathbf{i}_{h0}), \tag{5.3}$$

$$\mathbf{v}_i - \mathbf{v}_j = 2\,\mathrm{Re}(\overline{z}_{ij} S_{ij}) - |z_{ij}|^2 \mathbf{i}_{ij}, \forall (i,j) \in \mathcal{E}, \tag{5.4}$$

$$\mathbf{i}_{ij} = \frac{|S_{ij}|^2}{\mathbf{v}_i}, \forall (i,j) \in \mathcal{E}, \tag{5.5}$$

$$\mathbf{i}_{ij} \le \overline{\mathbf{i}}_{ij}, \forall (i,j) \in \mathcal{E}, \tag{5.6}$$

$$|S_{ij}| \le \overline{S}_{ij}, \forall (i,j) \in \mathcal{E}, \tag{5.7}$$

$$\underline{s_i} \le s_i \le \overline{s_i}, \forall i \in \mathcal{N}^+, \tag{5.8}$$

$$\underline{\mathbf{v}}_i \le \mathbf{v}_i \le \overline{\mathbf{v}}_i, \forall i \in \mathcal{N}^+, \tag{5.9}$$

where s_i (vector form: s) is the injection of plus node (other than node 0), named as sub-injection, s_0 is the injection of node 0, $S$is the reverse apparent power flow, z is the impedance, $\mathcal{E}$is the set of lines (edges) of the distribution network, $\mathcal{N}^+$ is the set of plus node (other than node 0), the direction of edge (i, j) or $h \to i$ is pointing to the root.

Its convex relaxation as an SOCP is shown below [75].

SOCP: (5.1),

s.t.

(5.2)-(5.4), (5.6)-(5.9), and

$$\mathbf{i}_{ij} \ge \frac{\left|S_{ij}\right|^2}{\mathbf{v}_i}, \forall (i, j) \in \mathcal{E}. \tag{5.10}$$

To clearly show the fundamental idea of the exactness of the convex relaxation as an SOCP, condition A1 for the convex relaxation to be exact is introduced first.

A1: The upper limit of the sub-injection fulfils: $\overline{s} \le 0$.

Though A1 is a special case of the condition proposed in [71], it needs to be proven to be a sufficient condition since the AC OPF has current and line capacity constraints compared to the one in [71].

The physical meaning of A1 is that all the nodes except the root will draw active and/or reactive power from the system. This condition is easy to understand and can be used in many applications where the generation from, e.g. renewable energy sources (RES), is less than the consumption.

5.2.2 Convexity of Sub-Injection Region

Before studying the exactness of the convex relaxation of the AC OPF, it is helpful to know more of the structure of the AC OPF. As shown in [69], [70], the feasible set $\mathcal{P}$ of the AC OPF, known as the feasible injection region of (p_0, p), is normally non-convex.

$$\mathcal{P} = \{p_0, p : (5.2)\text{-}(5.9)\}, \text{ where } (p_0, p) = \mathrm{Re}(s_0, s).$$

However, if the focus is put on the feasible injection region of p only, the feasible set can be proven to be convex. This partial injection region can be named as the feasible sub-injection region, denoted by $\mathcal{P}^+$ (the word "feasible" is omitted later on for brevity). Set $\mathcal{P}^+$ is an orthogonal projection of $\mathcal{P}$ to the subspace of vector p.

$$\mathcal{P}^+ = \{p : (5.2)\text{-}(5.9)\}, \text{ where } p = \mathrm{Re}(s).$$

In fact, a stronger statement regarding the sub-injection region with reactive power included, i.e. $\mathcal{S}^+$, can be made. Together with $\mathcal{S}$, they are defined as,

$$\mathcal{S}^+ = \{s : (5.2)\text{-}(5.9)\},$$

$$\mathcal{S} = \{s_0, s : (5.2)\text{-}(5.9)\}.$$

Proposition 5.1: $\mathcal{S}^+$ is convex if A1 holds.

The idea of focusing on the sub-injection region comes from the power flow calculation methods, such as the Newton-Raphson method or Forward-Backward method. In the power flow calculations, the power injection of the slack node is dependent on the power injections of other nodes, i.e. the sub-injection. In other words, only the sub-injections are free variables while the injection of node 0 is not. Since not all variables are free ones, $\mathcal{P}$ or $\mathcal{S}$ is not convex unless the relationships between these variables are linear, which is not true because of (5.5). Therefore, it is reasonable to put the focus on the sub-injection.

Proposition 5.1 will be proven after the proof of the following lemma.

Lemma 5.1: If A1 holds, then $\mathcal{S}^+ = \tilde{\mathcal{S}}^+$, i.e. the sub-injection region is equal to the convex-relaxed one, where

$$\tilde{\mathcal{S}} = \{s_0, s : (5.2)\text{-}(5.4),\ (5.6)\text{-}(5.10)\},$$

$$\tilde{\mathcal{S}}^+ = \{s : (5.2)\text{-}(5.4),\ (5.6)\text{-}(5.10)\}.$$

It is obvious that $\forall s \in \mathcal{S}^+$, then $s \in \tilde{\mathcal{S}}^+$ because of the relaxation. Therefore, there is $\mathcal{S}^+ \subseteq \tilde{\mathcal{S}}^+$. Then we only need to prove $\mathcal{S}^+ \supseteq \tilde{\mathcal{S}}^+$.

$\forall s \in \tilde{\mathcal{S}}^+$, $\exists (S^{(0)}, \mathbf{v}^{(0)}, \mathbf{i}^{(0)}, s_0^{(0)})$ such that $(s, S^{(0)}, \mathbf{v}^{(0)}, \mathbf{i}^{(0)}, s_0^{(0)})$ satisfies (5.2)-(5.4), (5.6)-(5.10). Then employ the following iteration method to construct a series of variables $(S^{(k)}, \mathbf{v}^{(k)}, \mathbf{i}^{(k)}, s_0^{(k)})$.

Reorganize the tree network as shown in Fig. 5-1 according to the depth (the distance to the root) of the nodes. Relabel the node number such that the deeper the node, the larger the number. In case of the same depth, the numbering is arbitrary.

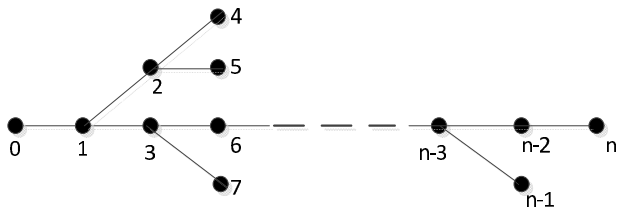

Fig. 5-1. Relabel the nodes according to their depth

Let $(S^{(k)}, \mathbf{v}^{(k)}, \mathbf{i}^{(k)}, s_0^{(k)}) = (S^{(0)}, \mathbf{v}^{(0)}, \mathbf{i}^{(0)}, s_0^{(0)}), \forall k \in \mathcal{Z}^-$, and $\mathbf{v}_0{}^{(k)} = \mathbf{v}_0$. Then in the k-th ($k > 0$) iteration, apply a Forward-Backward sweep algorithm as described below.

Forward: For $i = n, n-1, n-2, \cdots, 1$, and $(i, j) \in \mathcal{E}$,apply sequentially,

$$\begin{aligned} S_{ij}^{(k)} &= s_i + \sum_{h:h\to i} (S_{hi}^{(k)} - z_{hi}\mathbf{i}_{hi}^{(k)}) \\ &\geq s_i + \sum_{h:h\to i} (S_{hi}^{(k-1)} - z_{hi}\mathbf{i}_{hi}^{(k-1)}), \\ &= S_{ij}^{(k-1)} \end{aligned} \tag{5.11}$$

$$\mathbf{i}_{ij}^{(k)} = \frac{\left|S_{ij}^{(k)}\right|^2}{\mathbf{v}_i^{(k-1)}} \leq \frac{\left|S_{ij}^{(k-1)}\right|^2}{\mathbf{v}_i^{(k-1)}} \leq \frac{\left|S_{ij}^{(k-1)}\right|^2}{\mathbf{v}_i^{(k-2)}} \leq \mathbf{i}_{ij}^{(k-1)}. \tag{5.12}$$

For node 0,

$$\begin{aligned} s_0^{(k)} &= -\sum_{h:h\to 0} (S_{h0}^{(k)} - z_{h0}\mathbf{i}_{h0}^{(k)}) \\ &\leq -\sum_{h:h\to 0} (S_{h0}^{(k-1)} - z_{h0}\mathbf{i}_{h0}^{(k-1)}). \\ &= s_0^{(k-1)} \end{aligned} \tag{5.13}$$

Backward: For $i = 1,2,3,\cdots,n-1,n$, and $(i,j) \in \mathcal{E}$,apply,

$$\begin{aligned} \mathbf{v}_i^{(k)} &= \mathbf{v}_j^{(k)} + 2\,\mathrm{Re}(\overline{z}_{ij} S_{ij}^{(k)}) - \left|z_{ij}\right|^2 \mathbf{i}_{ij}^{(k)} \\ &\geq \mathbf{v}_j^{(k-1)} + 2\,\mathrm{Re}(\overline{z}_{ij} S_{ij}^{(k-1)}) - \left|z_{ij}\right|^2 \mathbf{i}_{ij}^{(k-1)}. \\ &= \mathbf{v}_i^{(k-1)} \end{aligned} \tag{5.14}$$

The above algorithm not only shows how to update the variables iteratively, but also ensures that the obtained series are monotonic.

In order to show the monotone of the series, let k=1. Since $\forall i > 0$, j is unique such that $(i,j) \in \mathcal{E}$, the subscription j is sometimes omitted in branch variables or parameters for brevity. In the forward sweep, when $i = n$, the inequality in (5.11) holds because it is a leaf node. Because $s_n \leq 0$ due to A1, $S_n^{(1)} \leq 0$. Therefore, the first inequality in (5.12) holds due to (5.11). Because $\mathbf{v}^{(k)} = \mathbf{v}^{(0)}$, $\forall k \leq 0$, the second inequality in (5.12) holds. According to (5.10), $\mathbf{i}_n^{(0)} \geq \left|S_n^{(0)}\right|^2 / \mathbf{v}_n^{(0)}$, the third inequality in (5.12) holds as well. When $i = n-1$, the inequality in (5.11) holds because (5.11) and (5.12) holds for any of its child nodes (if any) with the relabeling

shown in Fig. 5-1. Noticing that for any of its child nodes (if any), $S_{h,n-1}^{(1)} \le 0$, $z_{h,n-1} \ge 0$ and $\mathbf{i}_{h,n-1}^{(0)} \ge 0$, there is $S_{n-1}^{(1)} \le 0$. With (5.11) and $S_{n-1}^{(1)} \le 0$, the first inequality in (5.12) holds. Similar to the analysis for $i=n$, the second and third inequality in (5.12) holds for $i=n-1$. Similarly, it can be verified that (5.11) and (5.12) hold for the rest i. The analysis of (5.13) is the same as (5.11).

In the backward sweep, when $i=1$, the inequality holds in (5.14) because $\mathbf{v}_0^{(1)} = \mathbf{v}_0$, (5.11) and (5.12). When $i>1$, with the relabeling shown in Fig. 5-1, $\mathbf{v}_j^{(1)}$ is always determined before $\mathbf{v}_i^{(1)}$ and $\mathbf{v}_j^{(1)} \ge \mathbf{v}_j^{(0)}$ due to (5.14). Therefore, the inequality in (5.14) holds for $i = 2,3,...,n-1,n$, respectively. The second equation in (5.11), (5.13) and (5.14) holds because (5.2)-(5.4) hold for $(s, S^{(0)}, \mathbf{v}^{(0)}, \mathbf{i}^{(0)}, s_0^{(0)})$.

Because of the iterative nature of (5.11)-(5.14), it can be verified that they hold for $k = 2,3,4,\cdots$. Therefore, there exists the following monotonic series.

$$\{S^{(k)}\} : S^{(0)} \le S^{(1)} \le S^{(2)} \le \cdots \le 0$$

$$\{\mathbf{i}^{(k)}\} : \mathbf{i}^{(0)} \ge \mathbf{i}^{(1)} \ge \mathbf{i}^{(2)} \ge \cdots \ge 0$$

$$\{s_0^{(k)}\} : s_0^{(0)} \ge s_0^{(1)} \ge s_0^{(2)} \ge \cdots \ge 0$$

$$\{\mathbf{v}^{(k)}\} : \mathbf{v}^{(0)} \le \mathbf{v}^{(1)} \le \mathbf{v}^{(2)} \le \cdots \le \mathbf{v}_0$$

In the last series, $\mathbf{v}_0$ is a bound, because $2\mathrm{Re}(\bar{z}_{ij} S_{ij}^{(k)}) - |z_{ij}|^2 \mathbf{i}_{ij}^{(k)}$ in (5.14) is negative. Since all the above infinite monotonic series have bounds, they have limits. Denote $S^* = \lim_{k\to+\infty} S^{(k)}$, $\mathbf{i}^* = \lim_{k\to+\infty} \mathbf{i}^{(k)}$, $s_0^* = \lim_{k\to+\infty} s_0^{(k)}$ and $\mathbf{v}^* = \lim_{k\to+\infty} \mathbf{v}^{(k)}$.

It can be verified that $(s, S^*, \mathbf{v}^*, \mathbf{i}^*, s_0^*)$ fulfills the line flow constraints (5.2)-(5.5) and s satisfies (5.8). It can also be shown that $(S^*, \mathbf{v}^*, \mathbf{i}^*)$ satisfies constraints (5.6), (5.7) and (5.9) because of the assumption of $(S^{(0)}, \mathbf{v}^{(0)}, \mathbf{i}^{(0)})$ and the relation between $(S^{(0)}, \mathbf{v}^{(0)}, \mathbf{i}^{(0)})$ and $(S^*, \mathbf{v}^*, \mathbf{i}^*)$. Hence, $(s, s_0^*) \in \mathcal{S}$ and $s \in \mathcal{S}^+$. This means $\mathcal{S}^+ \supseteq \tilde{\mathcal{S}}^+$. It ends the proof of Lemma 5.1.

With Lemma 5.1 proved, Proposition 5.1 is easy to be proved because $\tilde{\mathcal{S}}^+$ is convex since it is an orthogonal projection of the convex set $\tilde{\mathcal{S}}$. Therefore, $\mathcal{S}^+$ is convex as well.

5.3 Exactness Analysis

5.3.1 Exactness of Convex Relaxation

In [71], a definition of the exactness of the convex relaxation is given as: the SOCP is exact if every of its optimal solutions satisfies the nonlinear line flow constraint (5.5). This requires (5.10) to be active at the optimal point and f_0 to be strictly increasing. However, this requirement can be relaxed.

It can be seen from the proof of Lemma 5.1 that any optimal point of the SOCP can be converted to a feasible point to the original AC OPF. In order to use this Lemma, the definition of the convex relaxation exactness is modified to an intuitive one: the SOCP is exact if the gap between the optimal values of the AC OPF and its convex relaxation is zero. It is shown below that f_0 is only required to be non-decreasing for the SOCP to be exact.

Proposition 5.2: When f_0 is non-decreasing, the SOCP is exact if A1 holds.

Proof: Assume that (s^*, s_0^*) is an optimal solution of the SOCP and the constructed feasible point of the AC OPF is (s^*, s_0^{**}), where s_0^{**} is the constructed feasible injection at node 0 using the Forward-Backward sweep method described in Section 5.2.2. It is obvious that,

$$f_0(\mathrm{Re}(s_0^*)) + f_1(\mathrm{Re}(s^*)) \le f_0(\mathrm{Re}(s_0^{**})) + f_1(\mathrm{Re}(s^*)),$$

because (s^*, s_0^*) is an optimal point of the SOCP. It is known from the construction process that $s_0^{**} \le s_0^*$. Therefore, if f_0 is non-decreasing, there is,

$$f_0(\mathrm{Re}(s_0^*)) + f_1(\mathrm{Re}(s^*)) \ge f_0(\mathrm{Re}(s_0^{**})) + f_1(\mathrm{Re}(s^*)).$$

Therefore, they are equal. It is obvious that (s^*, s_0^{**}) is an optimal solution of the AC OPF and it has the same optimal value. This ends the proof of Proposition 5.2.

An example of non-decreasing function f_0 is shown in Fig. 5-2. In fact, f_0 can be zero or constant, which is a special case of non-decreasing. In that case, the SOCP is equivalent to the AC OPF in terms of having the same sub-injection region and the same objective value for every feasible point. The significance of this argument can be seen from the EV planning application presented in [76], [77]. The charging service provider employs an OPF problem to make an optimal charging plan for the EVs with the network constraint information received from the DSO. The optimal planning considers only the cost of EV charging; therefore, the cost function f_0 is zero in this application. The authors of [76], [77] use an iterative method to solve the ACOPF problem, which is slow and complicated. However, employ the method proposed in this chapter, this application can be solved more efficiently (see section 5.4 and 5.6).

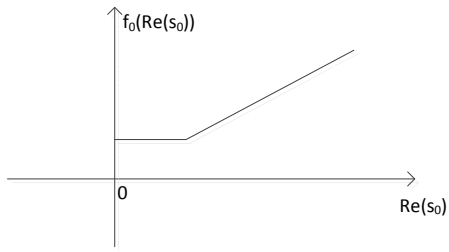

Fig. 5-2. An example of non-decreasing function f_0

5.3.2 The Proposed Sufficient Condition for Exactness

A new sufficient condition, denoted as C1, is proposed in this chapter, which also ensures an exact convex relaxation and a convex sub-injection region, but much wider applicability.

C1: The sub-injection s satisfies (5.15)-(5.18).

$$\hat{S}_{ij} = s_i + \sum_{h:h\to i} \hat{S}_{hi}, \forall (i,j) \in \mathcal{E}, \tag{5.15}$$

$$\hat{\mathbf{v}}_i - \hat{\mathbf{v}}_j = 2\,\mathrm{Re}(\bar{z}_{ij}\hat{S}_{ij}), \forall (i,j) \in \mathcal{E}, \tag{5.16}$$

$$\mathrm{Re}(\bar{z}_{ht}\hat{S}_{ij}) \le 0, \forall (i,j) \in \mathcal{E}, (h,t) \in \mathcal{E}_i, \tag{5.17}$$

$$\hat{\mathbf{v}}_i \le \overline{\mathbf{v}}_i, \forall i \in \mathcal{N}^+ . \tag{5.18}$$

In (5.16), $\hat{\mathbf{v}}_0 = \mathbf{v}_0$. Equation (5.15) and (5.16) are known as Linear Distribution Flow Model [78]. It can be verified that A1 is a special case of C1 (see section 5.3.3). Notice that the linear approximation of the voltage ($\hat{\mathbf{v}}$) and the reverse power ($\hat{S}$) is an upper bound of the voltage ($\mathbf{v}$) and reverse power (S). The physical meaning of (5.17) can be interpreted as that the network does not allow both active and reactive reverse power flow simultaneously on its non-leaf lines (neither of the line ends is a leaf node). C1 is suitable for the applications with light reverse power flow, such as EV planning problems with reactive power support functions or with capacitor banks (see the case study in section 5.6.3). Equation (5.18) will be always satisfied if the reverse power flow is not heavy.

Proposition 5.3: When f_0 is non-decreasing, the SOCP is exact if C1 holds.

Proof: In order to prove the exactness of the SOCP, the key is to check the monotone of the constructed series, $\{S^{(k)}\}$, $\{\mathbf{i}^{(k)}\}$, $\{s_0{}^{(k)}\}$, $\{\mathbf{v}^{(k)}\}$, using the Forward-Backward sweep method.

With k=1, for $i = n, n-1, n-2, \cdots, 1$, and $(i, j) \in \mathcal{E}$, there is,

$$\begin{aligned} \Delta S_{ij} &= S_{ij}{}^{(1)} - S_{ij}{}^{(0)} = \sum_{(h,t)\in\mathcal{E}_i} (-z_{ht}(\mathbf{i}_{ht}{}^{(1)} - \mathbf{i}_{ht}{}^{(0)}) \\ &= \sum_{(h,t)\in\mathcal{E}_i} (-z_{ht}\Delta\mathbf{i}_{ht}) \\ &\ge 0 \end{aligned} , \tag{5.19}$$

$$\begin{aligned}\Delta\left|S_{ij}\right|^2 &= \left|S_{ij}^{(1)}\right|^2 - \left|S_{ij}^{(0)}\right|^2 = (P_{ij}^{(1)})^2 + (Q_{ij}^{(1)})^2 \\ &\quad -(P_{ij}^{(0)})^2 - (Q_{ij}^{(0)})^2 \\ &= (\Delta P_{ij})(P_{ij}^{(1)} + P_{ij}^{(0)}) \\ &\quad +(\Delta Q_{ij})(Q_{ij}^{(1)} + Q_{ij}^{(0)}) \\ &\le (\Delta P_{ij})(2\hat{P}_{ij}) + (\Delta Q_{ij})(2\hat{Q}_{ij}) \\ &= 2(\sum_{(h,t)\in\mathcal{E}_i} -r_{ht}\Delta\mathbf{i}_{ht})\hat{P}_{ij} + \\ &\quad 2(\sum_{(h,t)\in\mathcal{E}_i} -x_{ht}\Delta\mathbf{i}_{ht})\hat{Q}_{ij} \\ &= 2\sum_{(h,t)\in\mathcal{E}_i} -\Delta\mathbf{i}_{ht}(r_{ht}\hat{P}_{ij} + x_{ht}\hat{Q}_{ij}) \le 0\end{aligned} \quad , \tag{5.20}$$

$$\begin{aligned}\Delta\mathbf{i}_{ij} = \mathbf{i}_{ij}^{(1)} - \mathbf{i}_{ij}^{(0)} &\le \frac{\left|S_{ij}^{(1)}\right|^2}{\mathbf{v}_i^{(0)}} - \frac{\left|S_{ij}^{(0)}\right|^2}{\mathbf{v}_i^{(-1)}} \\ &\le \frac{\left|S_{ij}^{(1)}\right|^2 - \left|S_{ij}^{(0)}\right|^2}{\mathbf{v}_i^{(0)}} = \frac{\Delta\left|S_{ij}\right|^2}{\mathbf{v}_i^{(0)}} \le 0\end{aligned} \quad . \tag{5.21}$$

Inequality constraints (5.19)-(5.21) can be verified sequentially, i.e. after verify all of them for $i=n$, start over again to verify (5.19)-(5.21) for $i=n-1$. For node 0, there is,

$$\begin{aligned}\Delta s_0 = s_0^{(1)} - s_0^{(0)} &= \sum_{ht\in\mathcal{E}} z_{ht}(\mathbf{i}_{ht}^{(1)} - \mathbf{i}_{ht}^{(0)}) \\ &= \sum_{ht\in\mathcal{E}} z_{ht}\Delta\mathbf{i}_{ht} \\ &\le 0\end{aligned} \quad . \tag{5.22}$$

For $i=1,2,3,\cdots,n-1,n$ and $(i,j)\in\mathcal{E}$,

$$\begin{aligned}\Delta\mathbf{v}_i = \mathbf{v}_i^{(1)} - \mathbf{v}_i^{(0)} &= \Delta\mathbf{v}_j + 2\,\mathrm{Re}(\overline{z}_{ij}\Delta S_{ij}) - \left|z_{ij}\right|^2\Delta\mathbf{i}_{ij} \\ &\ge 0\end{aligned} \quad . \tag{5.23}$$

Therefore, the voltage is increasing, which supports the first inequality in (5.21). The first inequality in (5.20) is due to the property of $\hat{P}_{ij}$ and $\hat{Q}_{ij}$ (they are upper limits). The second inequality in (5.20) is due to (5.17).

It is not difficult to verify that for $k \geq 2$, (5.19)-(5.23) are valid. Notice that $\mathbf{v}^{(k)} \leq \hat{\mathbf{v}} \leq \overline{\mathbf{v}}$, the new series will be,

$$\{S^{(k)}\}: S^{(0)} \leq S^{(1)} \leq S^{(2)} \leq \cdots \leq \hat{S},$$

$$\{\mathbf{i}^{(k)}\}: \mathbf{i}^{(0)} \geq \mathbf{i}^{(1)} \geq \mathbf{i}^{(2)} \geq \cdots \geq 0,$$

$$\{s_0{}^{(k)}\}: s_0{}^{(0)} \geq s_0{}^{(1)} \geq s_0{}^{(2)} \geq \cdots \geq \hat{s}_0,$$

$$\{\mathbf{v}^{(k)}\}: \mathbf{v}^{(0)} \leq \mathbf{v}^{(1)} \leq \mathbf{v}^{(2)} \leq \cdots \leq \hat{\mathbf{v}}.$$

Therefore, the above series have limits and the limits satisfy the constraints of the OPF. Moreover, the SOCP is exact. This ends the proof of Proposition 5.3.

5.3.3 Discussion on Sufficient Condition A1, B1 and C1

The sufficient condition proposed in [71], named as B1, is rewritten in this chapter.

B1: The positive linear approximation of the reverse power based on the upper limit of the sub-inject $\overline{s}$ fulfils (5.24), and the linear approximation of the voltage based on the sub-injection s fulfils (5.18). And

$$A_{i_1} A_{i_2} A_{i_3} \ldots A_{i_{n-1}} u_{i_n} > 0, \forall i_1 \sim i_n, i_1 > 0, \tag{5.24}$$

where i_x is the parent node of i_{x+1},

$$A_i = I - \frac{2}{\underline{\mathbf{v}}_i} \begin{pmatrix} r_i \\ x_i \end{pmatrix} \left((\hat{P}_i(\overline{p}))^+ \quad (\hat{\mathrm{Q}}_i(\overline{q}))^+ \right),$$

$u_i = \begin{pmatrix} r_i \\ x_i \end{pmatrix}$, i represents $i_1 \sim i_n$,

symbol a^+ means $\max(a,0)$.

It can be seen that A1 is a special case of B1 given that $r, x > 0$. According to A1, $\overline{s} \le 0$. There are $(\hat{P}_i(\overline{p}))^+ = 0$ and $(\hat{\mathrm{Q}}_i(\overline{q}))^+ = 0$. Therefore, $A_i = I$ and the left side of (5.24) equals to u_i, which is strictly positive since $r, x > 0$. Equation (5.18) is also satisfied because $\hat{\mathbf{v}} \le \mathbf{0} < \overline{\mathbf{v}}$.

A1 is also a special case of C1. Since $\overline{s} \le 0$, there is $s \le 0$. Therefore, $\hat{S} \le 0$ and the left side of (5.17) is always negative. Equation (5.18) is satisfied because $\hat{\mathbf{v}} \le \mathbf{0} < \overline{\mathbf{v}}$. Comparing to A1, C1 allows active reverse power flow or reactive reverse power flow while A1 doesn't allow any reverse power flow.

The differences between B1 and C1 are analyzed below. First of all, it should be emphasized that B1 is a sufficient condition for the exactness of the SOCP without line flow constraints while C1 is proposed for the case with line flow constraints.

Secondly, for B1 to be a sufficient condition, the cost function $\mathtt{f}_0$ is required to be strictly increasing, while for the case with C1, it only needs to be non-decreasing.

Thirdly, there is no requirement of the impedance for C1 (and A1 as well), but it is required that $r, x > 0$ for B1. This is because the 'greater than' symbol is used in (5.24).

At last, B1 does not imply C1 and vice versa. According to B1, the reverse power flow has an obvious upper limit, $\hat{P}_i(\overline{p}) < \frac{\underline{\mathbf{v}}_i}{2r_i}$ and $\hat{\mathrm{Q}}_i(\overline{q}) < \frac{\underline{\mathbf{v}}_i}{2x_i}$, due to (5.24) and the definition of A_i. However, according to C1, if the active power flow is very high, the allowed reactive reverse power flow will also be very high, without an explicit upper limit. On the other hand, B1 may allow both active and reactive reverse power flow at the same time. However, C1 does not allow both active and reactive reverse power flow at the same time.

5.4 AC OPF for Multi-Period EV Energy Planning

In this section, the AC OPF with EV charging planning over multi-period is described considering the line flow and voltage limits.

OPF-EV:
$$\min_{e,s,S,\mathbf{v},\mathbf{i},s_0} g = \sum_{t\in\mathcal{T}} (c_t \sum_{k\in\mathcal{V}} e_{kt}), \tag{5.25}$$

s.t.
$$S_{ijt} = s_{it} + \sum_{h:h\to i} (S_{hit} - z_{hi}\mathbf{i}_{hit}), \forall (i,j)\in\mathcal{E}, t\in\mathcal{T}, \tag{5.26}$$

$$0 = s_{0t} + \sum_{h:h\to 0} (S_{h0t} - z_{h0}\mathbf{i}_{h0t}), \forall t\in\mathcal{T}, \tag{5.27}$$

$$\mathbf{v}_{it} - \mathbf{v}_{jt} = 2\,\mathrm{Re}(\overline{z}_{ij}S_{ijt}) - \left|z_{ij}\right|^2 \mathbf{i}_{ijt}, \forall (i,j)\in\mathcal{E}, t\in\mathcal{T}, \tag{5.28}$$

$$\mathbf{i}_{ijt} = \frac{\left|S_{ijt}\right|^2}{\mathbf{v}_{it}}, \forall (i,j)\in\mathcal{E}, t\in\mathcal{T}, \tag{5.29}$$

$$\mathbf{i}_{ijt} \le \overline{\mathbf{i}}_{ij}, \forall (i,j)\in\mathcal{E}, t\in\mathcal{T}, \tag{5.30}$$

$$\left|S_{ijt}\right| \le \overline{S}_{ij}, \forall (i,j)\in\mathcal{E}, t\in\mathcal{T}, \tag{5.31}$$

$$\underline{\mathbf{v}}_i \le \mathbf{v}_{it} \le \overline{\mathbf{v}}_i, \forall i\in\mathcal{N}^+, t\in\mathcal{T}, \tag{5.32}$$

$$\mathrm{Re}(s_{it}) = -\sum_{k\in\mathcal{V}_i} e_{kt} - \mathrm{Re}(b_{it}), \forall i\in\mathcal{N}^+, t\in\mathcal{T}, (\rho_{i,t}), \tag{5.33}$$

$$\mathrm{Im}(s_{it}) = -\mathrm{Im}(b_{it}), \forall i\in\mathcal{N}^+, t\in\mathcal{T}, \tag{5.34}$$

$$\sum_{t\in\mathcal{T}_i} e_{kt} = d_k, \forall k\in\mathcal{V}, \tag{5.35}$$

$$0 \le e_{kt} \le \overline{e}_k a_{kt}, \forall k\in\mathcal{V}, t\in\mathcal{T}, \tag{5.36}$$

where e_{kt} is the EV charging power, $\overline{e}_k$ is the upper limit of the charging power, d_k is the total energy requirement of each EV, a_{kt} is the availability of EV, b_{it} is the total fixed consumption, $\mathcal{V}$ is the set of EVs, $\mathcal{T}$ is the set of planning periods.

The objective function is to minimize the total charging cost for the EVs. The EV charging related constraints (5.33)-(5.36) are all linear. Only (5.35) is coupling the

multiple periods, which is to satisfy the total charged energy required by each EV. Constraint (5.36) is to limit the charging power, which will lead to the limit of s_{it} through (5.33). Because of (5.29), the OPF-EV problem is nonconvex, which is very hard to solve. Similar to the method employed in the single period OPF, (5.29) can be relaxed. The corresponding SOCP is written below.

SOCP-EV: (5.25) s.t. (5.26)-(5.28), (5.30)-(5.36), and

$$\mathbf{i}_{ijt} \geq \frac{\left|S_{ijt}\right|^2}{\mathbf{v}_{it}}, \forall (i,j) \in \mathcal{E}, t \in \mathcal{T} \ . \tag{5.37}$$

Proposition 5.4: The SOCP-EV is exact if C1 holds.

Proof: Let (e^*, s^*) be an optimal solution of the SOCP-EV, and g^* is the optimal value. For any given period t, the corresponding sub-injection s_t^* can be used to construct a feasible power flow solution, denoted as $(S_t^*, \mathbf{v}_t^*, \mathbf{i}_t^*, s_{0t}^*)$, to the OPF-EV that satisfies the constraints (5.26)-(5.32). Therefore, the solution $(e^*, s^*, S^*, \mathbf{v}^*, \mathbf{i}^*, s_0^*)$ is feasible to the OPF-EV. It is obvious that the objective value for the OPF-EV based on this feasible solution is also equal to g^*. Hence, g^* is the optimal value of the OPF-EV because g^* is a lower bound of the optimal value due to the relaxation. This ends the proof of Proposition 5.4. Notice that, B1 cannot be used to determine whether the SOCP-EV is exact, not only because there are line flow constraints (5.30) and (5.31), but also there is no $\mathtt{f}_0$.

In some application cases with different market and business assumptions, the line losses are considered in the cost function. Then the objective function (5.25) can be replaced with the following function.

$$g = \sum_{t \in \mathcal{T}} c_t \, \mathrm{Re}(s_{0t}) \cdot \tag{5.38}$$

For these applications, a conclusion similar to Proposition 5.4 can be drawn. The proof is not difficult and is neglected for brevity.

5.5 AC OPF for DT determination

As discussed in Chapter 2, quadratic terms are needed in order to determine the DT without causing multiple-response problems in the DT method. Only the optimal energy planning at the DSO side is needed, which has the same model as OPF-EV defined in section 5.4, except that the objective function should be slightly modified. The model for determining DT through AC OPF is defined below, names as OPF-DT, where the quadratic terms have a very small coefficient β such that they can make the optimization problem strict convex without changing the total cost too much.

OPF-DT: $$\min_{e,s,S,\mathbf{v},\mathbf{i},s_0} g = \sum_{t\in\mathcal{T}} (\beta_t \sum_{k\in\mathcal{V}} {e_{kt}}^2 + c_t \sum_{k\in\mathcal{V}} e_{kt}) , \tag{5.39}$$

s.t.

(5.26)-(5.36).

The corresponding convex relaxed model is defined as below.

SOCP-DT: (5.39)

s.t.

(5.26)-(5.28), (5.30)-(5.37).

The DT equals to the Lagrangian multiplier of (5.33), i.e. $\rho_{i,t}$. Considering the strict convexity of SOCP-DT and the exactness between OPF-DT and SOCP-DT, it can be proven through the same method from Chapter 2 that the summarized energy planning at the aggregator side based on the above DT will be the same as the solution of SOCP-DT and OPF-DT. Hence, the DT method for congestion management based on the convex relaxed AC OPF model is valid.

5.6 Case Studies

Case studies were conducted using the Danish driving pattern and the Bus 4 distribution system of the RBTS [36] and the IEEE 123 node feeder [79]. The details of the case studies are presented in this section.

5.6.1 Grid Data

The single line diagram of the Bus 4 distribution network is shown in Fig. 5-3. Line segments and nodes of the feeder one are labeled in Fig. 5-3, among which L2-1, L4-3, L6-5, L8-7, L9-7, L11-10, and L12-10 refer to the transformers connecting the corresponding load points. Notice that the labelling follows the rules mentioned in section 5.2.2. The detailed data of these load points are listed in Table 5-1. The reactive power consumption is assumed to be 10% of the active power consumption for each load point. The peak conventional demands of residential customers occur at 18:00 when people come home and start cooking (shown in Fig. 5-4).

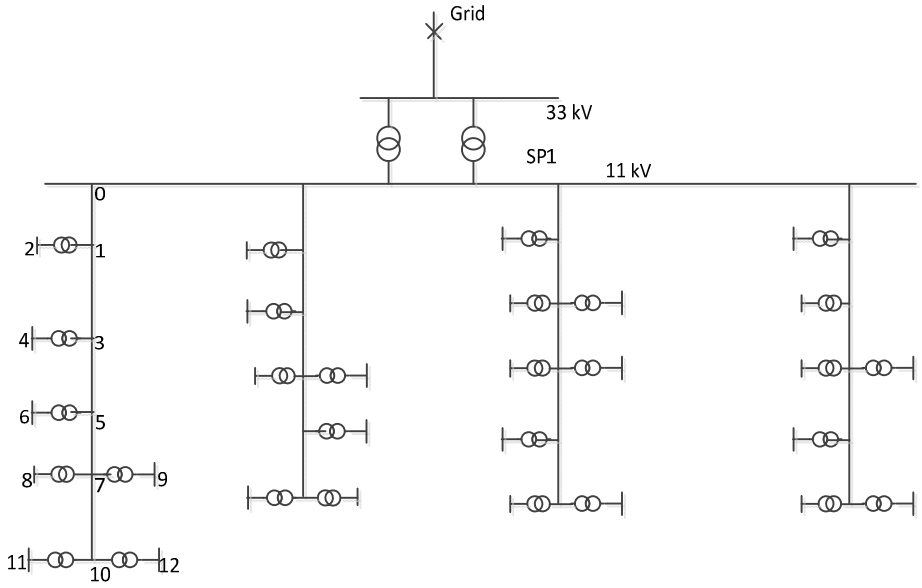

Fig. 5-3. Single line diagram of the distribution network

TABLE 5-1. LOAD POINT DATA

load points	customer type	peak conv. load / point (kW)	peak conv. load / point (kVar)	number of customers per point
node 2,4,6,8	residential	886.9	88.69	200
node 9	residential	813.7	81.37	200
node 11,12	commercial	671.4	67.14	10

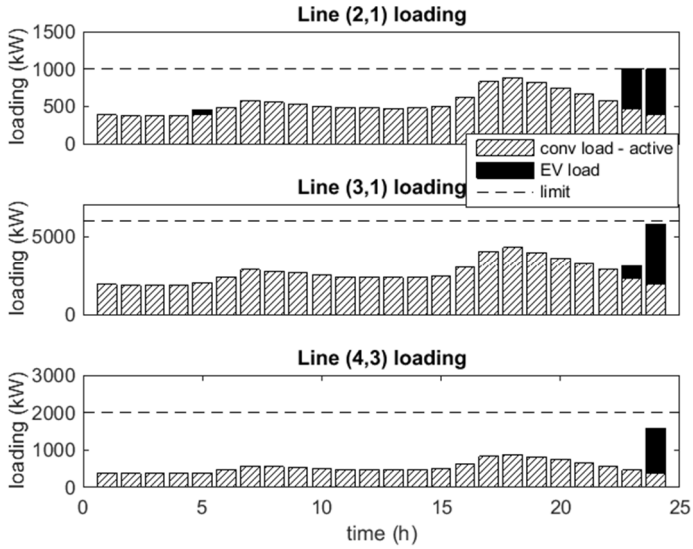

Fig. 5-4. Active power sharing of EV and conventional loads, where active power losses are very small

Voltage limits are set to be $\pm 5\%$ p.u., then the limits of the square voltage will be $\underline{v} = 0.95^2$ and $\overline{v} = 1.05^2$. Assume that $v_0 = 1$. The line parameters including resistance, reactance and line capacity limits can be seen in Table 5-2. The prices for the EV charging are the predicted day-ahead market system price, as shown in Appendix A.

TABLE 5-2. LINE PARAMETERS

From	To	r (ohm)	x (ohm)	x/r ratio	Capacity limit (kVA)
1	0	0.176	0.52	2.954	8000
2	1	0.4	2.4	6	1000
3	1	0.22	0.66	3	6100
4	3	0.4	2.4	6	2000
5	3	0.264	0.64	2.424	6000
6	5	0.4	2.4	6	2000
7	5	0.176	0.56	3.181	6000
8	7	0.4	2.6	6.5	2000
9	7	0.48	2.8	5.833	2000
10	7	0.22	0.6	2.727	6000
11	10	0.4	2.44	6.1	2000
12	10	0.44	2.8	6.363	2000

5.6.2 EV Data

Assume there are 1000 EVs in the network (except for Case Study Four), i.e., one EV per residential customer. The key parameters of the EVs are listed in the table in Appendix A. The EV availability (available for charge per hour) is also shown Appendix A.

5.6.3 Case Study Results

The simulation is carried out using CVX, a package for specifying and solving convex programs [80], [81]. CVX is a toolbox in Matlab and it supports several SOCP solvers, such as SeDuMi, SDPT3, Gurobi and MOSEK. In this chapter, CVX/MOSEK is chosen, and the platform is a personal computer (a laptop) with Intel Core i5-4310U, 2 GHz, 8 GB RAM, windows 64-bit Operation System.

5.6.3.1 Case Study One

The first case study is the application of EV energy planning. CVX can transform constraints (5.31) and (5.37) in SOCP-EV to conic ones, and thereby solved by the SOCP solvers. The optimal solution of the OPF-EV can be recovered using the Forward-Backward sweep method and used to describe the operation status of the network, as shown in Fig. 5-4, Fig. 5-5 and Fig. 5-6.

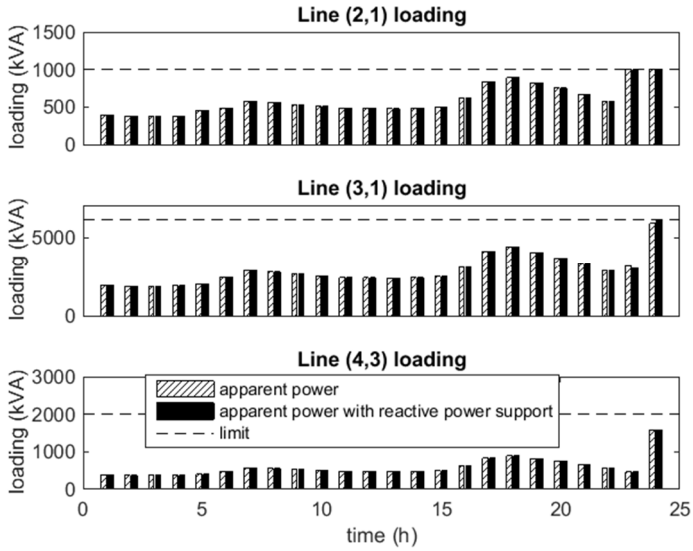

Fig. 5-5. Apparent power of three line segments

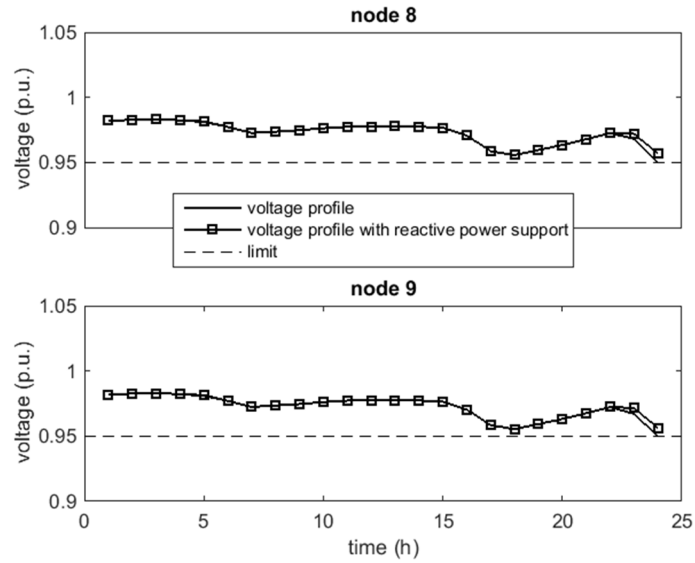

Fig. 5-6. Voltage profiles of node 8 and 9, which are critical node in the feeder

It can be seen from Fig. 5-4 that most of the EV charging loads are allocated at the hour with the lowest price, i.e., hour 24. However, due to the availability and the line capacity limit, part of the loads is allocated to the hours with the second and third lowest prices. Due to small resistances, the line losses are very small, which

is about 1%. Hence, it is not shown in the figure. The sharing of EV loads and conventional loads are calculated using the linear model, i.e. (5.15), and the losses are the gaps between the linear model and the full model.

The apparent power (magnitude) profile of three line segments is shown in Fig. 5-5. It can be seen that the apparent power is below or equal to the line capacity limit. Due to the heavy EV charging loads, the capacity limit of L2-1 is reached at hour 23 and hour 24. The apparent power of L3-1 is below the capacity limit at hour 24 because the voltage limit is hit first as shown in Fig. 5-6.

5.6.3.2 Case Study Two

The second case study is to calculate the DT through convex relaxed AC OPF. The parameters are the same as the first case study. The calculated DTs are shown in Table 5-3. Because of the line congestion of Line(2,1) as shown in Fig. 5-4 and Fig. 5-5, DTs are not zero for Node 2 at hour 23 and 24. Due to the fact that the voltage limits of Node 8 and 9 are bounded at hour 24 as shown in Fig. 5-6, the DTs are not zero for all nodes at hour 24.

TABLE 5-3. CALCULATED DT
(DKK/MWH, DT NOT SHOWN IN THIS TABLE IS ZERO)

time	**23**	**24**
Node 2	7.01	77.01
Node 4	0.00	27.11
Node 6	0.00	46.25
Node 8	0.00	70.00
Node 9	0.00	70.00

5.6.3.3 Case Study Three

A third case study was carried out, where the EVs were allowed to produce reactive power up to 10% of its active power, to test the reactive power support function of the EVs and the validity of C1. With the feed-in of reactive power, the voltage profile is improved (see Fig. 5-6), and the total cost is reduced a bit because the EVs are able to consume more energy at the lowest price up to the limit of the line capacity as shown in Fig. 5-5.

5.6.3.4 Case Study Four

At last, the efficiency of the SOCP-EV model was tested on distribution networks of different complexity scales. The results were tabularized in Table 5-4. The first simulation is the case described above. The simulation focuses on the first feeder of the network shown in Fig. 5-3. The 11-kV bus was deemed as the root node. Because it is a multi-period optimal planning problem, the number of scalar variables depends on the number of EVs and the number of planning periods (24 here). The optimizer only took 0.39 seconds to finish the optimization. The second simulation was done on the whole distribution network. The 33-kV bus was deemed as the root node. The optimizer took 1.56 seconds to finish the optimization. The third simulation was done with the IEEE 123 node test feeder [79]. The number of EVs was increased to 20000 and the total optimization time is 12.09 seconds for such a complicated feeder with high penetration of EVs.

TABLE 5-4. SOCP-EV MODEL EFFICIENCY TEST

Simulation	1	2	3
Number of nodes (exclude root)	12	50	123
Number of EVs	1000	4000	20000
Constraints	3280	13576	43592
Cones	576	2400	5904
Scalar variables	28217	113249	532521
Time (s)	0.39	1.56	12.09

5.7 Summary

This chapter has proven that if A1 holds, i.e., there is no net injection power, the sub-injection region will be convex. Moreover, if the cost function is non-decreasing, the convex relaxation of the AC OPF of distribution networks with line constraints will be exact under A1. When this condition holds, the NP-hard AC OPF of distribution networks can be solved through an SOCP. In order to expand the applicability of the convex relaxed AC OPF in distribution networks with line constraints as an SOCP, a weaker condition C1 is proposed and proved, which allows that the reverse power flow is only active or reactive, or none. The case study demonstrates the exactness of the convex relaxed AC OPF and the efficacy of using the convex relaxed AC OPF for solving a multi-period EV planning problem and determining DT with line and voltage constraints.

CHAPTER 6.

DS METHOD FOR CONGESTION MANAGEMENT[6]

In this chapter, the dynamic subsidy method will be presented, which is opposite to the DT method presented in previous chapters.

6.1 Introduction

The DT method is economically efficient for alleviating congestion in distribution networks, because only those consumers causing congestion pay the DT. However, considering the regulations of distribution networks in many countries nowadays [82], there are regulatory issues to deploy the DT method. Firstly, from the perspective of the customers, the DT method may not be viewed as a fair method, because the customers might have to accept different tariff rates because of their locations in the network. This is against the non-discrimination rules specified by the regulations. Secondly, the flexible demands that help alleviate congestion pay the DTs instead of getting rewards.

A monetary incentive based method was proposed in [23] for coordinating and rescheduling the flexible demands, where the capacity limit of the distribution networks was taken into account. With this method, the flexible demands will be rewarded if they are willing to reduce the consumption during the congestion hours. However, the method to determine a proper incentive is not optimal. This is because the authors of [23] choose the best one from a finite set of predefined incentives, however, it is not necessarily the optimal one. The rebound effect, i.e. the reduced flexible demand will cause an increase in a future period, is not considered because the method only handles one period at each execution. Another issue is that it does not consider the location of the incentives. The demand responses for

[6] This chapter is based on paper: S. Huang and Q. Wu, "Dynamic Subsidy Method for Congestion Management in Distribution Networks", IEEE Tr. Smart Grid, epub ahead.

solving congestion are usually needed at specific areas or nodes. Locational incentives can improve the efficiency of solving congestion because the responses of the flexible demands from uncritical areas or nodes (e.g. the upstream nodes to the congested point) have a limited effect. These issues also exist in other previous studies, such as in [20], [22].

In order to resolve the issues of the abovementioned demand response methods, this chapter proposes a dynamic subsidy (DS) method to handle the potential congestion problems in distribution networks. Same as the DT method, the DS method realizes the congestion management in a decentralized manner. The DS motivates the aggregators to re-profile their energy plans such that the network constraints are respected. The DS is a timed subsidy for the next day paid by the DSO to the aggregators while the DT is a tariff collected by the DSO from the aggregators. In the DS method, the DSO provides subsidies to the aggregators who are willing to consume the energy at the designated hours, when there are available capacities predicted by the DSO. As a result, the energy consumptions at "peak" hours or potential congestion hours are under the limits.

The motivations of proposing the DS method are summarized as the follows. Firstly, like other incentive-based methods, the DS method does not have regulatory issues. The DSO normally needs an official approval from the authorities to charge new types of tariffs. However, the DSO's purchase of services from the customers does not require a special approval. There isn't a direct statement in regulations about whether it is allowed for a DSO to pay DS. The idea is that paying DS is an alternative method to reinforcing the network to avoid congestion. The DSO should have some calculations to make sure that the expenditure on paying DS is less than the (annualized) cost of the network reinforcement; otherwise the DSO should choose to reinforce the network. In this sense, the DSO should be able to convince the regulators that this expenditure is due to a reasonable substitute to the investment on infrastructures.

Secondly, the DS determined by the DSO is always limited between zero and the maximum predicted energy price. The DT is unlimited in theory. In practice, the upper limit of the DT can be set, however, the efficacy of the DT method will be compromised [59]. Also, unlike other incentive-based methods, it provides an efficient method to determine the DS without iterative information exchanges between the DSO and the aggregators. And finally, it does not incur the rebound effect of the DR while other incentive-based DR methods do.

In this chapter, the DS concept, mathematical formulation of the DS method and the feasibility study are firstly presented. Then, the calculation of the DS through optimization is described. Afterwards, the analysis and comparison of the DS method with the DT method is presented. At last, case studies are presented and discussed.

6.2 DS Concept

In this section, the market mechanism of the DS method for congestion management of distribution networks is presented. Afterwards, the mathematical formulation of the DS concept is described.

6.2.1 Decentralized Congestion Management through the DS Concept

The DS method for congestion management in distribution networks is based on the day-ahead energy market mechanism and can be seamlessly integrated into the day-ahead energy market (spot market in Nordic). This is the same as the DT method, except that the DS is an income for the aggregators. The DS is a price signal from the DSO to the aggregators, which implies that the DSO has only an indirect control of the aggregators. The aggregators have the freedom of choosing their own optimal energy planning for the flexible demands. However, it is assumed that the aggregators as business units are economically rational and pursue the maximum profits. The DSO needs to predict the energy requirements of the flexible demands and determine an appropriate set of DSs to motivate the aggregators to re-profile the flexible demands as wished by the DSO. In this sense, the DS method for congestion management is a decentralized control method.

The process of the decentralized congestion management by using the DS method is described as follows. Firstly, the DSO obtains the flexible demand data, such as energy requirements and the availability, by its own prediction or from aggregators. The DSO also needs to collect the network information from its own sources and obtain the predicted day-ahead energy price from third parties. Secondly, a set of DSs is calculated through an optimal energy planning respecting the network constraints, and the DSs are published to all the aggregators before the closure of the day-ahead energy market. Thirdly, after receiving the DSs, the aggregators make their own optimal plans independently with the predicted energy prices, a fixed cost (in this chapter, it refers to fixed grid tariffs and tax) and the DSs. At last, the aggregators submit their energy plan/bids to the day-ahead energy market.

The DSO may use the money collected from the customers through distribution grid tariffs to pay the DS. The DSO has the right to collect grid tariffs to cover the cost of operation, maintenance and reinforcement of the distribution grid. The DSO pays the DS in order to solve congestion problems, which can effectively postpone the very costly reinforcement of the grids. Therefore, the DS method is of the interest of both the DSO and the customers because all the costs are ultimately paid by the customers. This also means that the congestion, wherever it is in the distribution grid, is solved by the contribution of every customer.

6.2.2 Mathematical Formulation of DS Method

6.2.2.1 Formulation at the aggregator side

At the aggregator side, the formulations of the DS and DT methods are similar. The aggregators are purely economic units without any consideration of the network constraints. They make energy plans based on the requirements of the flexible demands and the prices, including the energy price, and the fixed cost (such as grid tariffs and tax), and the DS (or DT). In both the DS and the DT methods, the aggregators use the following optimization problem to determine the energy plans of EVs and HPs in the day-ahead energy market. For aggregator i,

$$\begin{aligned}\min_{p_{i,t},\hat{p}_{i,t}} \quad & \sum_{t\in T}\frac{1}{2}{p_{i,t}}^{T}B_{i,t}p_{i,t}+(c_t\mathbf{1}+{E_i}^{T}r_t)^{T}p_{i,t}+\\ & \frac{1}{2}{\hat{p}_{i,t}}^{T}B_{i,t}\hat{p}_{i,t}+(c_t\mathbf{1}+{E_i}^{T}r_t)^{T}\hat{p}_{i,t}\end{aligned} \tag{6.1}$$

subject to,

$$e_i^{\min}\le\sum_{t\_\le t}(p_{i,t\_}-d_{i,t\_})+e_{i0}\le e_i^{\max},\forall \mathrm{t}\in\mathcal{T},(\mu_{i,t}^{-},\mu_{i,t}^{+}), \tag{6.2}$$

$$p_{i,t}^{\min}\le p_{i,t}\le p_{i,t}^{\max},\quad \forall t\in\mathcal{T},(\varsigma_{i,t}^{-},\varsigma_{i,t}^{+}), \tag{6.3}$$

$$K_{i,t}^{a,\min}\le\sum_{t\_\le t}A_{i,t,t\_}\hat{p}_{i,t\_}+u_{i,t}\ \le\ K_{i,t}^{a,\max},\forall \mathrm{t}\in\mathcal{T},(\hat{\mu}_{i,t}^{-},\hat{\mu}_{i,t}^{+}), \tag{6.4}$$

$$\hat{p}_{i,t}^{\min}\le\hat{p}_{i,t}\le\hat{p}_{i,t}^{\max}\quad t\in\mathcal{T},(\hat{\varsigma}_{i,t}^{-},\hat{\varsigma}_{i,t}^{+}). \tag{6.5}$$

The distributional regulation price r_t in (6.1) can be either positive or negative. When it is positive ($r_t > 0$), it is the DT. When it is negative ($r_t < 0$), it is the DS. The decision vector variables $p_{i,t}$ and $\hat{p}_{i,t}$ represent the charging power of EVs and consumption of HPs. Matrix B describes the sensitivity coefficients, E is a mapping from the customers to the load busses, parameter c_t is the baseline price, d is discharging power, e is SOC (kWh) of EV batteries, $\mathcal{T}$ is the set of planning periods. One planning period is assumed to be one hour in this chapter; therefore $(p_{i,t\_} - d_{i,t\_}) = (p_{i,t\_} - d_{i,t\_})\Delta t$, and Δt is omitted for brevity.

Constraints (6.2) - (6.3) are from the limits of EVs. Constraints (6.4) - (6.5) present the thermal and electrical limits of HPs. Constraint (6.4) is derived from the thermal process analysis of the household and the HP as shown in chapter 2.

6.2.2.2 Formulation at the DSO side

At the DSO side, the formulations of the DS and DT methods are quite different. The DT method will be briefly reviewed first.

The DSO needs to determine a proper distributional regulation price such that the sum of all aggregators' energy planning resulting from (6.1)-(6.5) will not exceed the network constraints. This is the key idea of the DT and DS methods. In order to determine DTs in the DT method, chapter 2 proposed a method using the following optimization problem (6.6)-(6.11). The DTs are calculated from the Lagrange multipliers of the network constraint (6.7).

$$\begin{aligned}\min_{p_{i,t},\hat{p}_{i,t}} \quad & \sum_{i\in\mathcal{B},t\in\mathcal{T}} \frac{1}{2} {p_{i,t}}^T B_{i,t} p_{i,t} + (c_t \mathbf{1})^T p_{i,t} + \\ & \frac{1}{2} {\hat{p}_{i,t}}^T B_{i,t} \hat{p}_{i,t} + (c_t \mathbf{1})^T \hat{p}_{i,t}\end{aligned} \tag{6.6}$$

subject to,

$$\sum_{i\in\mathcal{B}} DE_i(p_{i,t} + \hat{p}_{i,t}) \le f_t, \forall t \in \mathcal{T}, \ (\lambda_t) \tag{6.7}$$

$$e_i^{\min} \le \sum_{t\_\le t} (p_{i,t\_} - d_{i,t\_}) + e_{i,0} \le e_i^{\max}, \forall t \in \mathcal{T}, i \in \mathcal{B}, (\mu_{i,t}^-, \mu_{i,t}^+) \tag{6.8}$$

$$p_{i,t}^{\min} \le p_{i,t} \le p_{i,t}^{\max}, \forall t \in \mathcal{T}, i \in \mathcal{B}, (\varsigma_{i,t}^{-}, \varsigma_{i,t}^{+}) \tag{6.9}$$

$$K_{i,t}^{a,\min} \le \sum_{t\_ \le t} A_{i,t,t\_} \hat{p}_{i,t\_} + u_{i,t} \le K_{i,t}^{a,\max}, \forall t \in \mathcal{T}, i \in \mathcal{B}, (\hat{\mu}_{i,t}^{-}, \hat{\mu}_{i,t}^{+}) \tag{6.10}$$

$$\hat{p}_{i,t}^{\min} \le \hat{p}_{i,t} \le \hat{p}_{i,t}^{\max}, \forall t \in \mathcal{T}, i \in \mathcal{B}, (\hat{\varsigma}_{i,t}^{-}, \hat{\varsigma}_{i,t}^{+}) \tag{6.11}$$

The set of the aggregators is denoted as $\mathcal{B}$, the PTDF is denoted as D . The DT is determined to be $D^T \lambda_t$. Since λ_t is required to be non-negative and D has non-negative elements, the DT is always non-negative. The following proposition is the key principle of the DT method which has been proven in chapter 2 by comparing the KKT conditions of the optimization at the DSO side and the optimizations at the aggregator side.

Proposition 6.1: The sum of the optimal energy consumption resulting from (6.1) - (6.5) of all aggregators is the same as the optimal energy consumption resulting from (6.6)- (6.11) given that the distributional regulation price r_t (DT) is equal to $D^T \lambda_t$.

According to Proposition 6.1, the DT, as a distributional regulation price determined by the DSO using (6.6) - (6.11), is able to motivate the aggregators of the flexible demands (EVs and HPs) to make their schedule such that the network constraints are not violated. The DS, as another kind of distributional regulation price, should be able to play the same role as the DT does. The method used by the DSO to determine the proper DS is, however, quite different from the one to determine the DT. The DS is determined by a two-level optimization problem. The two-level optimization problem can be written as,

Optimization 6.1:

$$\min_{r_t, p_{i,t}, \hat{p}_{i,t}} \quad \varsigma = -\sum_{t \in \mathcal{T}, i \in \mathcal{B}} r_t^T E_i (p_{i,t} + \hat{p}_{i,t}) \tag{6.12}$$

subject to (6.7), and

$$r_t \le 0, \forall t \in \mathcal{T} , \tag{6.13}$$

$$(p_{i,t}, \hat{p}_{i,t}) \in \arg\min \{(6.1): (6.2) - (6.5)\}, \forall i \in \mathcal{B}.$$

The objective function $\mathcal{G}$ represents the total cost of the DSO to employ the DS method (notice that $r_t \leq 0$). Constraint (6.13) requires the distributional regulation price to be non-positive according to the definition of the DS. The inner optimization gives the outer optimization a constraint such that the energy plan $(p_{i,t}, \hat{p}_{i,t})$ must be the minimizer of (6.1) subject to (6.2)-(6.5), which represents the optimization problem of each aggregator. Finally, the energy plan $(p_{i,t}, \hat{p}_{i,t})$ must fulfill constraint (6.7). The Optimization 6.1 can be summarized as: the DSO needs to find the proper r_t that minimizes the cost function $\mathcal{G}$, and r_t is non-positive and the optimal energy plan of each aggregator with the given r_t respects the network constraints (6.7). Therefore, Optimization 6.1 represents exactly the DS concept in subsection 6.2.1.

It is obvious that the optimization result of each aggregator is the same as the optimal energy plan determined by Optimization 6.1 because it is assured by the inner optimization of Optimization 6.1. Hence, the sum of all aggregators' energy planning respects the network constraints assured by constraint (6.7) of Optimization 6.1. It implies that the decentralized congestion management through the DS method is realized.

6.2.3 Feasibility Discussion and a Feasible Solution

Optimization 6.1 is generally difficult to solve. Before trying to solve the problem, it is necessary to investigate its feasibility, i.e. whether there is any feasible solution and under what conditions there is. If the conditions under which the DS exists are too stringent, the DS method for congestion management will not be attractive to the DSO.

In the DT method, the DT exists as long as the optimization problem (6.6) - (6.11) is feasible, i.e. the feasible set determined by constraints (6.7) - (6.11) is not empty. The optimization problem (6.6)-(6.11) is a strictly convex problem and its feasible set is not unbounded because of the constraints (6.5) and (6.11). Therefore, the optimization problem has an optimal solution as long as the feasible set is not empty. Hence, λ_t exists and so does the $D^T\lambda_t$, i.e. the DT exists. Constraints (6.7)-(6.11) have defined the feasible condition for the DT method, i.e. there exists an energy plan respecting the network constraints as well as the requirements of each individual flexible demand.

It is desirable that the feasible condition for the DS method is as straightforward as the one for the DT method. This is possible if the inner optimization of Optimization 6.1 is slightly modified and the baseline price c_t is strictly positive. Though the energy price is sometimes negative due to the excess production of renewable energy, the total baseline price is usually positive. The modified inner optimization is,

$$\min_{p_{i,t},\hat{p}_{i,t}} \sum_{t\in\mathcal{T}} \frac{1}{2} p_{i,t}{}^T(\alpha B_{i,t}) p_{i,t} + (c_t \mathbf{1} + E_i{}^T r_t)^T p_{i,t} + \frac{1}{2} \hat{p}_{i,t}{}^T(\alpha B_{i,t}) \hat{p}_{i,t} + (c_t \mathbf{1} + E_i{}^T r_t)^T \hat{p}_{i,t}, \tag{6.14}$$

subject to

$$(6.2)\text{-}(6.5),$$

where α is a small positive number ($0 < \alpha \le 1$).

The coefficient α can be calculated through the following method. Firstly, the optimization problem (6.6)-(6.11) is solved and the Lagrange multiplier λ_t is found. Then the coefficient α is determined by,

$$\alpha = \min\left\{ \frac{c_t}{\{D^T \lambda_t\}_j + c_t} \middle| \forall t \in \mathcal{T}, j \in \mathcal{N}_d \right\}, \tag{6.15}$$

to assure that the calculated DS is nonpositive, where $\mathcal{N}_d$ is the set of load points.

The new two-level optimization problem can be written as,

Optimization 6.2:

$$(6.12) \text{ subject to } (6.7), (6.13),$$

$$\text{and } (p_{i,t}, \hat{p}_{i,t}) \in \arg\min \{(6.14): (6.2)\text{-}(6.5)\}, \forall i \in \mathcal{B}.$$

It can be proven that the distributional regulation price,

$$r_t = \alpha(D^T \lambda_t + c_t \mathbf{1}) - c_t \mathbf{1}, \forall t \in \mathcal{T}, \tag{6.16}$$

is a feasible point of Optimization 6.2; this implies that it is a feasible DS scheme which can re-profile the flexible demands such that the network constraints are respected.

Proof: Firstly, the distributional regulation price r_t determined by (6.16) is non-positive, because

$$\forall t \in \mathcal{T}, j \in \mathcal{N}_d,$$

$$\{r_t\}_j = \alpha(\{D^T \lambda_t\}_j + c_t) - c_t \leq$$

$$\frac{c_t}{\{D^T \lambda\}_j + c_t}(\{D^T \lambda_t\}_j + c_t) - c_t = 0.$$

Hence, constraint (6.13) is fulfilled.

Secondly, the inner optimization problem of Optimization 6.2 under the given r_t has the same optimal solution as the optimization (6.1)-(6.5) with $r_t = D^T \lambda_t$. With the given r_t, the inner optimization problem can be rearranged as,

$$\begin{aligned} \min_{p_{i,t}, \hat{p}_{i,t}} \quad & \alpha\Big(\sum_{t \in \mathcal{T}} \frac{1}{2} {p_{i,t}}^T B_{i,t} p_{i,t} + (c_t \mathbf{1} + {E_i}^T D^T \lambda_t)^T \\ & p_{i,t} + \frac{1}{2} {\hat{p}_{i,t}}^T B_{i,t} \hat{p}_{i,t} + (c_t \mathbf{1} + {E_i}^T D^T \lambda_t)^T \hat{p}_{i,t}\Big) \end{aligned} \tag{6.17}$$

subject to,

$$(6.2)\text{-}(6.5).$$

This is because,

$$c_t \mathbf{1} + {E_i}^T r_t = c_t \mathbf{1} + {E_i}^T (\alpha (D^T \lambda + c_t \mathbf{1}) - c_t \mathbf{1})$$

$$= \alpha {E_i}^T (c_t \mathbf{1} + D^T \lambda) = \alpha (c_t \mathbf{1} + {E_i}^T D^T \lambda) .$$

Assume that $({p_{i,t}}^*, {\hat{p}_{i,t}}^*)$ is the optimal solution of (6.17) subject to (6.2)-(6.5), i.e. it is the minimizer of the inner optimization of Optimization 6.2 since they are

equivalent to each other. Then, it is obviously also the optimal solution of (6.1)-(6.5) with $r_t = D^T \lambda_t$, because they have the same constraints and the proportional objective function with a constant factor α.

Finally, according to Proposition 6.1, $(p_{i,t}^*, \hat{p}_{i,t}^*)$ is also the optimal solution of (6.6)-(6.11) since it is the optimal solution of (6.1)-(6.5) with $r_t = D^T \lambda_t$. Therefore, constraint (6.7) is fulfilled with $(p_{i,t}^*, \hat{p}_{i,t}^*)$. This leads to the conclusion that the distributional regulation price determined by (6.16) is a feasible solution of Optimization 6.2 and its associated optimal energy plan is $(p_{i,t}^*, \hat{p}_{i,t}^*)$. (End of the proof)

It should be noted that in the DT method, the coefficient of the quadratic terms, i.e. $B_{i,t}$, is the sensitivity of the predicted energy price and plays the role of avoiding the multiple-response issue of the linear optimization problem where $B_{i,t} = 0$. In the DS method, the coefficient of the quadratic terms becomes $\alpha B_{i,t}$ which is smaller than $B_{i,t}$ and its main function is to avoid the multiple-response issue. Parameter $\alpha B_{i,t}$ will be chosen to be sufficiently small such that it has the least impact on the energy schedules.

6.3 Method to Determine DS

6.3.1 Calculate DS with One-level Optimization

Optimization 6.2 is to be solved in order to determine the efficient DS. Due to the strict convexity, the KKT conditions of the inner optimization problem are both necessary and sufficient. Hence, the inner optimization problem of Optimization 6.2 is equivalent to, $\forall i \in \mathcal{B}$,

$$\alpha B_i p_{i,t} + c_t 1 + E_i^T r_t + \sum_{t\_ \le t} (\mu_{i,t\_}^+ - \mu_{i,t\_}^-) + (\varsigma_{i,t}^+ - \varsigma_{i,t}^-) = 0, \forall t \in \mathcal{T} \tag{6.18}$$

$$\alpha B_i \hat{p}_{i,t} + c_t 1 + E_i^T r_t + \sum_{t\_ \le t} (\hat{\mu}_{i,t\_}^+ - \hat{\mu}_{i,t\_}^-) + (\hat{\varsigma}_{i,t}^+ - \hat{\varsigma}_{i,t}^-) = 0, \forall t \in \mathcal{T} \tag{6.19}$$

$$(\sum_{t\_ \le t} (p_{i,t\_} - d_{i,t\_}) + e_{i,0} - e_i^{\max}) \cdot \mu_{i,t}^+ = 0, \forall t \in \mathcal{T}, \tag{6.20}$$

$$(\sum_{t\_\le t}(p_{i,t\_}-d_{i,t\_})+e_{i,0}-e_i^{\min})\cdot\mu_{i,t}^{-}=0,\forall t\in\mathcal{T}, \tag{6.21}$$

$$(p_{i,t}-p_{i,t}^{\max})\cdot\varsigma_{i,t}^{+}=0,\forall t\in\mathcal{T}, \tag{6.22}$$

$$(p_{i,t}-p_{i,t}^{\min})\cdot\varsigma_{i,t}^{-}=0,\forall t\in\mathcal{T}, \tag{6.23}$$

$$(\sum_{t\_\le t}A_{i,t,t\_}\hat{p}_{i,t\_}+u_{i,t}-K_{i,t}^{a,\max})\cdot\hat{\mu}_{i,t}^{+}=0,\forall t\in\mathcal{T}, \tag{6.24}$$

$$(\sum_{t\_\le t}A_{i,t,t\_}\hat{p}_{i,t\_}+u_{i,t}-K_{i,t}^{a,\min})\cdot\hat{\mu}_{i,t}^{-}=0,\forall t\in\mathcal{T}, \tag{6.25}$$

$$(\hat{p}_{i,t}-\hat{p}_{i,t}^{\max})\cdot\hat{\varsigma}_{i,t}^{+}=0,\forall t\in\mathcal{T}, \tag{6.26}$$

$$(\hat{p}_{i,t}-\hat{p}_{i,t}^{\min})\cdot\hat{\varsigma}_{i,t}^{-}=0,\forall t\in\mathcal{T}, \tag{6.27}$$

$$\mu_{i,t}^{+},\mu_{i,t}^{-},\varsigma_{i,t}^{+},\varsigma_{i,t}^{-},\hat{\mu}_{i,t}^{+},\hat{\mu}_{i,t}^{-},\hat{\varsigma}_{i,t}^{+},\hat{\varsigma}_{i,t}^{-}\ge 0,t\in\mathcal{T}, \tag{6.28}$$

and (6.2)-(6.5).

Since the inner optimization problem is replaced with its KKT conditions, Optimization 6.2 is equivalent to a one-level optimization rewritten as,

Optimization 6.3: (6.12)

subject to

(6.7), (6.13) and

$\forall i\in\mathcal{B}$, (6.2)-(6.5), (6.18) - (6.28).

This one-level optimization, named as Optimization 6.3. However, it is still hard to solve.

6.3.2 Calculate DS with Tightened Constraints

This section presents a linearized method to determine the DS by tightening the constraints. The feasible energy planning set resulting from the Optimization 6.3's feasible set is tightened by assuming that the only allowed energy plan is $(p_{i,t}^{*}, \hat{p}_{i,t}^{*})$, i.e. the optimal energy plan of (6.6)-(6.11). The reason is explained as follows. There are two costs associated with the customers. The first one is the energy cost (including the fixed cost) paid to the day-head market, grid companies and tax authorities, depending on the energy price and the energy plan. The second cost is the DS. Though it is an income in the congestion management, it will ultimately be a cost to the customers as explained in subsection 6.2.1. The second cost is realized in a long-term process. The DSO will adjust the grid tariffs depending on how much it spends on the DS in the last few months. Therefore, it is reasonable to separate these two costs. In the first step, the energy cost is minimized using (6.6) -(6.11), which will end up with the energy plan $(p_{i,t}^{*}, \hat{p}_{i,t}^{*})$. Then, the DS will be minimized with the fixed energy plan, i.e. $(p_{i,t}^{*}, \hat{p}_{i,t}^{*})$.

With a fixed energy plan, all the switching conditions become linear and the objective function becomes linear as well. The resulting liner optimization can be written as,

Optimization 6.4:

$$\min_{r_t} \quad g = -\sum_{i\in N_B, t\in N_T} r_t^T E_i (p_{i,t}^{*} + \hat{p}_{i,t}^{*}) \tag{6.29}$$

subject to

(6.13), (6.18) - (6.28),

where $p_{i,t}$ and $\hat{p}_{i,t}$ are fixed to $(p_{i,t}^{*}, \hat{p}_{i,t}^{*})$.

If coefficient $E_i(p_{i,t}^{*} + \hat{p}_{i,t}^{*})$ becomes zero, r_t becomes free. In practice, the following constraint can be added to avoid such situation,

$$r_t \geq -ME_i(p_{i,t}^{*} + \hat{p}_{i,t}^{*}), \tag{6.30}$$

where coefficient M is a very big number such that, when $E_i(p_{i,t}^* + \hat{p}_{i,t}^*)$ is nonzero, the constraint will have no effect on r_t; otherwise, r_t is forced to be zero. The procedure of calculating the DS can be summarized as: Employ (6.6)-(6.11) to determine $(p_{i,t}^*, \hat{p}_{i,t}^*)$ and λ_t, then employ (6.15) to determine α and finally use Optimization 6.4 to determine the DS.

6.4 Discussions of DS and DT

6.4.1 Limited DS and Unlimited DT

Use the method proposed in Section 6.3, the calculated DS is always limited between zero and the maximum baseline price. The reason is explained as follows.

Same as the DT method, the DS method influence the behavior of the customers by changing the prices. The consumption of the flexible demands will be shifted from the hours with higher prices to the hours with lower prices. Without losing generality, consider a case with two hours. Assume hour t_1 has total price $c_1 + r_1$ and hour t_2 has total price $c_2 + r_2$. If the first price is sufficiently smaller than the second price, i.e. $c_1 + r_1 \ll c_2 + r_2$, the energy consumption of the flexible demands will be shifted from hour t_2 to hour t_1, no matter whether the flexible demands have very efficient storage system like EVs or inefficient storage system like HPs. On the other hand, the total price cannot be zero or negative; otherwise, it will attract infinite large consumption of the flexible demands. Therefore, both prices are positive, i.e. $c_1 + r_1 > 0$ and $c_2 + r_2 > 0$. For the case of the DS, i.e. $r \le 0$ and DS equals to $|r|$, there is $|r_1| < C_1$, and $|r_2| < C_2$. Therefore, the DS is always limited between zero and the maximum baseline price.

However, for the case of the DT, i.e. $r \ge 0$ and DT equals to r, the situation is in the opposite. In order to shift enough consumption from hour t_2 to hour t_1, the second price $c_2 + r_2$ should be sufficiently large, which might lead to a very high r_2, i.e. a very high DT at hour t_2. This is verified in the case study in Section 6.5.2.

6.4.2 Regulatory Issues

In this subsection, the regulatory issue refers to the non-discrimination requirement by the grid code [82]. This implies that customers in the same distribution network

should have an equal opportunity to access the network, and the same type of customers should have same network tariffs. However, the DT method may not fulfil this requirement, because the customers located at different nodes may have different network tariffs. Therefore, unless this requirement is removed from the grid code, the DT method cannot be employed by the DSO.

For the DS method, the non-discrimination requirement is fulfilled. The network tariff is always the same for the same type of customers. The DS is given to those customers who are willing to shift their consumption in a way that benefits the network. After employing the DS method, the high-energy prices become lower, and the customers who originally cannot consume cheap energy due to congestion are able to have the cheap prices like other customers who don't have congestion issues. In this sense, with the DS method, the customers have an equal and fair opportunity to access the network and the (cheap) energy. This will be further illustrated in subsection 6.5.2.

6.4.3 Social Welfare

With the method proposed in Section 6.3.2, the energy planning resulting from the DS method and the DT method is the same. Therefore, the social welfare from the supply side is the same in both methods.

The utility (benefits obtained from consuming energy) from the demand side is also the same in both methods, because the energy planning is the same. The cost at the demand side has two parts. The first part is the energy cost, which should be the same in both methods. The second part is the cost/reward due to the DT/DS. As the second part is a reallocation of money among the customers, the overall cost is zero for both methods. Therefore, the social welfare at the demand side is also the same for both methods. Hence, the social welfare using the DS method is the same as the one using the DT method.

6.5 Case Studies

6.5.1 Case Study with a One Node System

In order to illustrate the idea and efficacy of the DS method for congestion management, a straightforward case was studied first. Only one EV is considered which requires 4 kWh for its battery. The network constraint is the fuse outside the household, which gives a limit of 4 kW. Considering the basic load of 1 kW for each period, the allowed capacity for the EV charging is only 3 kW. Only three charging

periods are considered and the predicted energy prices are 0.5, 0.2, 0.6 DKK/kWh, respectively (the fixed cost is neglected).

6.5.1.1 DT method

The DT method was studied first which can not only give a comparison with the DS method but also offer some useful results needed by the DS method. The DSO solves the following optimization problem first in order to determine the DTs.

$$\min_{p_t} \sum_{1\le t\le 3} \frac{1}{2}\beta p_t^2 + c_t p_t \tag{6.31}$$

subject to,

$$p_t \le 3, t = 1,2,3 \tag{6.32}$$

$$\sum_{1\le t\le 3} p_t \ge 4 \tag{6.33}$$

$$p_t \ge 0, t = 1,2,3 \tag{6.34}$$

Constraint (6.32) assures the limit of the fuse, (6.33) reflects the energy requirement of the EV and (6.34) implies no discharging. The calculated DTs, which in this case are Lagrange multipliers of (6.32), are 0.2996 DKK/kWh for period 2 and zero for other periods (see Table 6-1). The DTs will be sent to the aggregator who will make an optimal energy planning for the EV by the following optimization.

$$\min_{p_t} \sum_{1\le t\le 3} \frac{1}{2}\beta p_t^2 + (c_t + r_t) p_t \ , \tag{6.35}$$

subject to (6.33)-(6.34). The results are listed in Table 6-1 (row "p_t (kW) – with DT").

6.5.1.2 DS method

In order to calculate the DS, the DSO formulates the following two-level optimization according to Optimization 6.2, where α is determined to be 0.4003 (Table 6-1– row "α") according to (6.15).

$$\min_{r_t, p_t} \sum_{1\le t\le 3} -r_t p_t \tag{6.36}$$

subject to (6.32), and

$$p_t \in \arg\min\{\sum_{1\le t\le 3}\frac{1}{2}\alpha\beta p_t^2 + (c_t + r_t)p_t : (6.33)\text{-}(6.34)\}.$$

TABLE 6-1. PARAMETERS AND RESULTS OF THE SIMPLE EXAMPLE

time	1	2	3
β **(DKK/kW/kW)**	0.0002		
c_t **(DKK/kW)**	0.5	0.2	0.6
DT (DKK/kW)	0	0.2996	0
p_t **(kW) – with DT**	1	3	0
α	0.2/(0.2+0.2996) =0.4003		
DS-1 (DKK/kW)	-0.2999	0	-0.3598
DS-2 (DKK/kW)	-0.29992	0	0
p_t **(kW) – with DS**	1	3	0

The above two-level optimization is difficult to solve directly, and therefore is transformed to the following one-level optimization according to Optimization 6.3.

(6.36) subject to (6.32), (6.33)-(6.34),

$$\alpha\beta p_t + c_t + r_t - \mu - \varsigma_t = 0, t = 1,2,3\,, \tag{6.37}$$

$$(\sum_{1\le t\le 3} p_t - 4)\mu = 0\,, \tag{6.38}$$

$$p_t\varsigma_t = 0, t = 1,2,3\,, \tag{6.39}$$

$$\mu \ge 0, \varsigma_t \ge 0, t = 1,2,3\,. \tag{6.40}$$

Though the above nonlinear optimization can be solved, it is desirable to transform it to a linear problem by fixing p_t according to Optimization 6.4. The final linear formulation is obtained as below,

(6.36)

subject to,

(6.37), (6.40), and

$$\varsigma_t = 0, t = 1,2\,. \tag{6.41}$$

where the 'parameter' p_t takes the value $p_t^* = (1,3,0)$. The final optimal DS is obtained by solving the above linear program using GAMS [38] and the results are list in Table 6-1 (row "DS-2 (DKK/kW)" and "p_t (kW) – with DS"). A feasible DS is directly calculated according to (6.16) and listed in Table 6-1 as well (row "DS-1 (DKK/kW)"), which is not as efficient as the optimal DS because the DS for t=3 has no effect on the EV charging planning and therefore should be zero. Though both of the DS sets can motivate the aggregator to make an optimal plan which respects the network constraint, only the optimal DS should be chosen by the DSO.

6.5.2 Case Study with the Bus 4 Distribution Network of RTBS

6.5.2.1 Case study parameters

The single line diagram of the Bus 4 distribution network of the RBTS [36] is shown in Fig. 6-1. The parameters of the grids and load points can be found in Appendix A.

The key parameters of the simulation are listed in Table 6-2. The parameters about EV and HP can be seen in Appendix A.

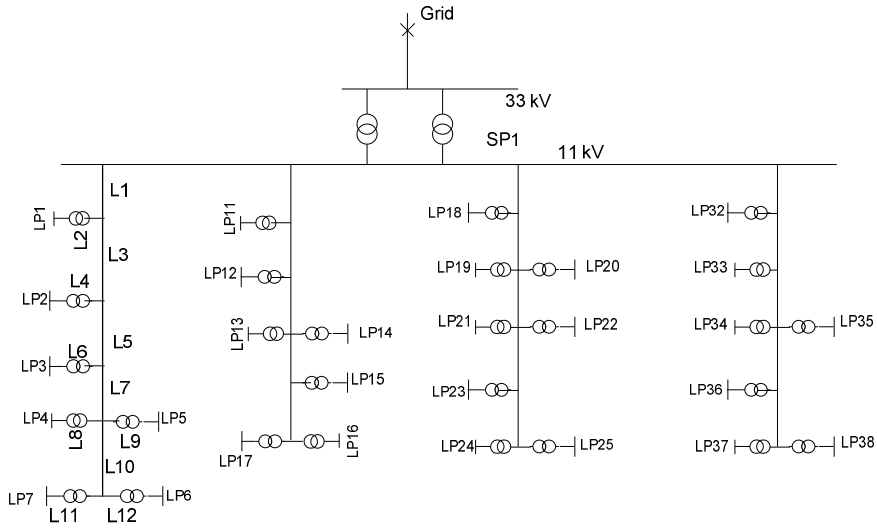

Fig. 6-1. Single line diagram of the distribution network

TABLE 6-2. KEY PARAMETERS OF THE SIMULATION MODEL

parameter	value
L2 limit (kW)	1100
L3 limit (kW)	7000
L4 limit (kW)	2700

6.5.2.2 Case study results

The simulation was carried out using the GAMS optimization software [38].

Firstly, the DT calculation was conducted. The DSO optimization problem with network constraints was solved and the optimal energy plan was found. The line loadings of L2, L3 and L4 with the DT method are shown in Fig. 6-2. Because the line loading limits are respected in the optimization, the line loadings of all line segments are lower than the limits. The base energy prices and the final energy prices with the DT for the customers at LP1 are shown in Fig. 6-3.

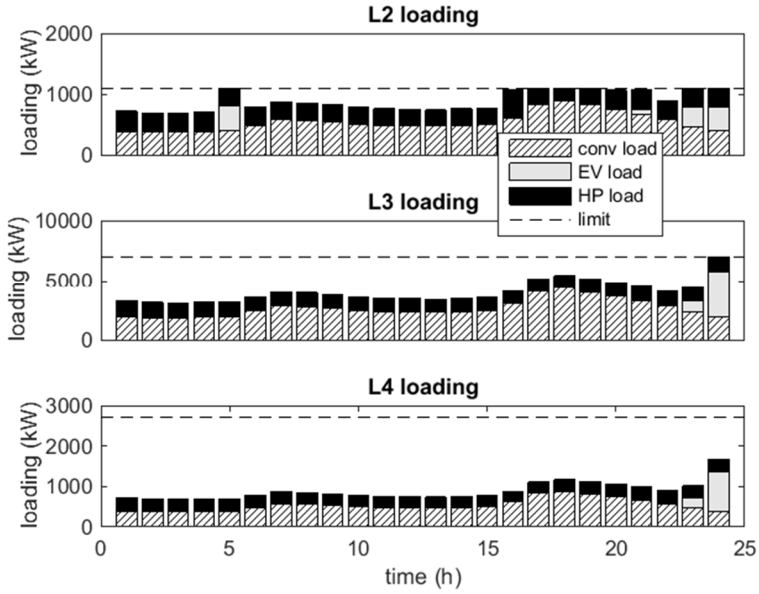

Fig. 6-2. Line loading with the DT method

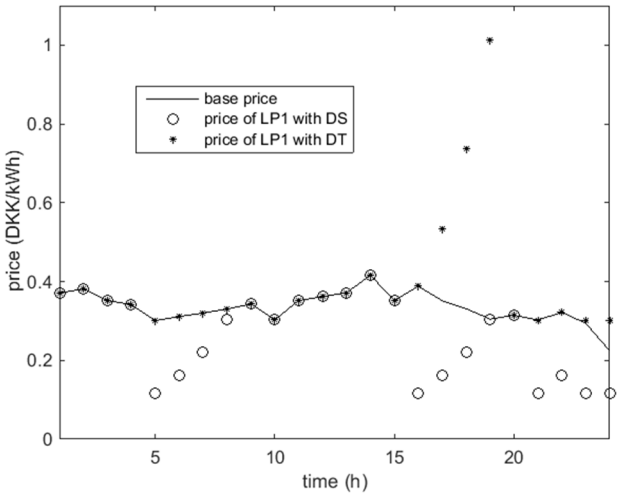

Fig. 6-3. System prices or baseline price and the final prices at LP1, including DT or DS

Secondly, the DS calculation was done using Optimization 6.4. The resulting prices (the base energy price minus the DS) for the customers at LP1 are also shown in Fig. 6-3. The DS is nonzero for many time periods for LP1 because the limit of L2 is tight. Therefore, many nonzero DS are needed to re-profile the flexible demands such that the line loading limit is respected. However, the DS is nonzero only for hour 23 for LP2-5 (shown in Table 6-3) due to the loose line loading limit of L3 and L4.

TABLE 6-3. PRICES, DKK/KWH, FOR LP2-5
('-' MEANS SAME AS BASE PRICE)

time		23	24
base price		0.29414	0.22414
price with DS	**LP2**	0.22425	-
	LP3	0.22425	-
	LP4	0.22425	-
	LP5	0.22425	-
price with DT	**LP2**	-	0.29378
	LP3	-	0.29378
	LP4	-	0.29378
	LP5	-	0.29378

Then, the DS was verified by sending to the aggregators. Each aggregator performed the optimization (6.1)-(6.5) and ended up with a total energy plan as shown in Fig. 6-4, which was the same as Fig. 6-2 with tolerable computation precision.

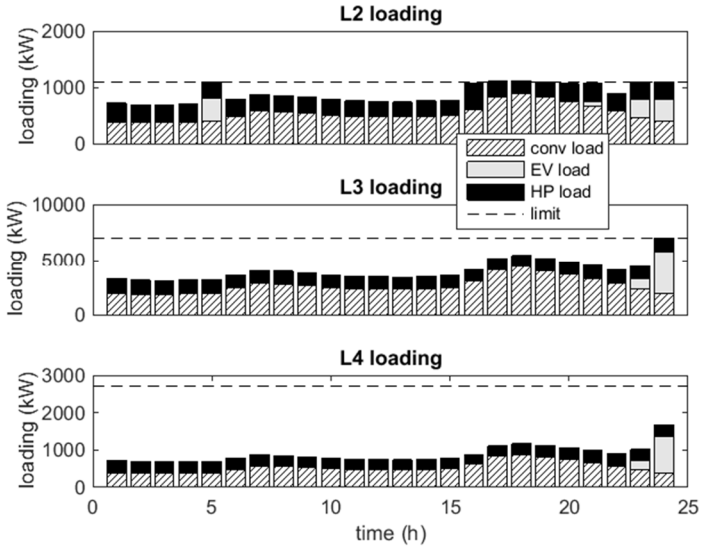

Fig. 6-4. Line loading with the DS method

6.5.2.3 Discussion

It can be observed from Fig. 6-3 that the final energy prices with the DS are always between zero and the base energy prices. Therefore, the DS is always limited between zero and the base energy prices, as it is the difference between the final energy price and the base energy price. In Fig. 6-3, it can be seen that the DT is always positive and can be very high. For instance, the maximum DT is about 0.709 (DKK/kWh) at hour 19, which is almost twice of the maximum base price. However, the maximum DS (absolute value) is only 0.27 (DKK/kWh) at hour 16. This is because the price difference determines the optimal energy plan, not the absolute value of the prices. Take LP1 as an example. In order to shift the HP demand from hour 19 to hour 16, the price at hour 19 should be several times higher than hour 16 in the DT method. However, in order to shift the same amount of the HP demand in the DS method, the price at hour 16 needs to be several times lower than hour 19. This results in a very high DT, but a moderate DS.

Moreover, receiving DS gives the customers a fair opportunity to the low energy prices. Take LP2 as an example. A customer wants to charge his EV in hour 24,

because the energy price is lower. However, due to the congestion, he is forced to charge his EV partially in hour 23 with a higher energy price. With the DS, he can charge his EV in hour 23 with an equally cheap price as in hour 24. This gives the customer the same opportunity to utilize the cheap energy price just as the customers at the load points where there is no congestion, such as LP11.

At last, it is obvious that there is no rebound effect with the DS (or the DT) method, because the optimization is conducted over the whole-time period (24 hour) corresponding to the day-ahead energy market.

6.6 Summary

This chapter proposes the DS method for congestion management in distribution networks with high penetration of EVs and HPs. The DS method employs a decentralized framework to realize the congestion management. A two-level optimization formulation is proposed to determine the DS. By using the KKT conditions of the inner optimization, the two-level optimization of calculating the DS is transformed into a one level optimization. By tightening the feasible set, the optimization is further simplified and easier to be solved. The case studies have demonstrated the DS method and validated its efficacy for congestion management.

Though it takes more efforts to determine the DS than the DT, the DS method is preferred to the DT method for congestion management nowadays. In addition to the fact that the DS method shares some of the advantages of the DT method, i.e. having the least cost energy planning without rebound effect. Unlike the DT method, the DS method does not have any regulatory issue. It provides a fair opportunity to customers to access cheap energy prices.

CHAPTER 7.

REAL-TIME CONGESTION MANAGEMENT BY SWAP[7]

After presenting the DT and DS methods, that are applicable at the time frame of day-ahead, this chapter will present a congestion management method that can be employed near the operation time.

7.1 Introduction

As important as the congestion management in the day-ahead market where the majority of energy production and consumption is planned, the congestion management close to the operation time (5 to 60 minutes ahead of the operation time) should be handled by the distribution system operator (DSO) because the discrepancy from the planning due to forecast error or component failure cannot be totally avoided in real life. This congestion management is referred as real-time congestion management. As approaching the operation time, new information about the grid condition, more accurate forecast of the energy production as well as the load demands, will be available with high certainties, which is an advantage of the real-time congestion management. However, as all market players have already made promises at the day-ahead energy market, it becomes more complicated to give proper incentives to the players to change their behaviors as close to the operation time.

In recent research, demand response (DR) is very promising in dealing with the real-time congestion management. Unless noted otherwise in this chapter, the Nordic electricity market (see Section 7.2) is used when discussing the DR cost, settlement and market procedure. There are two important aspects to be taken into account when designing the DR program for the real-time congestion management. The first one is the system balance, which is critical for the system to maintain the

[7] This chapter is based on the paper: S. Huang and Q. Wu, "Real-Time Congestion Management in Distribution Networks by Flexible Demand Swap", IEEE Tr. Smart Grid, in press.

frequency. And when there are system balance issues, additional costs to the DR providers may occur due to the settlement of the system imbalance. The second one is the rebound effect of the flexible demands, which can cause system balance issues and additional cost in future hours.

Either or both of the two important aspects have not been studied in the incentive-based DR programs, e.g. the FLECH method and the AD method, proposed in recent literatures. In [22], the coupon incentive-based DR program is proposed. However, the intertemporal feature of the flexible demands wasn't considered in the models of the coupon incentive-based DR program. Therefore, the rebound effect is not considered in this DR program. In [23], an optimal coordination and scheduling method for DR via monetary incentives is proposed, where the distribution network constraints and the rebound effect are taken into account. However, the system imbalance issue and the associated costs are not studied.

On the other hand, the DT method discussed in chapter 2 cannot be directly used in the real-time congestion management because they may cause system imbalance and the imbalance cost is unknown until the settlement of the regulation power market. The aggregators, as the provider of flexibility services, will not be willing to provide such services if the cost of them is not known or very difficult to forecast. Here, the cost refers to the settlement of system imbalance and the energy cost due to the future batteries/temperature recovery needs. In [83], the real-time market (5 minutes ahead of the operation time) architecture for European electricity markets is proposed, where the flexible demands are programmed to be simple price-responsive loads. However, the challenges of the real-time market lie in how to determine the real-time price, how to cooperate with the existing electricity markets and how to handle the rebound effect of the DR.

Because of the importance of the imbalance issue and the unknown-cost issue of providing flexibility services, this chapter proposes a real-time congestion management method by swapping the consumption of the flexible demands, i.e. the EV charging/discharging and the HP consumption increase/decrease. In the proposed method, the 'swap' occurs both temporally and spatially. The spatial swap helps maintain the system balance and avoid the cost of the system imbalance settlement. For instance, a decrease of consumption at one node is compensated by an increase with the same amount at another node; as such, the system balance is not affected. The temporal swap can help avoid the rebound effect. The flexible demands participating in the DR program will have the chance to restore their batteries or the temperature level of their households with the temporal swap. Taking either side of

the swap and providing the DR, the aggregators can be rewarded by the DSO according to the amount of the provided flexibility.

The 'buy back' method for transmission line congestion management [84] is also a swap method, but it only exchange the consumption/generation spatially to relieve the congestion between two price areas at the operation phase. The implementation of the 'buy back' method and the proposed swap method is also different. In the 'buy back' method, the bids from the producers or consumers are submitted to the TSO and then activated by the TSO according to the network conditions and the merit order of these bids. The implementation of the proposed swap method will be introduced later on in this chapter. The benefits of the proposed swap method are summarized as: (1) No system balance issue; (2) No rebound effect; (3) No unforeseen costs due to the system imbalance and the rebound effect; (4) The reward/cost for the aggregators/DSO is clear.

This chapter will first introduce the structure of the Nordic electricity markets, as their impacts on the behavior of the market players and the cost of providing DR must be considered in the real-time congestion management. Next, the method of swapping the EV charging and HP consumption is presented. Then, the algorithm for forming swaps is described. At last, results of the case studies are presented and discussed.

7.2 Electricity Markets and Potential Costs of Providing Flexible Services

As preknowledge of the proposed swap method, different types of markets and the potential costs of providing flexible services will be briefly discussed in this section.

7.2.1 Zonal price market

The detailed introduction of the Nordic electricity market, that represents many European electricity markets, can be seen from Appendix B. The Nordic electricity market is a typical zonal price market. It comprises chronologically the day-ahead spot market, intra-day market, regulation market and ancillary market.

The day-ahead spot market is the major market. The aggregators of flexible demands should buy the electricity from this market to fulfil the daily consumption requirement of the flexible demands. However, any deviation from the day-ahead energy plans, i.e. the difference between the actual production or consumption and the day-ahead schedule, will incur additional cost unless it is helping the system

balance according to the results of the regulation power market. Providing flexibility services, if activated, will cause such deviations and therefore will be subject to potential additional cost, which should be taken care of.

Due to the limited capacity and lifetime of storage systems of flexible demands, the flexibility services are not suitable to be traded in the intra-day market, but they are encouraged to participate in the regulating power market and ancillary service market. However, it is suggested that the bids should be checked by the DSO to ensure the security of the distribution networks before submitted to the regulating power market or ancillary service market.

Zonal price market is suitable for employing the proposed swap method for real-time congestion management. It will be the basic assumption for the analysis of the swap method, while the application of the swap method on other types of markets will be briefly discussed.

7.2.2 Nodal Price Market and Single Price Market

Employing the swap method for real-time congestion management is also suitable for single price markets, e.g. regulated electricity market in China, and the nodal price markets, e.g. many markets in North America. The technical issues of using swaps, e.g. the limitation of distribution networks and transmission networks, are the same for the three types of markets. The economic issues, i.e. the settlements of the swaps, will depend on the types of the markets, which will be partially illustrated through case studies in subsection 7.5.2. More detailed discussion of employing the swap method in single price markets or the nodal price markets will be carried out in the future work.

7.3 Memthod of Swapping

Flexibility services, e.g. charging/discharging batteries of EVs and increasing/decreasing consumption of HPs, can be employed to resolve congestion in distribution networks. However, it must be done with the coordination of the relevant electricity markets, such as day-ahead spot market, regulating power market, and ancillary services market, such that the settlement rules of these markets are considered and the power system security/balance is ensured. In this section, the proposed method of swapping EV or HP consumption is described, which can help the aggregators provide flexibility services without causing system imbalance and at the same time avoid additional cost in the settlement of other associated markets.

7.3.1 Swap within One DSO

If the congestion is not at the connection point of the distribution network to the transmission grid, it is possible that the congestion can be resolved by a swap within the same DSO.

One side of a swap (S_1) offered by the DSO can be defined as,

$$S_1 : \{LP_j \mid j \in N_1\}, t_1, -p_s, t_2, +p_s ,$$

where set $\{LP_j \mid j \in N_1\}$ represents the joint of load points where the flexibility service is needed, t_1 is the time period showing when and how long the flexibility is needed, $-p_s$ means a consumption decrease with the total amount p_s , t_2 is the time period that the opposite flexibility is needed, $+p_s$ means a consumption increase with the total amount p_s , which is the opposite flexibility. The opposite flexibility is to give the aggregator a chance to restore the storage system associated with the flexibility, e.g. maintain the state of charge (SOC) level of the batteries of EVs.

The other side of the swap (S_2) is defined as,

$$S_2 : \{LP_j \mid j \in N_2\}, t_1, +p_s, t_2, -p_s ,$$

which means a consumption increase of the total amount p_s is needed at t_1 and a consumption decrease of the total amount p_s is needed at t_2 at any or a joint of the load points in $\{LP_j \mid j \in N_2\}$. One aggregator can take one side of a swap and the other aggregator can take the other side. It is allowed that one aggregator takes both sides of a swap as long as it has the capacity of the required flexibility service.

Without losing generality, a distribution network (Fig. 7-1) from the RBTS [36] is employed to illustrate how the swap method can be used to handle real-time congestion in distribution networks. For instance, the DSO finds that there will be congestion, e.g. overloading by p_s , in 15 minutes at line L3 at Feeder 1, and the congestion will last for 30 minutes. The time information (t_1) is written as "hour: minute, duration in minutes", i.e. "18:00, 30". By forecast, the DSO finds that there is enough free capacity of line L1 and the other feeders at t_1 . The DSO also finds

that there is enough free capacity at t_2 to perform the opposite flexibility. Then, it will raise an offer requesting a consumption decrease, written as,

$$S_1 : \{LP_{2-7}\}, t_1, -p_s, t_2, +p_s .$$

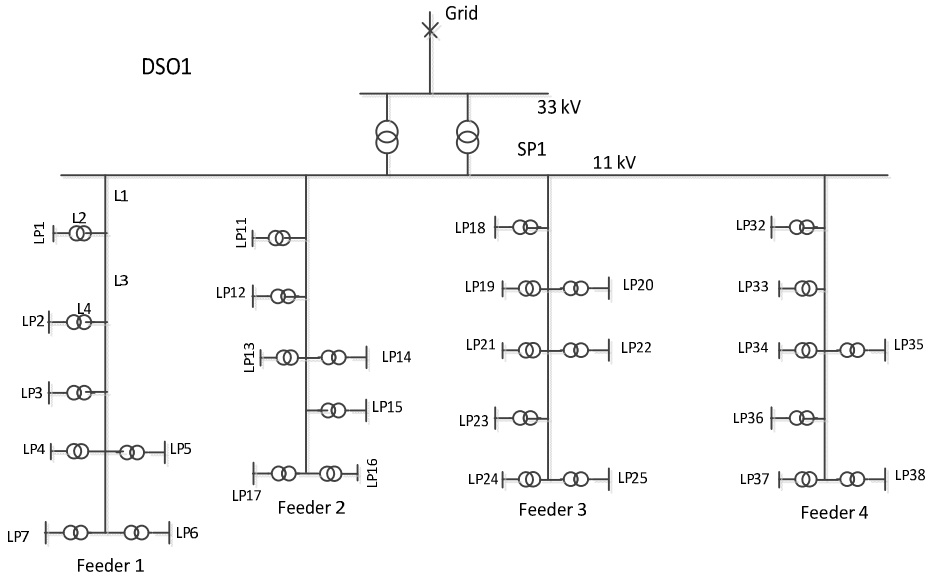

Fig. 7-1. Single line diagram of the distribution network

At the same time, it will raise an opposite offer requesting a consumption increase, written as,

$$S_2 : \{LP_1, LP_{11-38}\}, t_1, +p_s, t_2, -p_s .$$

The two offers form a swap. If both offers are taken by the aggregators, the congestion at L3 can be solved. It can be seen that the net change of consumption is zero at both t_1 and t_2, implying that the system balance is not influenced by the activation of the flexibility services.

The economics of the above swap is analyzed as follows. Firstly, the imbalance settlement as described in Appendix B.3 is analyzed. Assume that the one-price settlement is applied and the regulation prices at t_1 and t_2 are r_1 and r_2, respectively.

The first aggregator (A_1), who takes S_1 , should pay: $p_s t(r_1 - r_2)$, while the second aggregator (A_2), who takes S_2 , should pay: $p_s t(-r_1 + r_2)$, where t is the duration of the swap. As a whole, the two aggregators do not pay anything to the independent system operator (ISO) or transmission system operator (TSO) due to the imbalance. But one aggregator needs to pay another. However, it is assumed that the aggregators have a special agreement with the DSO that no one would have profit or loss due to the settlement of imbalance resulting from the swap. Hence, with this special agreement, the aggregators pay zero in the imbalance settlement. The DSO will help to neutralize the profit or loss of the aggregators either by notifying the ISO such that the two aggregators need not to be involved in the imbalance settlement or by collecting profit from one aggregator and covering the loss of another.

Secondly, the settlement of the swap is analyzed. Assume that the price of the swap offered by the DSO is c_s . Both A_1 and A_2 will receive the payment from DSO by the amount $p_s t c_s$, which is the profit from providing flexibility services. It should be noted that either side of the swap can be shared by several aggregators if one aggregator does not have enough flexibilities and the profit will be shared accordingly.

Because the payment of swap is based on the difference between the actual consumption and the baseline, there is incentive for the aggregator to exaggerate the amount of flexible demand (known as "inflating the baseline" problem [85], [86]). In the swap method, the schedule submitted to the day-ahead market is served as the baseline, which can reduce substantially the incentive for the aggregator to influence the baseline, because there is risk for the aggregator to exaggerate this number in the day-ahead market due to many uncertainties.

7.3.2 System-wide Swap

If there is not enough free capacity to implement S_2 inside the same distribution network which faces congestion issue identified by the DSO, denoted as D_1 , it will need to seek help from other DSOs and the TSO. If a neighboring DSO is able to help D_1 , the transmission limitation between different price zones does not need to be considered; otherwise, it needs to apply for the transmission capacity from relevant TSOs, which is considered free to use within the limitation in this chapter, and seek the help from a remote DSO. In either case, if the requested free capacity

to implement S_2 is identified in one or several other distribution networks, the system-wide swap can be formed, with S_1 implemented in the distribution network of D_1. The settlement of the system-wide swap is similar to the swap within one DSO since the help from the other DSOs and the TSO is "free".

7.3.3 Procedure of Swap Market

The concept of the swap market is shown in Fig. 7-2. "Swap" is a form of flexibility service proposed in this chapter to solve real-time congestion without causing imbalance to the transmission network. The procedure is described below.

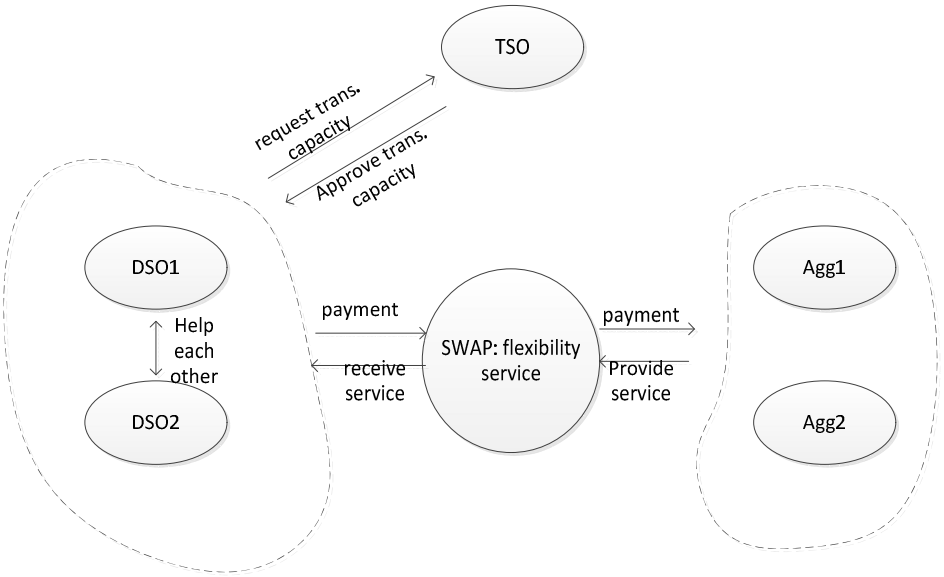

Fig. 7-2. Concept of the swap market

1) The DSO identifies the congestion problem within its network with at least 5 minutes in advance, such that there is enough time to set up a swap market.

2) The DSO identifies the free capacity to implement S_1 within its network.

3) The DSO identifies the free capacity to implement S_2 within its network; if not successful, it will ask help from a neighboring DSO; if not successful, it will ask help from a remote DSO within the allowed transmission capacity verified by the TSO.

4) If the free capacity to implement both S_1 and S_2 is found, the swap can be formed and published to the swap market by the DSO.

5) The aggregators can take the either side of the swap or both according to their flexibility service capacity.

6) The DSO confirms that both sides of the swap are taken by aggregators; otherwise, it will cancel the swap.

7) The aggregators activate S_1 or S_2 at the operation time.

8) The DSO settles the swap.

7.4 Algorithm for Formimg Swap

In this section, an algorithm for forming the swap is proposed. As shown in section 7.3.1, among the other parameters of the swap, the congestion time t_1 is identified by the DSO at first; otherwise, there is no need of swap. The amount of the exchange power p_s is standardized to a fixed number, e.g. 100 kW or 50 kW, to ease the programming. The size of the standardized exchange power is chosen such that the aggregators are easy to manage their flexible demands to provide the DR. The case with non-standardized p_s can be derived from the standardized case. The time of the swap, e.g. t_1 and t_2, is discretized with a fixed duration, e.g. 30 minutes, and indexed with natural numbers. The set of the time periods that the algorithm will search is denoted as $\mathcal{T} = \{1, 2, 3, ...n\}$ and $t_1 = 1$. The goal of the algorithm is to identify the suitable load points and t_2. The steps of the algorithm are presented as follows.

1) Step 1: Generate multiple solutions that can alleviate the congestion

In order to maximize the chance of the participation from the aggregators, it is desirable to have as many suitable load points as possible in S_1. Employ the following OPF, a MIP problem, to search for a feasible solution that can alleviate the identified congestion.

OPF1:

$$\min \sum_{i \in \mathcal{I}, j \in \mathcal{N}_d, t=1} x_{ijt} \tag{7.1}$$

Subject to,

$$\sum_{i \in \mathcal{I}, j \in \mathcal{N}_d} -p_s D_j x_{ijt} \le f_t, t = 1 \tag{7.2}$$

$$\sum_{i\in\mathcal{I},j\in\mathcal{N}_d} p_s D_j x_{ijt} \le f_t, \forall t>1, t\in\mathcal{T} \tag{7.3}$$

$$\sum_{j\in\mathcal{N}_d} x_{ijt} \le 1, \forall i\in\mathcal{I}, t=1 \tag{7.4}$$

$$\sum_{t>1,t\in\mathcal{T}} x_{ijt} = x_{ij1}, \forall i\in\mathcal{I}, j\in\mathcal{N}_d \tag{7.5}$$

$$x \in \{0,1\}$$

In OPF1, $\mathcal{I}$ is the set of swaps (one swap has a standardized exchange power p_s), $\mathcal{N}_d$ is the set of load points, x is the indicator of whether the load point is selected, D is the PTDF, f is the remaining capacity of the line loadings (negative means the corresponding line is overloaded).

The objective function (7.1) is to minimize the total number of swaps, which is also to minimize the cost of the swaps, since the cost of a standardized swap is fixed. Constraints (7.2)-(7.3) are power flow constraints, noticing that the swap is to reduce power at t_1 and to increase power at t_2. Constraint (7.4) means that only one load point is selected in one swap. Constraint (7.5) means that the power increase is the same as the power decrease at the same load point, which is the idea of the swap.

After solving OPF1, a solution is found. The solution tells how many swaps are needed. For instance, the DSO is willing to use a maximum of 10 swaps to solve the congestion by defining $\mathcal{I} = \{1,2,...,10\}$. If the solution has an objective value 2, it means that it only needs two swaps to solve the congestion. The solution also tells a candidate S_1 with e.g. two swaps: $S_1^{(1)} = \{LP_{j_1}, 1, -p_s, t_2^{(1)}, +p_s\}$ and $S_1^{(2)} = \{LP_{j_2}, 1, -p_s, t_2^{(2)}, +p_s\}$. Due to the symmetry of OPF1, the order of $S_1^{(1)}$ and $S_1^{(2)}$ does not matter.

Then exclude the above solution by adding new constraints to OPF1, e.g. if add new constraint $x_{i'j't'} + x_{i''j''t''} \le 1$, then $x_{i'j't'}$ and $x_{i''j''t''}$ cannot be one at the same time. Solve OPF1 again and find a new solution if any. Repeat the procedure till

there is no new solution or the objective value starts to increase or the total number of solutions reaches a predefined number, e.g. 100.

2) Step 2: Select t_2

Theoretically, one side of the swap, S_1, can be formed as a group of all optimal solutions found in Step 1. However, in order to reduce the complexity of forming S_2, the optimal solutions are further refined. To do so, t_2 is identified as an unordered n-tuple (n is the optimal value of OPF1) which has the maximum appearance in all optimal solutions found in Step 1. Form S_1 as the group of the optimal solutions having the selected t_2 and drop the rest of the optimal solutions.

3) Step 3: Form S_2

Employ the following OPF with a dummy objective function to find a candidate S_2.

OPF2: $$\min 0 \tag{7.6}$$

Subject to,

$$\sum_{i\in\mathcal{I}^*, j\in\mathcal{N}_d} p_s D_j y_{ijt} \le \tilde{f}_t, t=1 \tag{7.7}$$

$$\sum_{i\in\mathcal{I}^*, j\in\mathcal{N}_d} -p_s D_j y_{ijt} \le \tilde{f}_t, \forall t>1, t\in\mathcal{T}^* \tag{7.8}$$

$$\sum_{j\in\mathcal{N}_d} y_{ijt} = 1, \forall i\in\mathcal{I}^*, t=1 \tag{7.9}$$

$$y_{ijt_2^{(i)}} = y_{ij1}, \forall i\in\mathcal{I}^*, j\in\mathcal{N}_d \tag{7.10}$$

$$y\in\{0,1\}$$

In OPF2, $\mathcal{I}^*\subseteq\mathcal{I}$ is the set of active swaps according to S_1, $\mathcal{T}^*$ is the list of active time periods of t_2 in S_1, y indicates whether the load point is selected in the swap,

$\tilde{f}$ is the minimum remaining capacity of the line loadings after activating S_1 (as shown in Steps 1 and 2, S_1 has a group of selected candidates), subscript $t_2^{(i)}$ of $y_{ijt_2^{(i)}}$ is the i-th element in $\mathcal{T}^*$ (ordered list which may have duplicate elements) .

Constraints (7.7)-(7.8) are power flow constraints. Constraint (7.9) means that the number of selected load point is precisely one in one active swap. Constraint (7.10) is to match t_2 in S_2 and S_1 such that the system balance is maintained.

Similar to Step 1, after finding one candidate S_2, exclude the solution by adding new constraints to OPF2 and find new candidates. Repeat till there is no feasible solution or the number of candidates reaches a predefined number. In this way, S_2 is formed as the group of all possible candidates.

If there are not enough candidates within one DSO to form S_2 or it fails to attract the aggregators to take the formed S_2, the DSO should send a request to other DSOs. The other DSO can also employ OPF2 to find candidates and then form S_2 within its distribution network.

7.5 Case Study

Case studies have been carried out using the distribution network shown in Fig. 7-1. Key parameters particular to this case study are listed in Table 7-1, while the other common parameters about the grid and loading information can be found in Appendix A. The EV availability, implying EV is parked and connected, can be found in Appendix A as well. Assume each household has one EV and one HP. It is a typical winter day and almost all HPs are running.

TABLE 7-1. KEY PARAMETERS OF THE CASE STUDY

parameter	value
price of swap	2 DKK/kWh
L2 limitation	1400 kW
L3 limitation	7000 kW
L4 limitation	1700 kW

It is assumed that the line loadings resulting from the day-ahead planning, including conventional load, EV load and HP load, are respecting the line loading limits as shown in Fig. 7-3. The peak conventional consumption of residential customers occurs at 18:00 when people come home and start cooking or using other appliances (shown in Fig. 7-3).

Two cases are presented in the following two subsections. One case illustrates the fundamental idea of the swap method using a straightforward example, where the stakeholders of the swap are all in one distribution network. The second case has a rather complicated situation, where a remote DSO and remote aggregators are involved.

7.5.1 Case one

As approaching the real operation time, e.g. 18:00, the DSO finds that there will be an overloading of L2 by the amount of 100 kW and the overloading will last for 30 minutes due to a wrong forecast, e.g. the conventional consumption will be more than the day-ahead forecast, or a loss of generation from a wind power generator. The forecast line loadings are shown in Fig. 7-4, where each period has 30 minutes and there are 12 periods in total. The DSO has to solve the congestion and it considers buying flexibility services from the aggregators since they are managing a large number of EVs and HPs in this distribution network.

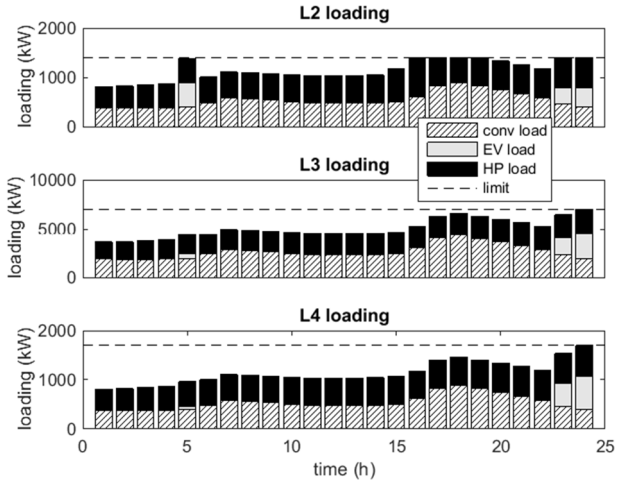

Fig. 7-3. Line loading resulting from the day-ahead planning

The DSO needs a reduction of consumption at 18:00 by 100 kW on L2 and an increase of consumption at 22:00 by the same amount, because the flexibility services need to restore their batteries or household temperatures and there is enough free capacity at 22:00 on L2 as shown in Fig. 7-4. The DSO observes that there is enough free capacity of other lines of feeder 1 and all lines of other feeders to implement S_2. Hence a swap can be formed within this distribution network, which is (the standardized exchange power is assumed to be 100 kW in the case study, see the beginning of Section 7.4):

$$S_1 : \{LP_1\}, (18:00, 30), -100, (22:00, 30), +100,$$

and,

$$S_2 : \{LP_{2-7}, LP_{11-38}\}, (18:00, 30), +100, (22:00, 30), -100.$$

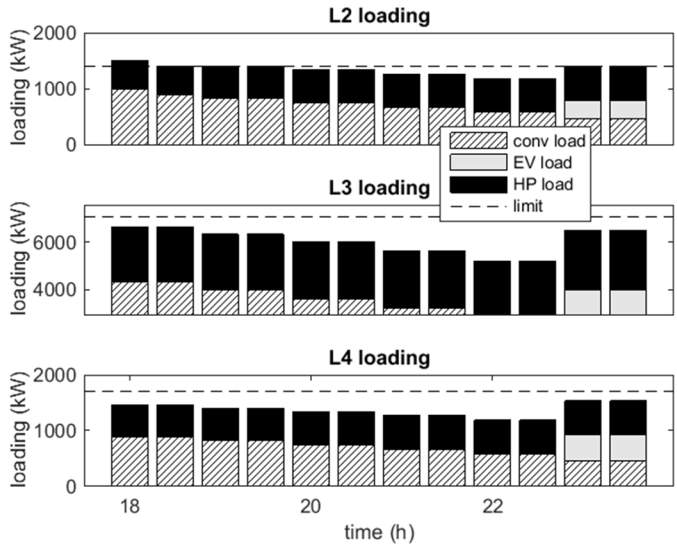

Fig. 7-4. Forecasted line loadings when close to the operating time

Because of the high HP availability indicated by high HP consumption as shown in Fig. 7-4, there is an aggregator taking both sides of the swap. After the confirmation of the swap from the DSO, the aggregator can activate the swap at the operation time. The aggregator will reduce HP consumption at LP1, which will result a reduction of the power flow of L2. At the same time, the aggregator will increase

HP consumption at LP2 in order to activate S_2 and maintain the system balance. Similarly, at 22:00, the aggregator will increase the HP consumption at LP1 to recover the household temperature. At the same time, the aggregator will reduce HP consumption at LP2 to maintain the system balance. The line loadings of L2, L3 and L4 after activating the swap are shown in Fig. 7-5, from which it can be seen that the congestion is solved.

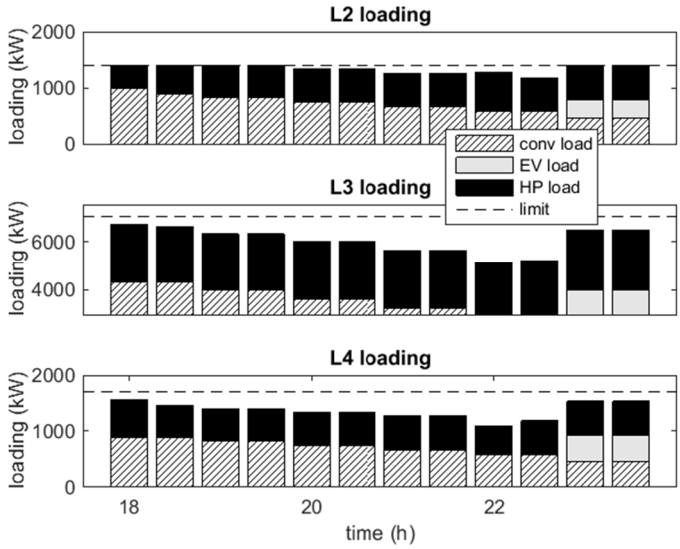

Fig. 7-5. Line loadings after activating swaps

The swap is settled by a payment made by the DSO with the amount $2 p_s tc_s = 2 \cdot 100 \cdot 0.5 \cdot 2 = 200$ DKK. The aggregator makes a profit of 200 DKK in this case by providing flexibility services to solve the congestion in the distribution network. If the aggregator would like to employ EV, e.g. discharge (V2G) or charge the batteries, to activate the swap, it can make the same profit from providing the swap and the DSO cannot see any difference.

7.5.2 Case Two

In Case Two, the algorithm for forming swaps is tested and the swap settlement involving remote DSO is considered. The DSO makes a forecast before 18:00 and the forecasted line loadings are shown in Fig. 7-6. Both L3 and L4 are overloaded: L3 is overload by 150 kW and L4 is overloaded by 60 kW. Because one swap has a standard 100 kW power exchange capacity, multiple swaps are employed.

OPF1 is employed to search for the first group of candidate swaps; each candidate swap has one load point and t_2. The minimum number of swaps is two, denoted as $S_1^{(1)}$ and $S_1^{(2)}$, after solving OPF1. Then exclude the solution and search for all other candidates. Observing all candidates, it is found that 20:00 and 20:30 are good time periods for consumption increase and load points 2~5 are suitable for activating S_1. And LP2 must be in one of the two swaps. To simplify the business between the DSO and the aggregators, the DSO decides to fix LP2 in $S_1^{(1)}$ with t_2 =20:00. Hence, one side of the two swaps are formed by combining selected candidates as,

$$S_1^{(1)}: \{LP_2\}, (18:00,30), -100, (20:00,30), +100,$$

and,

$$S_1^{(2)}: \{LP_{2-5}\}, (18:00,30), -100, (20:30,30), +100.$$

In order to form S_2, the DSO solves OPF2. It can be seen from Fig. 7-6 that there is no free capacity on L2 at 18:00. Assume that there is no free capacity on other feeders either. Therefore, OPF2 returns no feasible candidate. The DSO will broadcast a request to neighboring and/or remote DSOs. The request can be,

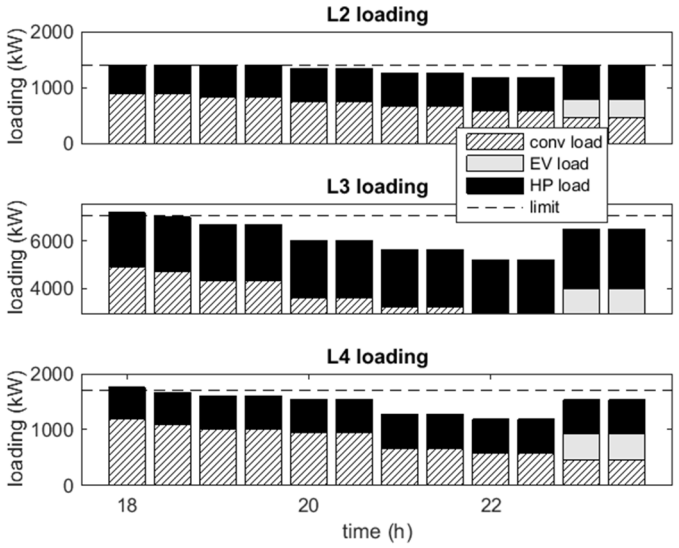

Fig. 7-6. The forecast line loadings when close to 18:00

$$S_2^{(1)} : \{LP_\times\}, (18:00,30), +100, (20:00,30), -100 ,$$

and,

$$S_2^{(2)} : \{LP_\times\}, (18:00,30), +100, (20:30,30), -100 .$$

Assume that there are a number of DSOs that have enough free capacity to implement S_2. They send the information to the sponsor DSO and the TSO. The TSO validates the technical limit of the transmission lines and rejects some candidate DSOs. The remaining DSOs will broadcast S_2 to attract potential interested aggregators in their own networks.

Finally, assume that one aggregator takes S_1 (including two standardized swaps) and another aggregator takes S_2 (including two standardized swaps). The line loadings of the local distribution network after activating S_1 are shown in Fig. 7-7, where there is no congestion. The line loadings of the remote distribution network after activating S_2 are also respecting the limits of the corresponding network.

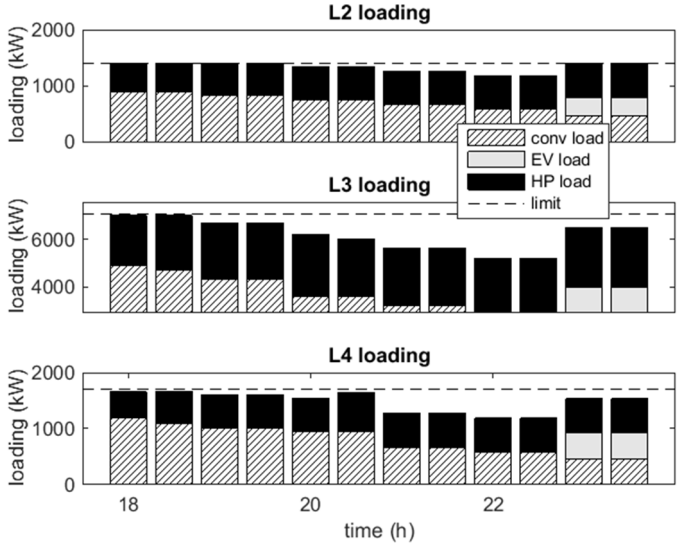

Fig. 7-7. Expected line loadings after activating S_1

The settlement of the two swaps depends on the market setup: single price market, zonal price market or nodal price market. For the single price market, the settlement will be the same as the situation in case one, i.e. the DSO should pay the two aggregators according to the swap price and the number of the swaps taken by the aggregators. For the nodal price market, the DSO should not only pay the cost of the swap as for the single price market, but also need to cover the possible losses due to different energy prices at t_1 and t_2. For instance, assume that the first aggregator has a profit/loss a_1 due to activating S_1 and the second aggregator has a profit/loss a_2. Then the DSO needs to pay $\max(0, -a_1 - a_2)$ to the two aggregators. This means if the two aggregators have a net loss, it will be covered by the DSO. But if the two aggregators have a net profit, one of the aggregators can keep the net profit.

For the zonal price market, if the neighboring/remote distribution network is within the same price zone with the local distribution network, the settlement will be the same as in the single price market. Otherwise, the settlement will be the same as in the nodal price market.

7.6 Summary

This chapter proposes a real-time congestion management method by swap of EV charging and HP consumption. By reducing consumption at the congestion points while increasing the same amount of consumption at other points, the total power balance is maintained and the congestion can be solved. There is no rebound issue because the same amount of consumption change in an opposite direction in a predefined future time is allowed by the swap to recover the batteries of EVs or household temperatures. The settlement of the swap is the payment made by the DSO based on the price of the swap, and the amount and duration of power being activated. The cost or profit resulting from the energy and regulation power market is neutralized by a special agreement made between the DSO and aggregators.

CHAPTER 8.

CONCLUSION AND FUTURE WORK

8.1 Conclusions

In this thesis, the market-based methods for congestion management on distribution networks have been investigated and a series of new methods have been proposed and validated.

The DT method has been shown in this thesis to be efficient in congestion management on distribution networks. The DT can motivate the aggregators to plan the flexible demands such that the sum of the planning will be the same as the DSO's planning, where the network constraints are expected. Because the DT method is based on the location marginal pricing concept, each bus or load point may receive different DT, leading to a discrimination of the customers of the same distribution network. This is against the regulation code of the distribution networks in many countries. In the future, an investigation of revising the regulation is needed for the DT method to be put into use.

Alternatively, the DS method can be employed in place of the DT method. The DS method rewards the customers who consume the power at desired hours, designated by the DSO according to the forecast energy price and the network conditions. As such, the customers can have the same opportunity to access the cheap energy. Therefore, the non-discrimination requirement is fulfilled.

The DT or DS is determined through a DC OPF model; however, the accuracy of the DC OPF model for distribution networks is a concern. This thesis has proposed a sufficient condition for the convex relaxation of the AC OPF to be exact. The assumption of the DT or DS method is that there is high penetration of the flexible demands on the distribution network; therefore, the sufficient condition is fulfilled

and the convex relaxation based AC OPF can be employed to determine the DT or DS, leading to a more accurate and more complete model.

Stochastic nature of the flexible demands and the error of the forecast data can affect the efficacy of the DT method. Uncertainty management has been carried out in this thesis through sensitive analysis and an iterative algorithm to determine the proper DT such that the probability of the network constraints being violated is less than a predefined level.

The market based methods, such as the DT or DS method, can be combined with the direct control methods, such as feeder reconfiguration, for a better solution for congestion management. In this thesis, it is shown that the combination of the DT and the feeder reconfiguration method can be employed for the congestion management and loss reduction of distribution networks more efficiently. It is suggested that the DSO should combine the control of self-owned resources first, such as OLTC, capacitor banks and voltage regulator, and at last combine the control of customer-owned resources, such as production curtailment and load shedding.

After the closure of the day-ahead market, the DT or DS method can't be employed any longer to influent the behavior of the flexible demands. The residual congestion can be handled before the actual operation time by the flexible demand swap method, as proposed lastly in this thesis. The swap is conducted both spatially and temporally; therefore, the power balance of the network can be maintained and the rebound effect of demand response can be avoided.

8.2 Future Work

In the future, it is interesting to further investigate the following points.

- Compare the DT or DS method with the transactive energy framework, to see which concept is more efficient and suitable for congestion management on distribution networks.

- Combine the DT or DS method with more direct control methods, such as OLTC and reactive power support of SVC or the flexible demands equipped with power electronic interfaces, to achieve a more efficient and powerful congestion management method.

- Further organize these market-based methods, as well as the direct control methods, to form a congestion management system, which can deal with the congestion more thoroughly.

- Study the convex relaxation of the AC OPF when there are heavy reverse power flows on the distribution networks.

- Study the coordination of the congestion management methods and the ancillary services provided by the flexible demands. Since they all rely on the management of the flexible demands, the potential conflicts and common interests should be studied.

APPENDIX A

PARAMETERS FOR THE SIMULATIONS

A.1 Grid Data

The Bus 4 distribution network of the Roy Billinton Test System (RBTS) [36] is employed in many case studies in this thesis. Its simplified structure is shown in Fig. A-1. The customer type at each load point and the peak conventional load per load point are listed in Table A- 1. The 24-hour conventional load profile for each load point can be obtained through the peak load of each load point multiplying the load coefficient shown in Table A- 5. Assume each residential customer has one EV and/or HP, while the commercial customer has no EV or HP.

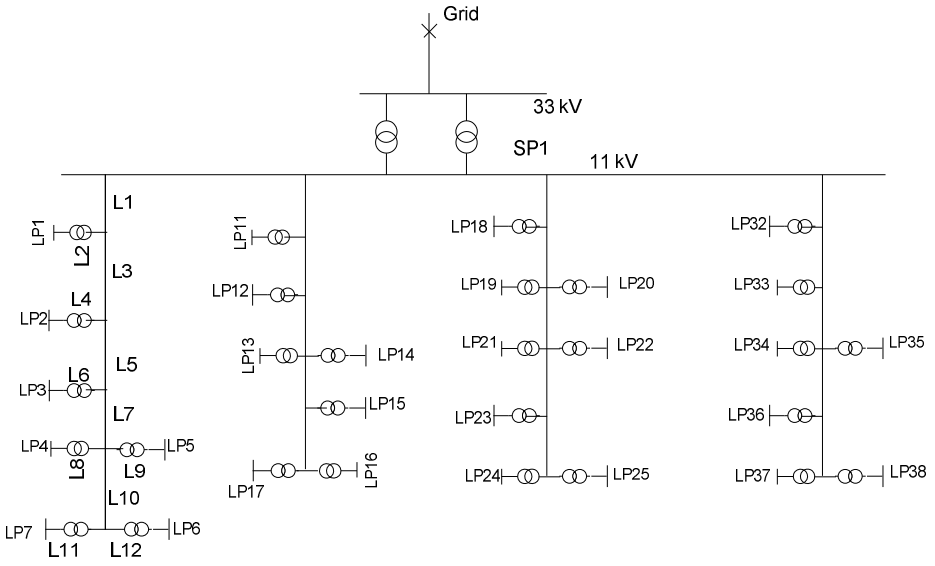

Fig. A-1. Single line diagram of the distribution network

A.2 EV Parameters.

The key parameters of EVs [37] are listed in Table A- 2. The EV availability shown in Fig. A-2 is from the driving pattern study in [37]. Detailed data for 50 EVs are drawn and shown in Table A- 3, which are assumed to represent the population of a large EV fleet in EV planning in the case studies. An EV is available means that the EV is home and plugged to the power socket.

TABLE A- 1. LOAD POINTS DATA

load points	customer type	peak conv. load per point (kW)	number of customers per point
1-4 11-13 18-21 32-35	residential	886.9	200
5 14 15 22 23 36 37	residential	813.7	200
6 7 16 17 24 25 38	commercial	671.4	10

TABLE A- 2. KEY PARAMETERS OF EVS

parameter	value
EV battery size	25 kWh
Peak charging power	11 kW (3 phase)
Energy consumption per km	150 Wh/km
Minimum SOC	20%
Maximum SOC	85%
Average driving distance	40 km

TABLE A- 3. EV AVAILABILITY OF A SAMPLE OF 50 EVS

	e0001	e0002	e0003	e0004	e0005	e0006	e0007	e0008	e0009	e0010	e0011	e0012	e0013	e0014	e0015	e0016	e0017	e0018	e0019
t01	1	1	0.16667	1	1	1	1	1	1	1	1	1	0	0	1	1	1	1	1
t02	1	1	1	1	1	1	1	1	1	1	1	1	0	0	1	1	1	1	1
t03	1	1	1	1	1	1	1	1	1	1	1	1	0	0	1	1	1	1	1
t04	1	1	1	1	1	1	1	1	1	1	1	1	1	1	1	1	1	1	1
t05	1	1	1	1	1	1	1	1	1	1	1	1	1	1	1	1	1	1	1
t06	1	1	1	1	1	1	1	1	1	1	1	1	1	1	1	1	1	1	1
t07	1	1	1	1	1	1	1	1	1	1	1	1	1	1	1	1	1	1	1
t08	1	1	1	1	1	1	1	1	1	0.35	0.76667	1	0.016667	1	0.85	1	1	1	0.51667
t09	1	1	1	1	1	1	1	1	0.016667	0	0	1	0	1	0	1	1	1	0
t10	0.51667	0.1	1	1	1	1	1	1	0.016667	0	0	1	0	1	0	1	0.016667	0.21667	0
t11	0	0	1	1	1	1	1	1	0	0	0	1	0	0.15	0	1	0.083333	1	0
t12	0	1	1	1	1	1	1	1	0	0	0	1	0	1	0	1	1	1	0
t13	0	1	1	1	1	0.51667	1	1	0	0	0	1	0	1	0	1	1	1	0
t14	0	1	1	1	1	0.25	1	1	0	0	0	1	0	1	0	1	0.016667	1	0
t15	0	1	1	1	0.6	1	1	1	0	0	0	1	0	1	0	1	0	1	0
t16	0	1	1	1	1	1	0.18333	1	0	0.26667	0	1	0.083333	1	0	1	0.66667	1	0
t17	0	1	0.016667	1	1	1	0	1	0.18333	0.91667	0	1	1	1	0.6	1	1	1	0
t18	0	1	0.55	1	1	1	0	1	0.91667	0.51667	0.91667	0.76667	1	1	1	1	1	1	0
t19	0	1	1	1	0.51667	1	0.8	1	1	0	0.35	0	1	1	1	1	1	1	0
t20	0	1	1	1	0	0.6	1	1	1	0	0.45	0	1	1	1	1	1	1	0.68333
t21	0	1	1	1	0	0	1	1	1	0	1	0	1	1	1	1	1	1	1
t22	0.58333	1	1	1	0	0	1	1	1	0	1	0	1	1	1	1	1	1	1
t23	1	1	1	1	0	0	1	1	1	0	1	0.91667	1	1	1	1	1	1	1
t24	1	1	1	1	0	0	0.6	1	1	0.41667	1	0.8	1	1	1	1	1	1	1

	e0020	e0021	e0022	e0023	e0024	e0025	e0026	e0027	e0028	e0029	e0030	e0031	e0032	e0033	e0034	e0035	e0036
t01	1	1	1	1	0	1	0	1	1	1	1	0	1	1	1	1	0
t02	1	1	1	1	0	1	0	1	1	1	1	0	1	1	1	1	0
t03	1	1	1	1	0	1	0	1	1	1	1	0	1	1	1	1	0
t04	1	1	1	1	1	1	1	1	1	1	1	1	1	1	1	1	1
t05	1	1	1	1	1	1	1	1	1	1	1	1	1	1	1	1	1
t06	1	1	1	1	1	1	1	1	1	1	1	1	1	1	1	1	1
t07	1	1	1	1	1	1	1	1	1	0.1	0.85	1	1	1	1	1	1
t08	0.68333	1	1	1	1	1	1	1	1	0	0	1	1	1	0.85	0.93333	1
t09	0	1	0.35	1	1	1	1	1	1	0	0	0.016667	0.26667	1	0	0.68333	1
t10	0	1	0.66667	1	0.26667	1	1	1	1	0	0	0	0	1	0	0.8	1
t11	0	1	0.016667	1	0	1	1	1	1	0	0	0	0	1	0	1	1
t12	0	1	0.91667	1	0.25	0.016667	1	1	1	0	0	0	0	1	0	0.35	1
t13	0	1	1	1	1	0	1	1	1	0	0	0	0	1	0	0.58333	1
t14	0	1	1	1	1	0	1	1	1	0	0	0	0	1	0	0.51667	1
t15	0	1	1	1	1	0	1	1	1	0	0	0	0	1	0	0.76667	1
t16	0	1	0.76667	1	1	0	1	1	1	0	0.58333	0	0	1	0	0	1
t17	0	1	0	1	1	0	1	1	1	0	1	0	0	1	0.91667	0	1
t18	0.35	0.55	0	1	1	0	1	1	1	0	1	0	0.33333	1	1	0	1
t19	1	1	0	1	1	0	1	1	1	0	1	0.41667	1	1	0.43333	0	1
t20	1	1	0.83333	1	1	0	1	1	1	0	1	1	0.016667	1	0	0	1
t21	1	1	1	1	1	0	1	1	1	0	1	1	0	1	0	0	1
t22	1	1	1	1	1	0	1	1	1	0	1	1	0.58333	1	0	0	1
t23	1	1	1	1	1	0	1	1	1	1	1	1	1	1	0.91667	0	1
t24	1	1	1	1	1	0.41667	1	1	1	1	1	1	1	1	1	0.65	1

	e0037	e0038	e0039	e0040	e0041	e0042	e0043	e0044	e0045	e0046	e0047	e0048	e0049	e0050
t01	1	1	1	1	1	1	1	1	1	0	1	1	1	1
t02	1	1	1	1	1	1	1	1	1	0	1	1	1	1
t03	1	1	1	1	1	1	1	1	1	0	1	1	1	1
t04	1	0.016667	1	1	1	1	1	1	1	1	1	1	1	1
t05	1	0	1	1	1	1	1	1	1	1	1	1	1	1
t06	1	0	1	1	1	1	1	1	1	1	1	1	1	1
t07	1	0	1	1	1	1	1	1	1	1	1	0.35	1	1
t08	0.68333	0.75	1	1	1	1	0.51667	1	1	0.93333	0.016667	0	0.93333	1
t09	0	1	1	1	1	1	0	1	0.016667	0.66667	0	0	0	1
t10	0	1	1	1	1	1	0	1	0	1	0	0	0	1
t11	0	1	0.016667	1	1	1	0	1	0	1	0	0	0	0.6
t12	0	1	0	1	1	1	0	1	0	1	0	0	0	0.58333
t13	0	1	0.86667	1	0.51667	1	0	1	0	1	0	0.25	0	1
t14	0	1	1	1	0	1	0	1	0	1	0	1	0	1
t15	0	1	1	1	0	1	0	1	0	0.51667	0	1	0	1
t16	0	1	1	1	0	1	0	0.26667	0	1	0	0.51667	0	1
t17	0.61667	1	1	1	0.66667	1	0	0.55	0.91667	1	0.083333	0.63333	0	1
t18	1	1	1	1	1	1	0.91667	1	1	1	1	0.26667	0	1
t19	1	1	1	1	1	1	1	1	1	1	1	0	0	1
t20	1	1	1	1	1	1	1	1	1	1	1	0	1	1
t21	1	1	1	1	1	1	1	1	1	1	0.76667	0	1	1
t22	1	1	1	1	1	1	1	1	1	1	0.66667	0	1	1
t23	1	1	1	1	1	1	1	1	1	1	1	0	1	1
t24	1	1	1	1	1	1	1	1	1	1	1	0.66667	1	1

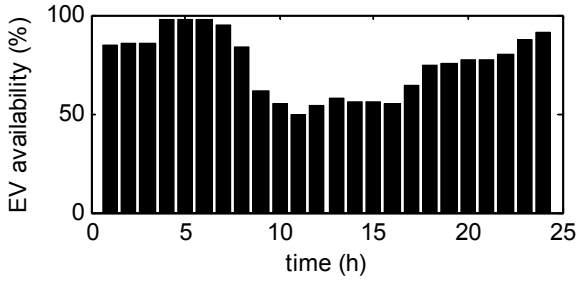

Fig. A-2. EV availability

A.3 HP and House Thermal Parameters

The key parameters of HPs [87] are listed in Table A-3.

TABLE A- 4. KEY PARAMETERS OF HPS

parameter	**value**
COP of HP of one hour	$2.3 \cdot 3600$ s
Initial Inside Air Temp.	20
Initial Structure Temp.	15
Min Temp. of the House	20 ℃
Max Temp. of the House	24 ℃

The household floor area A is a random number which has a uniform distribution between 100 and 200 (m^2). The parameters C_a, C_s, k_1, k_2, k_3 are all estimated based on the floor area through estimation functions [88], which are shown as follows.

Parameter C_a represents the heat capacity of the air and the furniture inside the house.

$$
\begin{aligned}
C_a &= Ah\rho_{air}c_{air} + Ah_{wood}\rho_{wood}c_{wood} \\
&= A \cdot 2.5\text{m} \cdot 1.205\frac{\text{kg}}{\text{m}^3} \cdot 1.005\frac{\text{kJ}}{\text{kg}^{\text{o}}\text{C}} + \\
&\quad A \cdot 1.25cm \cdot 500\frac{\text{kg}}{\text{m}^3} \cdot 1.7\frac{\text{kJ}}{\text{kg}^{\text{o}}\text{C}} \quad , \\
&\approx (A \cdot 3 + A \cdot 10)\frac{\text{kJ}}{\text{m}^{2\text{o}}\text{C}}
\end{aligned}
$$

where $h$is the height of the house (2.5m), ρ represents the density of air and wood, the heat capacity of the furniture is estimated as of 1.25cm wood of the living area A , c is the heat capacity of the substances.

According to [89], the heat capacity of the house structure (floor, wall and ceiling) is varying between 144 and 576 $\frac{\text{kJ}}{^{\text{o}}\text{C}}$ per square meter of the heated floor area depending on the material of the structure. In the previous case studies, 360 $\frac{\text{kJ}}{^{\text{o}}\text{C}}$ per square meter of heated floor area is used, i.e. $C_s = 360A\ \frac{\text{kJ}}{\text{m}^{2\text{o}}\text{C}}$.

The heat transfer between the inside and the outside is assumed to be the heat loss through ventilation. The inside air with temperature K_t^a will be replaced by the outside air with temperature K_t. Assume that the replacement rate n is $0.5\frac{1}{\text{h}}$ of the internal volume of the house. Hence, the HTC k_1 of one time unit (one hour, or h) is determined by,

$$
\begin{aligned}
k_1 &= nV\rho_{air}c_{air}t \\
&= \frac{0.5}{\text{h}} \cdot V \cdot 1.205\frac{\text{kg}}{\text{m}^3} \cdot 1.005\frac{\text{kJ}}{\text{kg}^{\text{o}}\text{C}} \cdot 1\text{h}\,, \\
&= 0.6 \cdot V\frac{\text{kJ}}{\text{m}^{3\text{o}}\text{C}}
\end{aligned}
$$

and $V = 2.5A$.

In order to calculate k_2 and k_3, the surface area of the house A_s is defined to be,

$$A_s = 2A + 4h \cdot \sqrt{A}\,.$$

The thermal resistance of the transition between the inside air and the wall, R_2, is approximated as $\frac{0.13}{A_s}\frac{\mathrm{m^{2o}C}}{\mathrm{W}}$ for isolated wall [90]; therefore,

$$k_2 = \frac{1}{0.13\frac{\mathrm{m^{2o}C}}{\mathrm{W}}} A_s \cdot 3600\mathrm{s} = 27.7 A_s \frac{\mathrm{kJ}}{\mathrm{m^{2o}C}}\,.$$

The HTC k_3 can be determined by estimating the total thermal resistance from the wall to the outside air, R_3. The total thermal resistance can be estimated by the summation of the thermal resistance of the series-connected layers of the wall and the transition between the wall and the outside air, which can be found in [90] for some specific wall materials. Alternatively, it can be estimated by the total thermal resistance from the inside air to the outside air, R_1, minus R_2 [88].

The parameter R_1 is estimated from the annual heat consumption for a normal Danish house, which is $4816\mathrm{kWh} + A \cdot 104\frac{\mathrm{kWh}}{\mathrm{m^2}}$ as shown in [88], minus the heat loss through ventilation. In this way, R_1 is estimated as $\frac{1}{69.05\mathrm{m^2} + 1.07A}\frac{\mathrm{m^{2o}C}}{\mathrm{W}}$ [88].

Finally,

$$k_3 = \frac{1}{R_1 - R_2} \cdot 3600\mathrm{s}$$
$$= \frac{7.69A_s \cdot (69.05\mathrm{m^2} + 1.07A)}{7.69A_s - (69.05\mathrm{m^2} + 1.07A)} \cdot 3600\frac{\mathrm{J}}{\mathrm{m^{2o}C}}\,.$$

A.4 Predicted Day-Ahead System Prices and Outside Temperature

The predicted day-ahead system prices are shown in Table A- 5, which are used as the predicted baseline price to calculated DT or DS in several simulations in this thesis. The outside temperatures employed in the case studies are also shown in Table A- 5.

TABLE A- 5. SOME PARAMETERS FOR PREVIOUS SIMULATIONS

Time	Outside Temp. (°C)	Day-ahead baseline price (DKK/kWh)	Conv. load coefficient
t01	1	0.37109	0.43491
t02	1.9799	0.38109	0.42124
t03	1.9942	0.35177	0.41575
t04	1.9449	0.34177	0.42715
t05	3.0281	0.30115	0.44823
t06	3.0027	0.31115	0.54529
t07	3.0019	0.32018	0.64725
t08	3.0258	0.33018	0.62588
t09	3.754	0.34309	0.60073
t10	3.9839	0.30309	0.56767
t11	4.0278	0.35185	0.54251
t12	4.6447	0.36185	0.54043
t13	5.0854	0.37168	0.5342
t14	3.9327	0.41612	0.54061
t15	4.5145	0.35155	0.55981
t16	5.0699	0.38838	0.6904
t17	3.8971	0.35125	0.93859
t18	4.0556	0.33125	1
t19	2.5406	0.30465	0.92232
t20	2.0209	0.31465	0.843
t21	2.0014	0.30212	0.75081
t22	1.9993	0.32212	0.64897
t23	1.9902	0.29414	0.52515
t24	1.8782	0.22414	0.43786

A.5 β and B

In the case studies, diagonal matrix B (price sensitive matrix) has same diagonal elements, which are equal to β=0.0001.

APPENDIX B

INTRODUCTION TO THE NORDIC ELECTRICITY MARKET

The Nordic electricity market is traded at Nord Pool, which is owned by several TSOs in Nordic and Baltic countries. Nord Pool has both day-ahead market and intraday market, which will be briefly introduced in the following sections.

B.1 Day-ahead Spot Market

The day-ahead spot market is the most important energy market in the Nordic electricity market, as the majority of the electricity is traded in this market. The market players submit their bids into a pool, and the market operator clears the market. After the clearance, the market players will receive the accepted bids, and the hourly zonal prices as well as the hourly system prices will be published. If there is no congestion between zones, the zonal prices will be equal to the system prices.

Due to the participation of renewable energy, the electricity price fluctuates and is largely dependent on the weather forecast.

B.2 Intra-day Market

The intra-day market is a bilateral contract market and is closed at one hour before the actual operation time. The bids not selected at the day-ahead market can be traded here. Market players can make contracts here and avoid the potential cost of causing system imbalance if they have failed components or inaccurate forecast and need balance help from other participants.

B.3 Regulating Power Market

The regulating power market is an auction market managed by the transmission system operator (TSO) where the up regulation (increase production or reduce consumption with duration of e.g. 30~60 minutes) and the down regulation (decrease production or increase consumption) are separated. The market is closed at 45 minutes before the operation time and the bids cannot be modified (price and quantity) after the closure.

The bids are activated in a sequence according to their prices. For a given hour, the up-regulation price (RP) is set as the last activated up regulation bid and the down RP is set as the last activated down regulation bid. It is possible that both up regulation bids and down regulation bids are activated; then a common RP is determined to be one of the up and down regulation price depending on the net effect of the total up and down regulation power. For instance, if the net effect of the total regulation power is up regulation, the common regulation price is determined to be the up-regulation price. In this case, all the up-regulation bids are settled at the common RP while all the down regulation bids are settled by pay-as-bid.

The imbalance of each balance responsible party (BRP), i.e. the difference between the metered data and the scheduled or notified plan resulting from spot market and regulating market, will be settled after the operation time. The imbalance that contributes to the system total imbalance will be settled at the common RP, and the imbalance that is in the opposite direction of the system total imbalance will be settled at the day-ahead spot price. This settlement method is referred as two-price settlement. If one-price settlement applies, the imbalance is always settled at the common RP.

B.4 Ancillary Service Market

Ancillary services, including primary reserve, secondary reserve, manual reserve, and black-start capacity, are traded in this market. EVs are believed to be a good source for providing ancillary services due to the ability of quick response. Bids from the aggregators should be first checked by the DSO to ensure the security of the distribution networks.

BIBLIOGRAPHY

[1] (2011, Feb.). Energy strategy 2050. The Danish government, Copenhagen. [online]. Available: http://www.ens.dk/sites/ens.dk/files/dokumenter/publikationer/downloads/energy_strategy_2050.pdf.

[2] Global Wind Energy Council. (2016). Global wind report. [online]. Available: http://www.gwec.net/wp-content/uploads/vip/GWEC-Global-Wind-2015-Report_April-2016_22_04.pdf. [Accessed: 11-May-2016].

[3] Energinet.dk,"New record-breaking year for Danish wind power." Available: http://energinet.dk/EN/El/Nyheder/Sider/Dansk-vindstroem-slaar-igen-rekord-42-procent.aspx. [Accessed: 11-May-2016].

[4] IEA PVPS Programme. (2016). 2015 snapshot of global photovoltaic marktes. [online]. Available: http://www.iea-pvps.org/fileadmin/dam/public/report/PICS/IEA-PVPS_-__A_Snapshot_of_Global_PV_-_1992-2015_-_Final_2_02.pdf. [Accessed: 11-May-2016].

[5] G. Delille, B. Francois, and G. Malarange,"Dynamic frequency control support by energy storage to reduce the impact of wind and solar generation on isolated power system's inertia," *IEEE Trans. Sustain. Energy*, vol.3, no.4, pp. 931–939, Oct. 2012.

[6] Z. H. Rather, Z. Chen, and P. Thogersen,"Impact of wind energy integration on reactive power reserve and its smart solution: A danish power system case study," in *Proc. IEEE International Conference on Power System Technology (POWERCON)*, pp. 1–6.

[7] U.S. Department of Energy,"Global plug-in light vehicle sales increased by about 80% in 2015," 2016. Available: http://energy.gov/eere/vehicles/fact-918-march-28-2016-global-plug-light-vehicle-sales-increased-about-80-2015. [Accessed: 11-May-2016].

[8] R. Bohn, M. Caramanis, and F. Schweppe,"Optimal pricing in electrical networks over space and time," *RAND J. Econ.*, vol.15, no.3, pp. 360–376, 1984.

[9] P. M. Sotkiewicz and J. M. Vignolo,"Nodal pricing for distribution networks: Efficient pricing for efficiency enhancing DG," *IEEE Trans. Power Syst.*, vol.21, no.2, pp. 1013–1014, May 2006.

[10] R. K. Singh and S. K. Goswami,“Optimum allocation of distributed generations based on nodal pricing for profit, loss reduction, and voltage improvement including voltage rise issue,” *Int. J. Electr. Power Energy Syst.*, vol.32, no.6, pp. 637–644, Jul. 2010.

[11] F. Meng and B. H. Chowdhury,“Distribution LMP-based economic operation for future smart grid,” in *Proc. 2011 IEEE Power and Energy Conference at Illinois*, pp. 1–5.

[12] G. T. Heydt, B. H. Chowdhury, M. L. Crow, D. Haughton, B. D. Kiefer, F. Meng, and B. R. Sathyanarayana,“Pricing and control in the next generation power distribution system,” *IEEE Trans. Smart Grid*, vol.3, no.2, pp. 907–914, Jun. 2012.

[13] K. Shaloudegi, N. Madinehi, S. H. Hosseinian, and H. A. Abyaneh,“A novel policy for locational marginal price calculation in distribution systems based on loss reduction allocation using game theory,” *IEEE Trans. Power Syst.*, vol.27, no.2, pp. 811–820, May 2012.

[14] N. O’Connell, Q. Wu, J. Østergaard, A. H. Nielsen, S. T. Cha, and Y. Ding,“Day-ahead tariffs for the alleviation of distribution grid congestion from electric vehicles,” *Electr. Power Syst. Res.*, vol.92, pp. 106–114, 2012.

[15] R. Li, Q. Wu, and S. S. Oren,“Distribution locational marginal pricing for optimal electric vehicle charging management,” *IEEE Trans. Power Syst.*, vol.29, no.1, pp. 203–211, Jan. 2014.

[16] R. A. Verzijlbergh, L. J. De Vries, and Z. Lukszo,“Renewable energy sources and responsive demand. Do we need congestion management in the distribution grid?,” *IEEE Trans. Power Syst.*, pp. 1–10, 2014.

[17] P. Bach Andersen, J. Hu, and K. Heussen,“Coordination strategies for distribution grid congestion management in a multi-actor, multi-objective setting,” in *Proc. 3rd IEEE PES Innovative Smart Grid Technologies Europe (ISGT Europe)*, pp. 1–8.

[18] J. Hu, S. You, M. Lind, and J. Ostergaard,“Coordinated charging of electric vehicles for congestion prevention in the distribution grid,” *IEEE Trans. Smart Grid*, vol.5, no.2, pp. 703–711, Mar. 2014.

[19] B. Biegel, P. Andersen, J. Stoustrup, and J. Bendtsen,“Congestion management in a smart grid via shadow prices,” in *Proc. 2012 8th IFAC Symposium on Power Plant and Power System Control*, pp. 518–523.

[20] C. Zhang, Y. Ding, N. Nordentoft, P. Pinson, and J. Østergaard,“FLECH-A danish market solution for DSO congestion management through DER flexibility services,” *J. Mod. Power Syst. Clean Energy*, vol.2, no.2, pp. 126–133, 2014.

[21] C. Evens, S. Hänninen, F. Pettersson, and S. Melin. Aggregate consumer’s flexibility in consumption and generation to create “Active Demand.” [online]. Available:

http://www.addressfp7.org/config/files/Nordac10_ADDRESS.pdf.
[22] H. Zhong, L. Xie, and Q. Xia,"Coupon incentive-based demand response: theory and case study," *IEEE Trans. Power Syst.*, vol.28, no.2, pp. 1266–1276, May 2013.
[23] M. R. Sarker, M. A. Ortega-Vazquez, and D. S. Kirschen,"Optimal coordination and scheduling of demand response via monetary incentives," *IEEE Trans. Smart Grid*, vol.6, no.3, pp. 1341–1352, May 2015.
[24] A. R. Malekpour, A. R. Seifi, M. R. Hesamzadeh, and N. Hosseinzadeh,"An optimal load shedding approach for distribution networks with DGs considering capacity deficiency modelling of bulked power supply," in *Proc. Power Engineering Conference*, pp. 1–7.
[25] M. Alonso, H. Amarís, C. Álvarez, and R. Albarracín,"Reactive power planning in distribution networks with distributed generation," in *Proc. 7th Mediterranean Conference and Exhibition on Power Generation, Transmission, Distribution and Energy Conversion (MedPower 2010)*, pp. 1–7.
[26] W. Liu and F. Wen,"Discussion on 'Distribution Locational Marginal Pricing for Optimal Electric Vehicle Charging Management,'" *IEEE Trans. Power Syst.*, vol.29, no.4, pp. 1866–1866, Jul. 2014.
[27] R. A. Verzijlbergh, Z. Lukszo, and M. D. Ilic,"Comparing different EV charging strategies in liberalized power systems," in *Proc. 9th International Conference on the European Energy Market*, pp. 1–8.
[28] P. Bacher and H. Madsen,"Identifying suitable models for the heat dynamics of buildings," *Energy Build.*, vol.43, no.7, pp. 1511–1522, Jul. 2011.
[29] S. Boyd and L. Vandenberghe,*Convex Optimization*. Cambridge University Press, 2004.
[30] EURELECTRIC. Network tariff structure for a smart energy system. [online]. Available: http://www.eurelectric.org/media/80239/20130409_network-tariffs-paper_final_to_publish-2013-030-0409-01-e.pdf.
[31] D. Kirschen and G. Strbac,*Fundamentals of Power System Economics*. England: John Wiley & Sons Ltd, 2004.
[32] R. Djabali, J. Hoeksema, and Y. Langer. (2011). COSMOS description - CWE Market Coupling algorithm. [online]. Available: https://www.apxgroup.com/wp-content/uploads/COSMOS_public_description2.pdf.
[33] IEA Statistics,"Electric power transmission and distribution losses (% of output)," 2014. Available: http://data.worldbank.org/indicator/EG.ELC.LOSS.ZS. [Accessed: 02-May-2016].

[34] S. Huang, J. R. Pillai, M. Liserre, and B. Bak-Jensen,“Improving photovoltaic and electric vehicle penetration in distribution grids with smart transformer,” in *Proc. 2013 4th IEEE/PES Innovative Smart Grid Technologies Europe, ISGT Europe 2013*, pp. 1–5.

[35] S. Bolognani and S. Zampieri,“On the existence and linear approximation of the power flow solution in power distribution networks,” *IEEE Trans. Power Syst.*, vol.31, no.1, pp. 163–172, Jan. 2016.

[36] R. N. Allan, R. Billinton, I. Sjarief, L. Goel, and K. S. So,“A reliability test system for educational purposes-basic distribution system data and results,” *IEEE Trans. Power Syst.*, vol.6, no.2, pp. 813–820, May 1991.

[37] Q. Wu, A. H. Nielsen, J. Østergaard, F. Marra, and C. Træholt,“Driving pattern analysis for electric vehicle (EV) grid integration study,” in *Proc. 2010 IEEE PES Innovative Smart Grid Technologies Conference Europe (ISGT Europe)*, pp. 1–6.

[38] R. E. Rosenthal. (2014, Aug.). GAMS — A user’s guide. GAMS Development Corporation, Washington, DC, USA. [online]. Available: http://www.gams.com/dd/docs/bigdocs/GAMSUsersGuide.pdf.

[39] D. Shirmohammadi and H. W. Hong,“Reconfiguration of electric distribution networks for resistive line losses reduction,” *IEEE Trans. Power Deliv.*, vol.4, no.2, pp. 1492–1498, Apr. 1989.

[40] E. RomeroRamos, A. GomezExposito, J. RiquelmeSantos, and F. LlorensIborra,“Path-based distribution network modeling: application to reconfiguration for loss reduction,” *IEEE Trans. Power Syst.*, vol.20, no.2, pp. 556–564, May 2005.

[41] J. D. McDonald,“Distribution network reconfiguration: single loop optimization,” *IEEE Trans. Power Syst.*, vol.11, no.3, pp. 1643–1647, 1996.

[42] R. A. Jabr, R. Singh, and B. C. Pal,“Minimum loss network reconfiguration using mixed-integer convex programming,” *IEEE Trans. Power Syst.*, vol.27, no.2, pp. 1106–1115, May 2012.

[43] B. Enacheanu, B. Raison, R. Caire, O. Devaux, W. Bienia, and N. HadjSaid,“Radial network reconfiguration using genetic algorithm based on the matroid theory,” *IEEE Trans. Power Syst.*, vol.23, no.1, pp. 186–195, Jul. 2008.

[44] R. Balakrishnan and K. Ranganathan,*A Textbook of Graph Theory*. New York: Springer, 2012.

[45] M. Lavorato, J. F. Franco, M. J. Rider, and R. Romero,“Imposing radiality constraints in distribution system optimization problems,” *IEEE Trans. Power Syst.*, vol.27, no.1, pp. 172–180, Feb. 2012.

[46] M. Guzelsoy and T. Ralphs,“Duality for mixed-integer linear programs,” *Internat. J. Oper. Res*, vol.4, no.3, pp. 118–137, 2007.

[47] MathWorks,“Mixed-integer linear programming (MILP).” Available:

http://www.mathworks.se/help/optim/ug/intlinprog.html#outputarg_output . [Accessed: 20-Aug-2014].

[48] J. Liu, G. M. Huang, Z. Ma, and Y. Geng,“A novel smart high-voltage circuit breaker for smart grid applications,” *IEEE Trans. Smart Grid*, vol.2, no.2, pp. 254–264, Jun. 2011.

[49] J. J. Carmona Cataln and S. S. Martn,“New medium voltage circuit-breaker switchgear with advanced functionality,” in *Proc. 22nd International Conference and Exhibition on Electricity Distribution (CIRED 2013)*, pp. 1–4.

[50] C. Meyer and R. W. De Doncker,“Solid-state circuit breaker based on active thyristor topologies,” *IEEE Trans. Power Electron.*, vol.21, no.2, pp. 450–458, Mar. 2006.

[51] R. Kapoor, A. Shukla, and G. Demetriades,“State of art of power electronics in circuit breaker technology,” in *Proc. 2012 IEEE Energy Conversion Congress and Exposition (ECCE)*, pp. 615–622.

[52] R. J. Sarfi, M. M. A. Salama, and A. Y. Chikhani,“Distribution system reconfiguration for loss reduction: an algorithm based on network partitioning theory,” in *Proc. 1995 Power Industry Computer Applications Conference*, pp. 503–509.

[53] S. Deilami, A. S. Masoum, P. S. Moses, and M. A. S. Masoum,“Real-time coordination of plug-In electric vehicle charging in smart grids to minimize power losses and improve voltage profile,” *IEEE Trans. Smart Grid*, vol.2, no.3, pp. 456–467, Sep. 2011.

[54] E. Sortomme, M. M. Hindi, S. D. J. MacPherson, and S. S. Venkata,“Coordinated charging of plug-in hybrid electric vehicles to minimize distribution system losses,” *IEEE Trans. Smart Grid*, vol.2, no.1, pp. 198–205, Mar. 2011.

[55] A. Abur,“A modified linear programming method for distribution system reconfiguration,” *Int. J. Electr. Power Energy Syst.*, vol.18, no.7, pp. 469–474, Oct. 1996.

[56] T. N. dos Santos and A. L. Diniz,“A dynamic piecewise linear model for DC transmission losses in optimal scheduling problems,” *IEEE Trans. Power Syst.*, vol.26, no.2, pp. 508–519, May 2011.

[57] K. Clement-Nyns, E. Haesen, and J. Driesen,“The Impact of Charging Plug-In Hybrid Electric Vehicles on a Residential Distribution Grid,” *IEEE Trans. Power Syst.*, vol.25, no.1, pp. 371–380, Feb. 2010.

[58] Y. Cao, Y. Tan, C. Li, and C. Rehtanz,“Chance-constrained optimization-based unbalanced optimal power flow for radial distribution networks,” *IEEE Trans. Power Deliv.*, vol.28, no.3, pp. 1855–1864, Jul. 2013.

[59] Shaojun Huang, Qiuwei Wu, Zhaoxi Liu, and Haoran Zhao,“Sensitivity analysis of dynamic tariff method for congestion management in distribution networks,” in *Proc. 2015 IEEE Power & Energy Society*

General Meeting, pp. 1–6.
[60] H. Dommel and W. Tinney,"Optimal Power Flow Solutions," *IEEE Trans. Power Appar. Syst.*, vol.PAS-87, no.10, pp. 1866–1876, Oct. 1968.
[61] B. Stott, J. Jardim, and O. Alsac,"DC Power Flow Revisited," *IEEE Trans. Power Syst.*, vol.24, no.3, pp. 1290–1300, Aug. 2009.
[62] W. Min and L. Shengsong,"A trust region interior point algorithm for optimal power flow problems," *Int. J. Electr. Power Energy Syst.*, vol.27, no.4, pp. 293–300, May 2005.
[63] A. A. Sousa, G. L. Torres, and C. A. Canizares,"Robust Optimal Power Flow Solution Using Trust Region and Interior-Point Methods," *IEEE Trans. Power Syst.*, vol.26, no.2, pp. 487–499, May 2011.
[64] E. BAPTISTA, E. BELATI, and G. DACOSTA,"Logarithmic barrier-augmented Lagrangian function to the optimal power flow problem," *Int. J. Electr. Power Energy Syst.*, vol.27, no.7, pp. 528–532, Sep. 2005.
[65] R. A. Jabr,"A Primal-Dual Interior-Point Method to Solve the Optimal Power Flow Dispatching Problem," *Optim. Eng.*, vol.4, no.4, pp. 309–336, Dec. 2003.
[66] R. A. Jabr,"Radial distribution load flow using conic programming," *IEEE Trans. Power Syst.*, vol.21, no.3, pp. 1458–1459, Aug. 2006.
[67] X. Bai, H. Wei, K. Fujisawa, and Y. Wang,"Semidefinite programming for optimal power flow problems," *Int. J. Electr. Power Energy Syst.*, vol.30, no.6–7, pp. 383–392, Jul. 2008.
[68] J. Lavaei and S. H. Low,"Zero duality gap in optimal power flow problem," *IEEE Trans. Power Syst.*, vol.27, no.1, pp. 92–107, Feb. 2012.
[69] B. Zhang and D. Tse,"Geometry of feasible injection region of power networks," in *Proc. 2011 49th Annual Allerton Conference on Communication, Control, and Computing (Allerton)*, pp. 1508–1515.
[70] B. Zhang and D. Tse,"Geometry of injection regions of power networks," *IEEE Trans. Power Syst.*, vol.28, no.2, pp. 788–797, May 2013.
[71] L. Gan, N. Li, U. Topcu, and S. H. Low,"Exact convex relaxation of optimal power flow in radial networks," *IEEE Trans. Automat. Contr.*, vol.60, no.1, pp. 72–87, Jan. 2015.
[72] B. C. Lesieutre, D. K. Molzahn, A. R. Borden, and C. L. DeMarco,"Examining the limits of the application of semidefinite programming to power flow problems," in *Proc. 2011 49th Annual Allerton Conference on Communication, Control, and Computing (Allerton)*, pp. 1492–1499.
[73] S. H. Low,"Convex Relaxation of Optimal Power Flow—Part I: Formulations and Equivalence," *IEEE Trans. Control Netw. Syst.*, vol.1, no.1, pp. 15–27, Mar. 2014.
[74] S. H. Low,"Convex relaxation of optimal power flow—Part II: Exactness," *IEEE Trans. Control Netw. Syst.*, vol.1, no.2, pp. 177–189,

Jun. 2014.
[75] M. Farivar and S. H. Low,“Branch flow model: relaxations and convexification—Part I,” *IEEE Trans. Power Syst.*, vol.28, no.3, pp. 2554–2564, Aug. 2013.
[76] O. Sundstrom and C. Binding,“Planning electric-drive vehicle charging under constrained grid conditions,” in *Proc. 2010 International Conference on Power System Technology*, pp. 1–6.
[77] O. Sundstrom and C. Binding,“Flexible Charging Optimization for Electric Vehicles Considering Distribution Grid Constraints,” *IEEE Trans. Smart Grid*, vol.3, no.1, pp. 26–37, Mar. 2012.
[78] M. E. Baran and F. F. Wu,“Optimal capacitor placement on radial distribution systems,” *IEEE Trans. Power Deliv.*, vol.4, no.1, pp. 725–734, 1989.
[79] IEEE PES,“Distribution Test Feeders.” Available: http://ewh.ieee.org/soc/pes/dsacom/testfeeders/index.html. [Accessed: 04-Mar-2016].
[80] CVX Research Inc.. (2012, Aug.). CVX: Matlab Software for Disciplined Convex Programming, version 2.0. [online]. Available: http://cvxr.com/cvx/.
[81] M. Grant and S. Boyd,“Graph implementations for nonsmooth convex programs,” *Recent Advances in Learning and Control*. Springer-Verlag Limited, pp. 95–110, 2008.
[82] EU Comission. (2015, Jan.). Study on tariff design for distribution systems. [online]. Available: https://ec.europa.eu/energy/sites/ener/files/documents/20150313 Tariff report fina_revREF-E.PDF.
[83] Y. Ding, S. Pineda, P. Nyeng, J. Ostergaard, and E. M. Larsen,“Real-Time Market Concept Architecture for EcoGrid EU—A Prototype for European Smart Grids,” *IEEE Trans. Smart Grid*, vol.4, no.4, pp. 2006–2016, Dec. 2013.
[84] N. Flatabo, G. Doorman, O. S. Grande, H. Randen, and I. Wangensteen,“Experience with the Nord Pool design and implementation,” *IEEE Trans. Power Syst.*, vol.18, no.2, pp. 541–547, May 2003.
[85] B. Stephan and M. Paterson,“The politics of carbon markets: an introduction,” *Env. Polit.*, vol.21, no.4, pp. 545–562, Jul. 2012.
[86] E. Woerdman,*The institutional economics of market-based climate policy*. Elsevier B.V., 2004.
[87] J. M. Nyers and A. J. Nyers,“COP of heating-cooling system with heat pump,” in *Proc. IEEE 3rd International Symposium on Exploitation of Renewable Energy Sources (EXPRES)*, pp. 17–21.
[88] C. F. Mieritz,“Aggregate Modeling and Simulation of Price Responsive

Heat Pumps," M.S. thesis, Dept. of Elec. Eng., Technical University of Denmark, 2010.
[89] S. Aggerholm and K. G. Sørensen,*Bygningers energibehov*. Hørsholm: SBI forlag, 2005.
[90] *Beregning af bygningers varmetab : DS 418*. Dansk Standard, 2002.